

# **Development of an on-line process monitoring for yeast cultivations via 2D-fluorescence spectroscopy**

Dissertation for Obtaining the Doctoral Degree of Natural Sciences

(Dr. rer. nat.)

Faculty of Natural Sciences  
University of Hohenheim

Institute of Food Science and Biotechnology  
Department of Process Analytics and Cereal Science  
Prof. Dr. Bernd Hitzmann

submitted by

Supasuda Assawajaruwan

from Bangkok

Stuttgart 2019

Dean: Prof. Dr. rer. nat. Uwe Beifuß  
1<sup>st</sup> reviewer: Prof. Dr. rer. nat. Bernd Hitzmann  
2<sup>nd</sup> reviewer: Prof. Dr.-Ing. Rudolf Hausmann  
Submitted on: 15.10.2018  
Oral examination on: 16.01.2019

This work was accepted by the Faculty of Natural Sciences at the University of Hohenheim on 16.01.2019 as “Dissertation for Obtaining the Doctoral Degree of Natural Sciences”.

# **Chapter 1**

## **Preface**

## 1.1 Acknowledgements

Undertaking this PhD has been a truly life-changing experience for me and it would not have been possible to do without the support and guidance that I received from many people.

Firstly, I am especially indebted to my supervisor, Prof. Dr. Bernd Hitzmann who has been supportive of my career goals and who worked actively to provide me with the protected academic time to pursue those goals. Without his guidance and constant feedback this PhD would not have been achievable.

Apart from my supervisor, my thanks also go out to the support I received from following people:

To Dr. Olivier Paquet-Durand, I am hugely appreciative for his assistance in computer settings, programming in MATLAB and other helpful suggestions. Similar, profound gratitude goes to Lucas Ranzan, who helped in MATLAB codes for the fed-batch control. I am also grateful to Annika Hitzemann and Saskia Faassen, who provided me the fundamental knowledge of fluorescence spectroscopy and yeast cultivations. Additionally, the work could not be done well without the help of these students: Jasmin Reinalter, Ramona Diekmann, Philomena Eckard, Fiona Kuon and Matthias Funke. Many thanks also to Almut von Wrochem and Herbert Götz who assisted in the lab equipment and supplies. Last but not least, my deep appreciation goes out to all research team members in Process Analytics and Cereal Science.

Nobody has been more important to me in the pursuit of this project than the members of my family. I would like to thank my parents whose love and guidance are with me in whatever I pursue. They are the ultimate role models.

## 1.2 Co-authors

This work has been partially published previously with the knowledge and approval of the supervisor Professor Dr. Bernd Hitzmann. The scientific work presented in this thesis was partially conducted in cooperation with co-authors from the university of Hohenheim.

### **Comparison of methods for wavelength combination selection from multi-wavelength fluorescence spectra for on-line monitoring of yeast cultivations**

By Supasuda Assawajaruwan, Jasmin Reinalter and Bernd Hitzmann published in *Analytical Bioanalytical Chemistry*. Volume 409, Pages 707-717, January 2017

Jasmin Rheinalter assisted in the yeast cultivations and the analytical methods of the off-line measurements.

### **On-line monitoring of relevant fluorophores of east cultivations due to glucose addition during the diauxic growth**

By Supasuda Assawajaruwan, Philomena Eckard and Bernd Hitzmann published in *Process Biochemistry*. Volume 58, Pages 51-59, July 2017

Philomena Eckard carried out the experiments of yeast cultivations and determined the concentration of glucose, ethanol and biomass.

### **Feedback-control based on NADH fluorescence intensity for *Saccharomyces cerevisiae* cultivations**

By Supasuda Assawajaruwan, Fiona Kuon, Matthias Funke and Bernd Hitzmann published in *Bioresources and Bioprocessing*. Volume 5, Issue 24, May 2018

Matthias Funke performed the yeast cultivations in the part of “Investigation of fluorescence signals corresponding to the metabolic change”. Fiona Kuon performed the experiments of the feedback control of the yeast cultivations.

## 1.3 Publication lists

### Peer-reviewed publications

- Supasuda Assawajaruwan, Jasmin Reinalter and Bernd Hitzmann  
Comparison of methods for wavelength combination selection from multi-wavelength fluorescence spectra for on-line monitoring of yeast cultivations, *Analytical Bioanalytical Chemistry*, Volume 409, Pages 707-717, January 2017
- Supasuda Assawajaruwan, Philomena Eckard and Bernd Hitzmann  
On-line monitoring of relevant fluorophores of yeast cultivations due to glucose addition during the diauxic growth, *Process Biochemistry*, Volume 58, Pages 51-59, July 2017
- Supasuda Assawajaruwan, Fiona Kuon, Matthias Funke and Bernd Hitzmann  
Feedback-control based on NADH fluorescence intensity for *Saccharomyces cerevisiae* cultivations, *Bioresources and Bioprocessing*, Volume 5, Issue 24, May 2018
- Olivier Paquet-Durand, Supasuda Assawajaruwan, Bernd Hitzmann  
Artificial neural network for bioprocess monitoring based on fluorescence measurements: Training without offline measurements, *Engineering in Life Sciences*, Volume 17, Issue 8, Pages 874-880, August 2017

### Oral Presentations

- Supasuda Assawajaruwan, Jasmin Reinalter, Bernd Hitzmann  
Selection techniques for significant fluorescence wavelength combinations, *Analytica*, Munich, 2016
- Supasuda Assawajaruwan, Philomena Eckard and Bernd Hitzmann  
On-line detection of proportional changes of tryptophan and NADH fluorescence intensity due to glucose pulse during ethanol growth phase, 10<sup>th</sup> World Congress of Chemical Engineering, Barcelona, 2017

### Poster Presentations

- Jasmin Reinalter, Supasuda Assawajaruwan, Ramona Diekmann, Bernd Hitzmann

- Auswahl von Fluoreszenz-Wellenlängenkombinationen zum Monitoring von Kultivierungsprozessen, 11. Kolloquium für Prozessanalytik, Vienna, 2016
- Ramona Diekmann, Supasuda Assawajaruwan, Jasmin Reinalter, Bernd Hitzmann  
Alternierende Bestimmung von Glucose und Ethanol während einer Bäckerhefe Kultivierung mit einem Fließinjektionsanalyzesystem, 11. Kolloquium für Prozessanalytik, Vienna, 2016
  - Supasuda Assawajaruwan, Jasmin Reinalter, Bernd  
Selection techniques for significant fluorescence variables from two-dimensional (2D) fluorescence spectroscopy, ProcessNet-Jahrestagung, Aachen, 2017
  - Supasuda Assawajaruwan, Jasmin Reinalter, Bernd Hitzmann  
Selection of wavelength combinations from two-dimensional fluorescence spectra for on-line monitoring of yeast cultivation, ESBES, Dublin, 2017
  - Supasuda Assawajaruwan, Philomena Eckard and Bernd Hitzmann  
Quantification of changes of tryptophan and NADH fluorescence due to glucose pulses during ethanol growing yeast cells, Europact, Potsdam 2017
  - Supasuda Assawajaruwan, Fiona Kuon, Matthias Funke, Bernd Hitzmann  
On-line fluorescence measurements for feed-rate control during yeast cultivations, ESBES, Lisbon, 2018
  - Supasuda Assawajaruwan, Fiona Kuon, Matthias Funke, Bernd Hitzmann  
Feed rate control based on fluorescence measurements during *Saccharomyces cerevisiae* cultivations, ProcessNet-Jahrestagung und 33. DECHEMA-Jahrestagung der Biotechnologen, Aachen, 2018
  - Supasuda Assawajaruwan, Fiona Kuon, Matthias Funke, Bernd Hitzmann  
Closed-loop control for yeast cultivations based on on-line fluorescence measurements, Smart Sensors - mechanistic and data driven modelling, Frankfurt/Main, 2018

## 1.4 Summary

An optimum process is required in the field of food, pharmaceutical and biotechnological industry with the ultimate goal of achieving high productivity and high-quality products. In order to achieve this goal, there are many different parameters to be realized and controlled, e.g., physical, chemical and biological aspects of microbial bioprocesses. Microbial cultivations are a very complex process, therefore, reliable and efficient tools are required to receive as much real-time information for an on-line monitoring as possible, so that the processes can be controlled in time.

The primary objective of this research was to apply a two-dimensional (2D) fluorescence spectroscopy to monitor glucose, ethanol and biomass concentrations of yeast cultivations. The measurement of one spectrum has 120 fluorescence intensity variables of excitation and emission wavelength combinations (WLCs) without consideration of the scattered light. To investigate which WLCs carry important and relevant information regarding the analyte concentrations, the three wavelength selection methods were implemented: a method based on loadings, variable importance in projection (VIP) and ant colony optimization. The five selected WLCs from each method for a particular analyte were evaluated by multiple linear regression (MLR) models. The selected WLCs, which showed the best predictive performance of the MLR models, were relevant to the analyte concentrations. Regarding the results of the MLR models, the most significant WLCs contained seven different excitation and emission wavelengths. They can be combined to have 38 WLCs for one spectrum based on the principle of fluorescence. They were in the area of NADH, tryptophan, pyridoxine, riboflavin and FAD/FMN. The 38 WLCs were used to predict the glucose, ethanol and biomass concentrations via partial least squares (PLS) regression. The best prediction from the PLS models with 38 WLCs had the percentage of root mean square error of prediction (pRMSEP) in the range of 3.1-6.3 %, which was not significantly different from the PLS models with the 120 variables. Therefore, the specific fluorescence sensor for yeast cultivations could be built with less filters, which would make it a low-cost device.

The following plan of the research goal was to investigate the attribute of fluorophores inside cells in real time using a 2D fluorescence spectrometer. The considered intracellular fluorophores, such as NADH, tryptophan, pyridoxine, riboflavin and FAD/FMN were observed during the yeast cultivations under three different conditions: batch, fed-batch with the glucose pulse during a glucose growth phase (GP) and fed-batch with the glucose pulse during an ethanol growth phase (EP) after a diauxic shift. With the help of principal component analysis,



the different states of the yeast cultivations, particularly the glucose pulse during EP, can be recognized and identified from the on-line fluorescence spectra. On the other hand, the change of the fluorescence spectra in the fed-batch process with the glucose pulse during GP was not recognizable. Remarkably, the intensities of the fluorophores due to the glucose pulse during EP did not change in the same direction. The fluorescence intensities of NADH and riboflavin increased, but the intensity of tryptophan, pyridoxine and FAD/FMN decreased. The conversion between tryptophan and NADH intensities was quantified as a proportional factor. It was calculated from the ratio of the area of NADH and tryptophan fluorescence intensity after the glucose addition until depletion. The proportional factor was independent on various glucose concentrations with the coefficient of determination,  $R^2 = 0.999$ . The correlative intensity changes of these fluorophores demonstrate a metabolic switch from ethanol to glucose growth phase.

Based on the previous experiments, a closed-loop control has been implemented for yeast cultivations. 2D fluorescence spectroscopy was applied for an on-line monitoring and control of yeast cultivations to attain pure oxidative metabolism. A glucose concentration is an important factor in a fed-batch process of *Saccharomyces cerevisiae*. Therefore, it has to be controlled under a critical concentration to avoid overflow metabolism and to gain high productivity of biomass. The characteristic of the NADH intensity can effectively identify the metabolic switch between oxidative and oxidoreductive states. Consequently, the feed rates were regulated using the NADH intensity as a metabolic signal. With this closed-loop control of the glucose concentration, a biomass yield was obtained at  $0.5 \text{ g}_{\text{biomass}}/\text{g}_{\text{glucose}}$ . Additionally, ethanol production could be avoided during the controlled feeding phase. The fluorescence sensor with the signal of the NADH intensity has potential to control a glucose concentration under the critical value in real time.

The experiments carried out show that 2D fluorescence spectroscopy has great potential in on-line monitoring and process control of the yeast cultivations. Consequently, it is promising to build up a compact and economical fluorescence sensor with the specific wavelengths using light-emitting diodes and photodiodes. The sensor would be a cost-effective and miniaturized device for routine analysis, which could be advantageous to real-time bioprocess monitoring.

Stuttgart 20.9.2018

Place and Date



Signature of supervisor

## 1.5 Zusammenfassung

Im Bereich der Lebensmittel-, Pharma- und Biotech-Industrie ist ein optimaler Prozess mit dem Ziel einer hohen Produktivität und hohen Produktqualität erforderlich. Um dieses Ziel zu erreichen, sind viele verschiedene Parameter zu überwachen und zu regeln, z.B. physikalische, chemische und biologische Aspekte von mikrobiellen Bioprozessen. Kultivierung von Mikroorganismen ist ein komplexer Prozess, der für ein Online-Monitoring zuverlässige und effiziente Werkzeuge benötigt, um möglichst viele Informationen in Echtzeit zu erhalten, so dass eine Regelung realisiert werden kann.

Das Hauptziel der Forschung war die Anwendung von 2D-Fluoreszenzspektroskopie zur Überwachung der Glukose-, Ethanol- und Biomassekonzentrationen von Hefekultivierung. Die Messung eines Spektrums besteht aus 120 Wellenlängenkombinationen (WLK) ohne Berücksichtigung des Streulichts. Um zu untersuchen, welche WLK wichtige und relevante Informationen über die Prozessgrößen enthalten, wurden drei Wellenlängenauswahlmethoden implementiert: Methode basierend auf Loadings, Variable Importance in Projection (VIP) und Ameisenkolonieoptimierung. Die fünf ausgewählten WLK jeder Methode für eine bestimmte Substanz wurden mit Hilfe der multilinearen Regression (MLR) bewertet. Die ausgewählten WLK, die die beste Vorhersageleistung des MLR-Modells zeigten, waren für die Prozessgrößen relevant. Bezüglich der Ergebnisse des MLR-Modells enthielten die wichtigsten WLK sieben verschiedene Anregungs- und Emissionswellenlängen. Basierend auf dem Prinzip der Fluoreszenz können sie zu 38 WLK für die Messung eines Teilspektrums kombiniert werden. Sie lagen im Bereich der Fluoreszenz von NADH, Tryptophan, Pyridoxin, Riboflavin und FAD/FMN. Diese 38 WLK wurden verwendet, um die Glukose-, Ethanol- und Biomassekonzentrationen über Partial Least Squares (PLS) Regression vorherzusagen. Die besten Vorhersagen der PLS-Modelle mit 38 WLK hatte relative Fehler im Bereich von 3,1-6,3 %. Das ist nicht signifikant schlechter als die PLS-Modellen mit 120 Variablen. Ein spezifischer Fluoreszenzsensor für die Hefekulturen könnte daher mit weniger Filtern gebaut werden, was ein kostengünstiges Gerät wäre.

Forschungsziel war es, die Eigenschaften von Fluorophoren in den Zellen in Echtzeit mit einem 2D-Fluoreszenzspektrometer zu untersuchen. Die betrachteten intrazellulären Fluorophore wie NADH, Tryptophan, Pyridoxin, Riboflavin und FAD/FMN wurden während der Hefekultivierung unter drei verschiedenen Bedingungen beobachtet: Batch-Kultivierung, Fed-Batch-Kultivierung mit einem Glukose-Puls während der Glukosewachstumsphase (GP) und Fed-Batch-Kultivierung mit einem Glukose-Puls während der Ethanolwachstumsphase (EP) nach einer Diauxie. Mit Hilfe der Hauptkomponentenanalyse können die verschiedenen

Zustände der Hefekultivierung, insbesondere der Glukose-Puls während des EP, aus den Online-Fluoreszenzspektren erkannt und identifiziert werden. Andererseits war die Änderung in den Fluoreszenzspektren der Fed-Batch-Kultivierung mit dem Glukose-Puls während der GP nicht erkennbar. Bemerkenswert war, dass sich die Intensitäten der Fluorophore durch den Glukose-Puls während des EP nicht alle in die gleiche Richtung verändert haben. Die Fluoreszenzintensitäten von NADH und Riboflavin nahmen zu, aber die Intensitäten von Tryptophan, Pyridoxin und FAD/FMN nahmen ab. Die Umwandlung von Tryptophan zu NADH konnte aufgezeigt und ein linearer Zusammenhang nachgewiesen werden. Der Proportionalfaktor war unabhängig von verschiedenen Glukosekonzentrationen mit einem Bestimmtheitsmaß von  $R^2 = 0,999$ . Die korrelative Intensitätsänderung von den Fluorophoren zeigte die Stoffwechselveränderung von der Ethanol- zur Glukosewachstumsphase.

Basierend auf den vorherigen Experimenten wurde eine Regelung für die Hefekultivierung implementiert. Die 2D-Fluoreszenzspektroskopie wurde zur Online-Überwachung und Kontrolle der Hefekultivierung eingesetzt, um einen reinen oxidativen Stoffwechsel zu erreichen. Die Höhe der Glukosekonzentration ist ein wichtiger Faktor in einem Fed-Batch-Prozess von *Saccharomyces cerevisiae*. Daher ist es notwendig die Glukosekonzentration unter einer kritischen Konzentration zu halten, um einen Überlaufstoffwechsel zu vermeiden und eine hohe Produktivität der Biomasse zu erreichen. Die Charakteristik der NADH-Intensität kann den metabolischen Wechsel zwischen oxidativen und oxidoreduktiven Zuständen effektiv identifizieren. Folglich wurde die Fütterungsrate auf Basis der Fluoreszenzintensität von NADH als Stoffwechselsignal geregelt. Mit dieser Regelung der Glukosekonzentration wurde ein Ausbeutekoeffizient von  $0,5 \text{ g}_{\text{Biomass}}/\text{g}_{\text{Glucose}}$  erzielt. Die Ethanolproduktion wurde so effektiv vermieden. Der Fluoreszenzsensor hat das Potenzial, die Glukosekonzentration unter dem kritischen Wert zu regeln.

Die durchgeführten Experimente zeigen, dass die 2D-Fluoreszenzspektroskopie ein großes Potenzial in der Online-Überwachung und Prozesskontrolle hat. Daher ist es vielversprechend mit Hilfe von Leucht- und Photodioden einen kompakten und kostengünstigen Fluoreszenzsensor mit den spezifischen Wellenlängen aufzubauen. Der Sensor wäre ein preiswertes und miniaturisiertes Gerät für die Routineanalytik, was für die Online-Bioprozessüberwachung von Vorteil ist.

Stuttgart 20. 9. 2018

Ort und Datum



Unterschrift des Betreuers

# Contents

<b>1 Preface</b>	<b>1</b>
1.1 Acknowledgements	2
1.2 Co-authors	3
1.3 Publication lists	4
1.4 Summary	6
1.5 Zusammenfassung	8
<b>2 Introduction and outline</b>	<b>11</b>
2.1 Introduction	12
2.1.1 <i>Saccharomyces cerevisiae</i>	12
2.1.2 Cellular metabolism in yeasts	14
2.1.3 Cultivation processes	16
2.1.4 Fluorescence spectroscopy	18
2.1.5 Signal processing	20
2.1.6 Chemometrics	21
2.1.7 Quality criteria	24
2.1.8 Variable selection methods	25
2.2 Outline	29
<b>3 Publications</b>	<b>31</b>
3.1 Comparison of methods for wavelength combination selection from multi-wavelength fluorescence spectra for on-line monitoring of yeast cultivations	32
3.2 On-line monitoring of relevant fluorophores of east cultivations due to glucose addition during the diauxic growth	44
3.3 Feedback-control based on NADH fluorescence intensity for <i>Saccharomyces cerevisiae</i> cultivations	54
<b>4 Conclusion and final remarks</b>	<b>64</b>
4.1 Conclusion	65
4.2 Final remarks	68
<b>Bibliography</b>	<b>69</b>
<b>Appendixes</b>	<b>74</b>
A Affidavit	75
B Curriculum Vitae	76

# **Chapter 2**

## **Introduction and outline**

## 2.1 Introduction

Biological processes are used in various fields of industrial production, such as pharmaceutical, food and bioenergy industries. To optimize bioprocesses, it is important to receive high productivity and high-quality products. In microbial bioprocesses, there are many different parameters, e.g., physical, biological and chemical aspects to be realized. Due to complex processes of microbial cultivations, efficient and reliable sensors are required to monitor essential substances like cell mass, substrate and product concentrations. On-line bioprocess monitoring has been studied and developed for many years. During the last years, this process monitoring area was brought into more focus to get more effective progress; for example, in 2002, the US Food and Drug Administration (FDA) launched the Process Analytical Technology (PAT) initiative to be applied in this field (Junker and Wang, 2006). During the past decade, there were many investigations on in-line/on-line monitoring of bioprocesses by using various optical technologies, such as in-situ-microscopy, near infrared, Raman and fluorescence spectroscopy (Marquard et al., 2016; Havlik et al., 2013; Singh et al., 2015; Schalk et al., 2017; Haack et al., 2004).

### 2.1.1 *Saccharomyces cerevisiae*

Yeasts are extensively used in industry of foods, beverages and pharmaceuticals. Besides, they are used as a model for eukaryotic cells, which are applied for fundamental knowledge in the biological and biomedical sciences. For these applications, they are important for research in several areas. Yeasts are unicellular fungi in subdivisions of Ascomycota or Basidiomycota (Boekhout and Kurtzman, 1996). According to Barnett, 1992, yeasts were classified into the genus *Saccharomyces*. Baker's yeast is known as *Saccharomyces cerevisiae* (*S. cerevisiae*). In laboratory and industry, yeasts basically grow best with temperature between 20-30 °C and at pH values between 4.5-6.5 (Walker, 1998). Most of yeasts are aerobic microbes, therefore, oxygen is required for the growth. However, some yeasts can also grow in an anaerobic condition like *S. cerevisiae*. Sugar is an essential carbon source for yeast cultivations, particularly, monosaccharides, i.e., glucose, fructose, mannose and galactose. Glucose is a primary carbon source for *S. cerevisiae* (Johnston, 1999). The main characteristics of glucose transport are that (Walker, 1998):

- (1) Glucose uptake does not need metabolic energy
- (2) Glucose will be not accumulated in cells when glucose uptake reaches equilibrium
- (3) There are several carriers for glucose to help glucose diffusion in the cell

There are two main glucose transporters in *S. cerevisiae* to set up an intracellular glucose signal. The high-affinity glucose transporters are to serve a low glucose level, and another type is low-affinity glucose transporters for a high level of glucose (Ozcan et al., 1996; Johnston, 1999). Thus, the glucose metabolism is based on the amount of glucose and oxygen. A phenomenon named Crabtree effect occurs when yeasts have an overload of glucose during an aerobic condition. Then the fermentation prevails over respiration under an aerobic condition because the glucose inactivates respiratory enzymes (Walker, 1998). In addition to the excess of glucose leading to the Crabtree effect, there is another factor to be realized, which is the limited respiratory capacity in cells (Käppeli et al., 2008). The glucose repression of *S. cerevisiae* solely degrades glucose to ethanol and CO<sub>2</sub> on condition that *S. cerevisiae* is cultivated in an overload of a glucose concentration with the limited respiratory capacity (Walker, 1998). It can be explained with the concept of the respiratory bottleneck, which points out the overflow of glucose to ethanol when the respiration of pyruvate is restricted as illustrated in Fig. 1. The produced ethanol is accumulated as a second carbon source for yeasts. When glucose is completely consumed from a medium, yeasts turn to an oxidative consumption of the accumulated ethanol. The fermentative metabolism under an aerobic condition is named as a respirofermentative or oxidoreductive growth (Käppeli et al., 2008). In the yeast growth, a diauxic shift can be recognized when yeasts switch their metabolism to grow on ethanol after the depletion of glucose (Walker, 1998). In industries, the oxidoreductive growth of yeasts is necessarily avoided to reach a high biomass yield. Consequently, substrate feed rates are controlled under the critical glucose concentration to maintain oxidative metabolism. Fundamentally, the yield coefficient ( $Y_{X/G}$ ) of an oxidative growth of yeasts attains in the range of 0.47-0.50 g<sub>biomass</sub>/g<sub>glucose</sub> (Pham et al., 1998; Hantelmann et al., 2006; Sonnleitner and Käppeli, 1986).

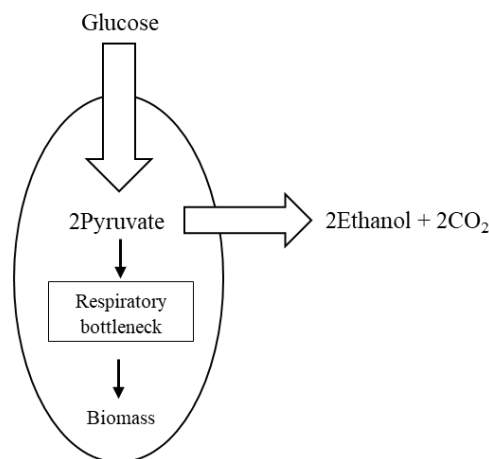
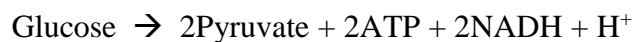


**Figure 1.** The respiratory bottleneck in *S. cerevisiae* (Walker, 1998).

### 2.1.2 Cellular metabolism in yeasts

As mentioned above, glucose is a primary carbon source for yeasts. Glucose is catabolized via the glycolysis pathway. Glycolysis is carried out in the cytoplasm of yeast cells and can function in either an aerobic or anaerobic condition. A glucose molecule is broken down by many enzymes into two molecules of pyruvate. Additionally, in the glycolysis pathway, a glucose molecule provides yeasts energy in the form of two molecules of adenosine triphosphate (ATP) and two molecules of nicotinamide adenine dinucleotide (NADH) as an electron carrier (Walker, 1998).



The molecules of pyruvate in a respiratory metabolism can be mainly proceeded into two ways, which depends on a glucose concentration and respiratory capacity of cells. At low glycolytic fluxes, the pyruvate is mostly oxidized to acetyl-CoA (Lei et al., 2001), but when the glycolytic fluxes reach to a certain value, some molecules of pyruvate are also oxidized to acetaldehyde. Then it is converted further to ethanol as demonstrated in Fig. 2 (Pham et al., 1998). The overflow metabolite like ethanol is produced to balance the NADH/NAD<sup>+</sup> ratio. NADH/NAD<sup>+</sup> as redox carriers are prerequisite for catabolic and anabolic reactions, particularly, for providing cells with energy in the form of ATP. Due to the overflow metabolism, NADH is accumulated and yeast cells need to maintain their cellular redox balance or metabolic homeostasis of NADH/NAD<sup>+</sup> ratio. Therefore, the accumulation of NADH due to high glycolytic fluxes leads to the formation of byproducts, such as ethanol and glycerol (Chen et al., 2014; Vemuri et al., 2007). Then these fermentation products, e.g., ethanol and glycerol, are further oxidized through the tricarboxylic acid cycle (TCA cycle) and oxidative phosphorylation for generating ATP to reach the requirement of growth (Brauer et al., 2005). The TCA cycle will take place only in an aerobic condition. The acetyl-CoA is completely oxidized in the TCA cycle into molecules of CO<sub>2</sub> and energy, which is in the form of ATP and also held in the electron carriers like NADH and FADH<sub>2</sub>. The terminal step of cellular respiration is the electron transport chain. This step will convert the energy in electrons from the electron carriers to generate ATP. In the electron transport chain, oxygen plays an important role as an electron acceptor to receive electrons from NADH and FADH<sub>2</sub>. Then NAD<sup>+</sup> and FAD can take electrons further from the glycolysis and TCA cycle to keep the metabolic process going.



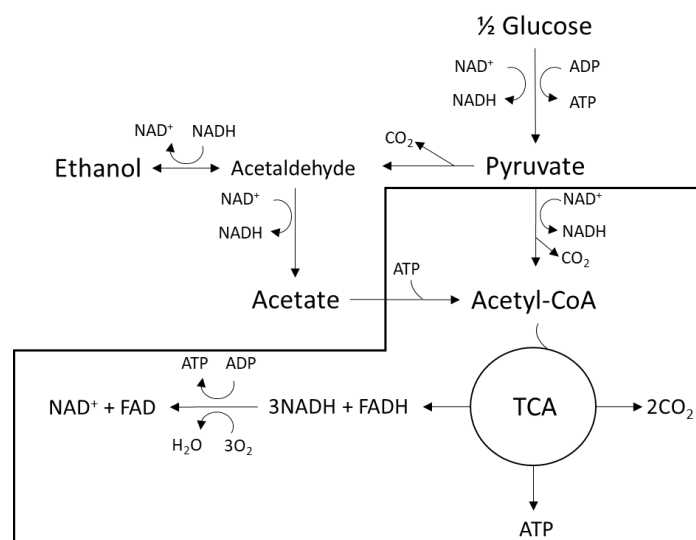


**Figure 2.** Main components of the energy metabolic pathways of *S. cerevisiae* (Pham et al., 1998)

Apart from the glycolysis, TCA cycle and oxidative phosphorylation, other metabolic pathways of intrinsic fluorophores are also considered to understand the process of yeast cultivations. The intrinsic fluorophores, which are relevant to yeast metabolism, are NADH, tryptophan, riboflavin (vitamin B<sub>2</sub>), FAD and pyridoxine (vitamin B<sub>6</sub>). NADH is an essential coenzyme synthesized by many pathways in eukaryotic cells. NADH plays an important role as an electron carrier in metabolic pathways. Another form of NADH is NAD<sup>+</sup>, which is an oxidized form. NAD<sup>+</sup> is synthesized through two main pathways, such as the de novo and salvage biosynthesis pathways (Knepper et al., 2008; Sporty et al., 2009). According to Knepper et al., 2008, Sporty et al., 2009, Ahmed and Moat, 1966, tryptophan is used as a precursor for synthesizing NAD<sup>+</sup> in the de novo pathway as illustrated in Fig. 3. For another pathway, NAD<sup>+</sup> is synthesized from either extracellular nicotinic acid or the recycled intermediates, which are shown in the dashed-line frame (Fig. 3). The biosynthesized NAD<sup>+</sup> is converted to the reduced form, NADH, therefore, it is an indirect relationship between NADH and tryptophan. Bacher et al., 2000 referred that riboflavin can be synthesized by yeasts. The biosynthesis of a molecule of riboflavin needs two molecules of ribulose 5-phosphate and guanosine 5-triphosphate (GTP) as substrates. Riboflavin is used to synthesize flavin adenine dinucleotide (FAD) (Bafunno et al., 2004; Pallotta et al., 1998). Besides, pyridoxine can be also synthesized by *S. cerevisiae* (Shane and Snell Esmond E., 1976; Ishida and Yamada, 2002).

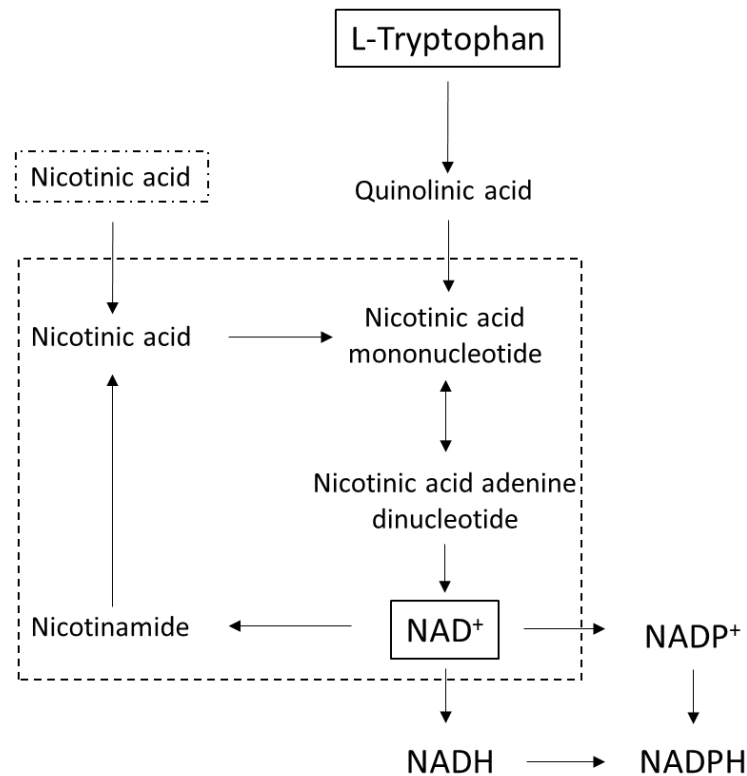


**Figure 3.** Scheme of NAD(P)<sup>+</sup> and NAD(P)H biosynthetic reactions in *S. cerevisiae* (Knepper et al., 2008)

## 2.1.3 Cultivation processes

### 2.1.3.1 Batch process

The main definition of a batch process is no addition of new carbon sources after the cultivation runs with the initial substrate. It means the batch will run until all initial carbon sources are depleted. The main concern in industry of the batch cultivations is a low product yield. However, it is necessary to perform batch cultivations to understand the process of unknown microorganisms or organisms in order to find their optimum growth conditions.

The mathematical models, which are illustrated in Eq. 1-3, were applied to simulate the growth of the yeast batch cultivation (Solle et al., 2003; Grote et al., 2011). The conditions of the specific growth rate ( $\mu$ ) in different phases are presented in Eq. 4-5. The specific growth rate on glucose ( $\mu_G$ ) will function on the condition of the presence of glucose. On the contrary, the specific growth rate on ethanol ( $\mu_E$ ) will be on duty if the glucose is depleted. The simulation is based on the Euler method and the simulation process is performed by using the particle swarm optimization algorithm.

$$\frac{dX}{dt} = \mu_G X + \mu_E X \quad (1)$$

$$\frac{dG}{dt} = -\frac{\mu_G X}{Y_{X/G}} \quad (2)$$

$$\frac{dE}{dt} = \frac{\mu_G X}{Y_{E/G}} - \frac{\mu_E X}{Y_{X/E}} \quad (3)$$

$$\mu_G = \begin{cases} 0 & G = 0 \\ \mu_G & G > 0 \end{cases} \quad (4)$$

$$\mu_E = \begin{cases} 0 & G > 0 \text{ or } E = 0 \\ \mu_E & G = 0 \text{ and } E > 0 \end{cases} \quad (5)$$

where  $X$ ,  $G$  and  $E$  are cell mass, glucose and ethanol concentrations, respectively.  $\mu_G$  and  $\mu_E$  are the specific growth rates on glucose and ethanol, respectively.  $Y_{X/G}$ ,  $Y_{E/G}$  and  $Y_{X/E}$  are the yield coefficients for glucose with respect to biomass and ethanol, and for ethanol with respect to biomass.

### 2.1.3.2 Fed-batch process

To improve a product yield, a fed-batch process is widely operated in various areas, such as chemical, biochemical, biotechnological and pharmaceutical industries (Kristensen, 2002). For the operation of a fed-batch process, a substrate feed rate plays a significant role to attain a high productivity of cultivation processes. Hence, it is important to understand the processes and find efficient strategies to control substrate feed rates. The below equations (Eq. 6-9) are a theoretical model of a fed-batch process (Kristensen, 2002).

$$\frac{dX}{dt} = \mu_S X - \frac{FX}{V} \quad (6)$$

$$\frac{dS}{dt} = -\frac{\mu_S X}{Y_{X/S}} + \frac{F(S_F - S)}{V} \quad (7)$$

$$\frac{dV}{dt} = F \quad (8)$$

$$F = \frac{\mu_S X V}{Y_{X/S}(S_F - S_{const.})}, \text{ if } \frac{dS}{dt} = 0 \quad (9)$$

where  $X$ ,  $S$  and  $V$  are cell mass, substrate concentrations and working volume.  $F$  is a substrate feed rate.  $\mu_S$  is the specific growth rate on the substrate.  $Y_{X/S}$  is the yield coefficient for the substrate with respect to biomass.  $S_F$  is the substrate concentration of the feed solution.  $S_{const.}$  is the substrate concentration in the bioreactor at the start of a fed-batch process.

### 2.1.4 Fluorescence spectroscopy

Molecules absorb photons at some wavelengths and are excited by irradiation of the light to go to the excited electronic states ( $S_1$  or  $S_2$ ). Then the molecules emit photons as fluorescence to return from the excited electronic states to the ground electronic state ( $S_0$ ) at different wavelengths as illustrated in Fig. 4 (Bass, 2000; Faassen and Hitzmann, 2015). The energy levels of molecules in absorption and emission can exist in different vibrational energy states (V). The electronic transitions are described as vertical lines because they occur in too short a period of time for significant displacement of nuclei (Lakowicz, 2006; Albani, 2007). Calculation of absorption ( $h\nu_A$ ) and emission energy ( $h\nu_F$ ) is based on the Planck-Einstein relation as shown in Eq. 10.

$$E = h\nu = h \frac{c}{\lambda} \quad (10)$$

where  $E$  represents the energy (J),  $h$  is the Planck's constant ( $6.626 \times 10^{-34}$  J.s),  $\nu$  is the frequency ( $s^{-1}$ ),  $c$  is the speed of the light ( $2.998 \times 10^8$  m/s) and  $\lambda$  is the wavelength (nm).

While the molecules are returning from the excited electronic states to the ground electronic state, some energy is changed to other forms. The emission energy is typically lower than the absorption one (Albani, 2007). Substances containing aromatic compounds are fluorescent and they are called fluorophores (Lakowicz, 2006). Each fluorophore has its own attribute of the peak intensity in different excitation and fluorescence emission wavelengths. In Table 1, the excitation and emission wavelengths of the peak intensity of significant biogenic fluorophores are presented.

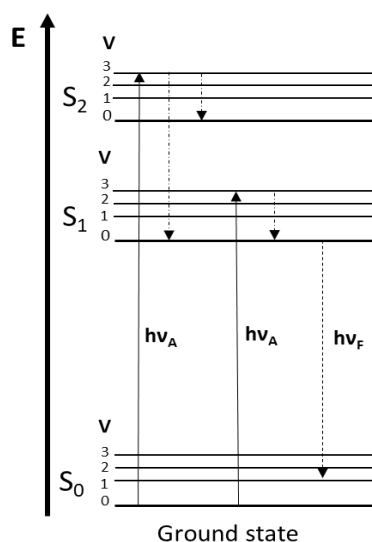


**Figure 4.** Jablonski diagram demonstrating transitions of absorption and fluorescence emission spectra (Faassen and Hitzmann, 2015).

The fluorescence intensity of the fluorophores can be influenced by different surroundings, such as pH, turbidity, aeration and viscosity of the culture (Li and Humphrey, 1991). The environment around them can affect energy transfer and absorption in molecules, which is called inner filter effects. For example, non-fluorescent components in cultivation media absorb excitation or emission radiation from fluorophores, therefore, the fluorescence intensity of these fluorophores is reduced from the original fluorescence yield (Srinivas and Mutharasan, 1987).

**Table 1.** Optimal excitation and emission wavelengths for the peak intensity of biogenic fluorophores (Faassen and Hitzmann, 2015; Stärk, 2000)

<b>Biogenic fluorophore</b>	<b>Excitation wavelength [nm]</b>	<b>Emission wavelength [nm]</b>
NAD(P)H	330, 370	450, 460
Riboflavin	365, 370	520, 530
FAD, FMN	450	530
Pyridoxine	330, 340	390, 400
Tryptophan	280, 290	350, 370

Fluorescence spectroscopy has been used in several applications for many years. According to the problem of overlapping and quenching of excitation or emission wavelengths from different fluorophores, it was developed to measure the wider range of excitation and emission wavelengths, which is called 2-dimensional (2D) fluorescence spectroscopy (Lindemann et al., 1998; Marose et al., 1998; Li et al., 1991). The scheme of the connection between the BioView<sup>®</sup> sensor (DELTA Lights & Optics, Hørsholm, Denmark) and a bioreactor is demonstrated in Fig. 5. The sensor contains two filter wheels as shown in Fig. 5. Each wheel has 16 slots, but containing only 15 filters for the different excitation and emission wavelengths, respectively. It is equipped with a xenon (Xe) flash lamp as a light source. Excitation light from the Xe lamp goes through the excitation filters to the bioreactor via fiber optic bundles as a light conductor. The fluorescence emitted in 180° angle is guided through the light conductor to the photomultiplier as a detector. One spectrum is completely measured in 90 s and the data is interpreted in matrix data or graphs. The 2D fluorescence spectroscopy is possible to perform a non-invasive measurement without interfering an inner system of cultivation processes.

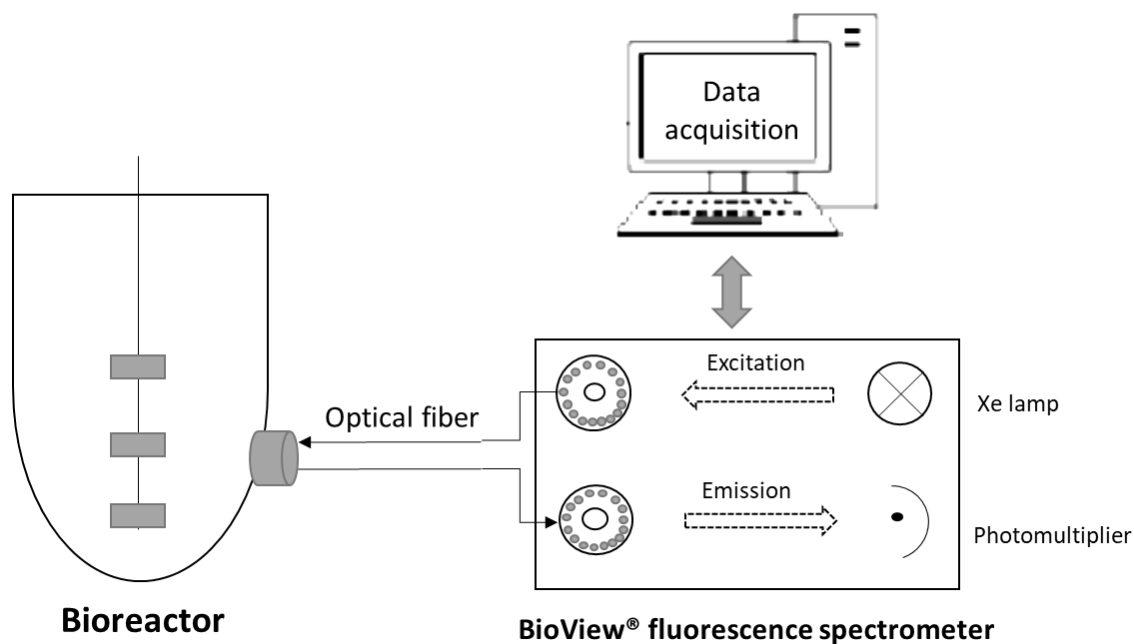


**Figure 5.** The schematic overview of the BioView® sensor connecting to a bioreactor (Faassen and Hitzmann, 2015).

### 2.1.5 Signal processing

Analytical signals, which are obtained from spectroscopies, are basically recorded as spectra. These signals are monitored in wavelength, wavenumber or frequency. The signals from analytical processes contain not only significant data, but also noise data, therefore, signal processing is required to enhance informative signals versus noises. There are several methods of the signal processing to serve different purposes, such as smoothing, derivation and integration of signals (Otto, 1999). Median filter is an effective and simple technique for smoothing signals. It is often used to remove noise from an image or signal, but all smoothing techniques can adversely affect the edge of data (Tukey, 1974). Apart from the smoothing filter, the derivation of signals is usually used for subtraction of background and for improvement of visual resolution. Savitzky-Golay filter is another signal processing method, which can be applied for the purpose of smoothing and derivation of signals (Gorry, 2002; Otto, 1999). This method calculates smoothing and differentiation of data by a least-squares technique. The coefficient ( $c_j$ ) of a selected data point ( $y_k$ ) is calculated as a weighted combination of itself as a center-point and  $m$  points on either side of it as in Eq. 11. The convolution weights correspond to performing a moving least squares fit across the data,  $2m+1$  points. The  $2m+1$  of the data points presents a size of the window called filter width. The size of the filter width should not be too large because it can affect the informative original data.

$$y_k^* = \frac{1}{NORM} \sum_{j=-m}^{j=m} c_j y_{k+j} \quad (11)$$

where NORM is a normalization factor obtained from the sum of the coefficients,  $c_j$ . The values of NORM and coefficients in different cases of Savitzky-Golay filter can be found in the literatures (Gorry, 2002; Otto, 1999).

## 2.1.6 Chemometrics

### 2.1.6.1 Multiple linear regression

Multiple linear regression (MLR) is fundamentally based on the concept of simple linear regression, but it is a regression of a single dependent variable,  $y$ , on two or more independent variables,  $x$ . MLR analyzes the correlation between  $y$  and  $x$  (Otto, 1999; Martens and Naes, 1989). Principally, the least squares functions by calculating parameters called regression coefficients,  $b$ , which are calculated as in Eq. 12.  $X$  is the matrix containing ones and independent variables (see Eq. 13). As shown in Eq. 12, the equation is solved by the inversion of the matrix,  $X^T X$ . It is necessary that there is no collinearity between data in the independent variables.

$$b = (X^T X)^{-1} X^T y \quad (12)$$

where  $b$  represents the vector of the regression coefficients and  $y$  is the vector of dependent variables.

These regression coefficients are used for predicting values of the dependent variable from the independent variables, which is demonstrated in Eq. 13 and 14 (Otto, 1999):

$$\begin{pmatrix} y_1 \\ y_2 \\ \vdots \\ y_n \end{pmatrix} = \begin{pmatrix} 1 & x_{11} & x_{12} & \cdots & x_{1k} \\ 1 & x_{21} & x_{22} & \cdots & x_{2k} \\ \vdots & \vdots & \vdots & \ddots & \vdots \\ 1 & x_{n1} & x_{n2} & \cdots & x_{nk} \end{pmatrix} \begin{pmatrix} b_0 \\ b_1 \\ \vdots \\ b_k \end{pmatrix} + \begin{pmatrix} e_1 \\ e_2 \\ \vdots \\ e_n \end{pmatrix} \quad (13)$$

$$y = Xb + e \quad (14)$$

where  $y$  is the dependent variable,  $x$  is the independent variable in  $X$ ,  $b$  is the regression coefficient,  $k$  and  $n$  are subscription indexes of the number of variables and measurements, respectively, and  $e$  represents the error between measured and predicted data.

### 2.1.6.2 Principal component analysis

Principal component analysis (PCA) is a method to handle the collinearity in the data of the  $X$ -matrix in order to carry the most relevant information and cut out noise and redundancy from

the data (Otto, 1999; Martens and Naes, 1989). Therefore, PCA helps to reduce non-useful data in order to visualize the structure of the significant information. PCA model, which consists of two main parts, such as scores and loadings is illustrated in Fig. 6. Besides, it also contains residuals ( $E$ ) as in Eq. 15.

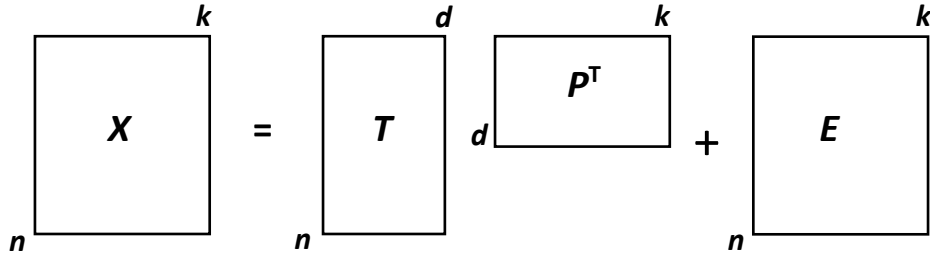


**Figure 6.** PCA model containing the data, scores, loadings and residuals,  $X$ ,  $T$ ,  $P$  and  $E$ -matrices, respectively.  $n$ ,  $k$  and  $d$  represent the size of  $X$ ,  $T$ ,  $P$  and  $E$ -matrices.

The objective of PCA is to lower the number of variables of the original data. The PCA process finds a direction that carries the most information of the original data. The direction is called principal component (PC) or score, which is represented as  $t$ . The PC or score containing the maximum variance of the data is called the first PC ( $t_1$ ). The second PC ( $t_2$ ) carries the maximum of the rest variance in the data and so on. These PCs are orthogonal to each other as shown in Fig. 7 (Otto, 1999; Martens and Naes, 1989). The mathematical equation of the PCA model is thoroughly written in Eq. 15-16, which show each score and loading. The data as shown in Fig. 7b is preprocessed by the mean centering, which is shown in Eq. 17-18. PCA can be computed with the non-linear iterative partial least squares (NIPALS) algorithm to find principal components (Otto, 1999; Martens and Naes, 1989).

$$X = TP^T + E \quad (15)$$

$$X = t_1p_1^T + t_2p_2^T + \dots + t_ap_a^T + E \quad (16)$$

where  $X$  represents the mean-centered data matrix,  $T$  is the score matrix which contains  $t$ ,  $P^T$  is the transpose of the loading matrix containing  $p^T$ , and  $E$  represents residuals or errors.



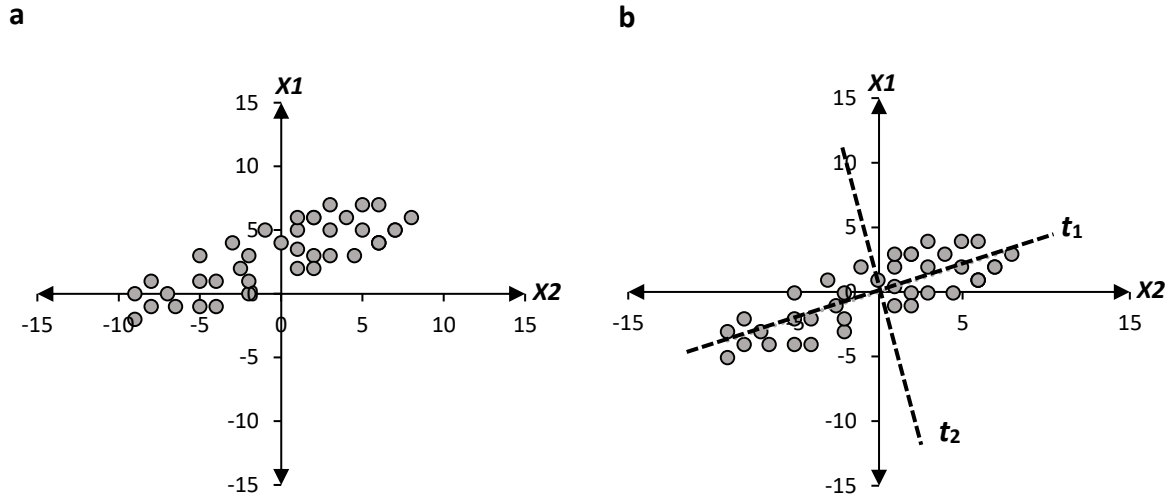


**Figure 7.** (a) The original data and (b) The mean-centered data of two variables ( $x_1$  and  $x_2$ ) with the first and second PCs,  $t_1$  and  $t_2$ , respectively.

$$\bar{x}_k = \frac{1}{n} \sum_{i=1}^n x_{ik} \quad (17)$$

$$x_{ik}^* = x_{ik} - \bar{x}_k \quad (18)$$

where  $x$  is the data in  $X$ ,  $i$  is the row index,  $k$  is the column index,  $\bar{x}_k$  is the mean value from the  $k^{\text{th}}$  column and  $x_{ik}^*$  is the mean-centered value.

### 2.1.6.3 Partial least squares regression

Partial least squares regression (PLSR) is a method to regress the response variables ( $Y$ ), i.e., measured data as the off-line data, on the predictors ( $X$ ), i.e., spectra as the on-line data. PLSR is based on a bilinear model with the maximal covariance between the latent variables (principal components) in the  $X$  and  $Y$ -matrices (CAMO Process AS, 2006; Martens and Naes, 1989; Otto, 1999; Wold et al., 2001b). The parameters, which are in the  $X$ -matrix, are represented as in Eq. 15. For the  $Y$ -matrix, it also consists of a score matrix ( $U$ ), loadings ( $Q$ ) and residuals ( $F$ ) as shown in Eq. 19. The correlation between the score  $T$  and  $U$ -matrices with  $B$ -coefficients is presented in Eq. 20. The  $B$ -coefficients are calculated from the correlation of the transpose of the loading matrices ( $P^T$  and  $Q^T$ ) with the parameter named loading weights,  $W$  in Eq. 21. The loading weights are obtained by maximizing the covariance between the linear combination of the score vector  $t$  and  $u$  under the condition that the loading weight are normalized as 1 (Martens and Naes, 1989; CAMO Process AS, 2006; Otto, 1999; Wold et al., 2001b). The NIPALS algorithm is also applied in PLSR to calculate the parameters.

$$Y = UQ^T + F \quad (19)$$

$$U = BT \quad (20)$$

$$B = W(P^TW)^{-1}Q^T \quad (21)$$

where  $Y$  is the measured data,  $U$  is the score matrix with respect to  $Y$ -matrix,  $Q$  is the loading matrix with respect to  $Y$ -matrix,  $F$  is the errors,  $B$  is the regression coefficients,  $T$  and  $P$  are the score and loading matrices with respect to the  $X$ -matrix and  $W$  is the loading weights. The process of PLSR model is demonstrated in Fig. 8. Firstly, a calibration model is created by using spectra and measured data. Subsequently, the model is used to predict the new off-line data set ( $Y'$ ) from a new set of spectra ( $X'$ ) as shown in the diagram.

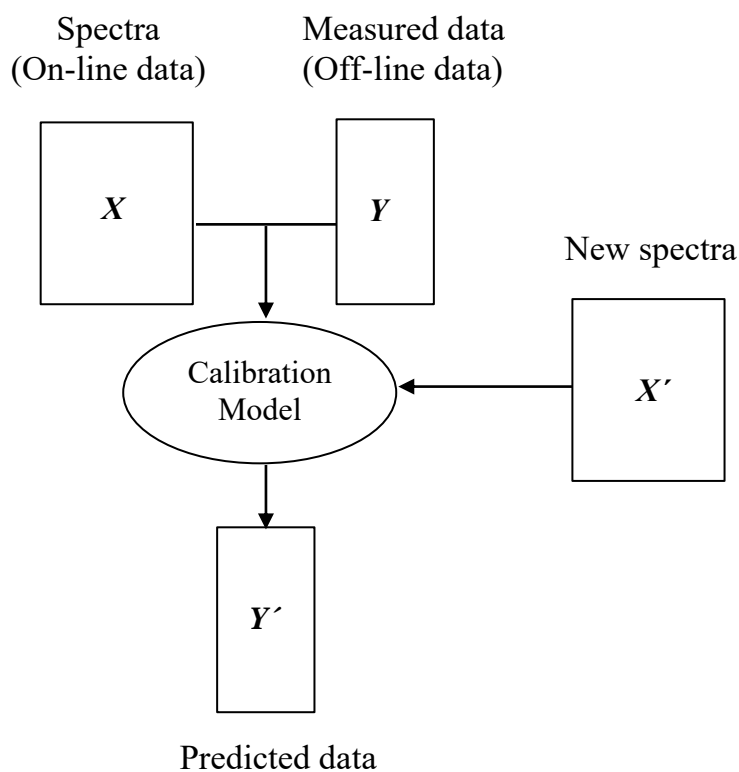


**Figure 8.** The process of PLSR model.

### 2.1.7 Quality criteria

The calibration and prediction models created by MLR or PLSR should be evaluated to examine the quality of the models. The root mean square error of calibration and prediction (RMSEC/P) as shown in Eq. 22 are used for calculating the errors between measured and predicted data. In addition, the percentage of RMSEP (pRMSEP) in Eq. 23 is computed for comparing the error of one process with other different processes.

$$\text{RMSEC/P} = \sqrt{\frac{\sum_{i=1}^n (y'_{i,model} - y_i)^2}{n}} \quad (22)$$

$$\text{pRMSECP} [\%] = \frac{\text{RMSEP} \times 100}{\text{max. } y_{measured}} \quad (23)$$

where  $y'_{i,model}$  is the predicted value of the target analyte for the object  $i$ ,  $y_i$  is the measured value for the object  $i$ ,  $n$  is the number of sample data, and  $\text{max. } y_{measured}$  is the maximum value of the measured off-line data.

## 2.1.8 Variable selection methods

According to analytical measurements, there are a number of variables, but the question is which ones are significantly related to the experimental response. For this reason, variable selection methods are required to find the most relevant variables, which helps to neglect non-significant variables and reduce noise to obtain the most informative data from the measurements.

### 2.1.8.1 A method based on loadings

This method chooses relevant variables based on loadings in PCA. The positive and negative signs of loadings do not determine the value of them, but the signs represent the direction of the vectors. High absolute value of the elements in loadings shows the corresponding variables, which have more influence on the considered PC than the variables with low values. Basically, the first few PCs are regarded as significant, therefore, a few variables with the magnitude of the loadings in the first few PCs are selected (Otto, 1999; Guo et al., 2002). These selected variables have an influence on the data.

### 2.1.8.2 Variable importance in projection

VIP is known as “variable influence on projection” or “variable importance in projection” (Wold et al., 2001). This variable selection method is based on PLSR. The variable selection methods based on PLSR can be divided into three main categories: (1) filter, (2) wrapper and (3) embedded methods (Mehmood et al., 2012). VIP is categorized into the filter method. The filter method works principally in two steps: (1) creating a PLSR model and (2) selecting variables based on an optimum threshold. The method calculates a VIP score for each variable ( $K$ ). The score of each variable basically depends on the explained variance of each  $a^{\text{th}}$  PLS component, which is  $\frac{w_{ak}}{\|w_a\|^2}$  as shown in Eq. 24. For the VIP method, the selection criterion is

that the variables with a VIP score over than 1.0 are chosen because the average threshold values equal to 1.0 (Gosselin et al., 2010).

$$VIP_k = \sqrt{K \sum_{a=1}^A [(q_a^2 t_a^T t_a) (\frac{w_{ak}}{\|w_a\|^2})]} / \sum_{a=1}^A (q_a^2 t_a^T t_a) \quad (24)$$

where  $a$  is a subscription index,  $A$  is the number of latent variables in PLS,  $K$  is the number of variables,  $w_{ak}$  is the loading weight of the  $k^{\text{th}}$  variable in the  $a^{\text{th}}$  component and  $\|w_a\|$  is the norm of matrix  $w_a \cdot t_a$ ,  $w_a$  and  $q_a$  are the  $a^{\text{th}}$  column vectors of  $T$  (scores of the  $X$ -matrix),  $W$  (weight matrix) and  $Q$  (loadings of the  $Y$ -matrix), respectively (Gosselin et al., 2010; Mehmood et al., 2012).

### 2.1.8.3 Ant colony optimization

Ant colony optimization (ACO) algorithm was firstly introduced in the early 1990s to find optimal solutions for problems (Mullen et al., 2009; Blum, 2005). The ACO algorithm is inspired from the real ants in wild (Dorigo et al., 1996). The ants find the shortest path between their nest and the food source by the strongest pheromone concentration on trails. As shown in Fig. 9, there are two paths from the nest to the food source and two groups of ants going to the different ways. The ants that go to the upper path being shorter arrive earlier, therefore, they return to the same path to their nest. While they are going to the food source and back to the nest, they leave the pheromone on the track. Thus, this higher pheromone concentration of the upper path guides other ants to follow the way to reach the food. The upper path that other ants follow collects more and more pheromone, on the contrary, the pheromone concentration of the lower (long) path decreases due to the evaporation and no visiting from other ants. Then it ends up with no ant using the lower path and the shortest path is found (Blum, 2005; Mullen et al., 2009). The indirect communication between ants by pheromone is called stigmergy.

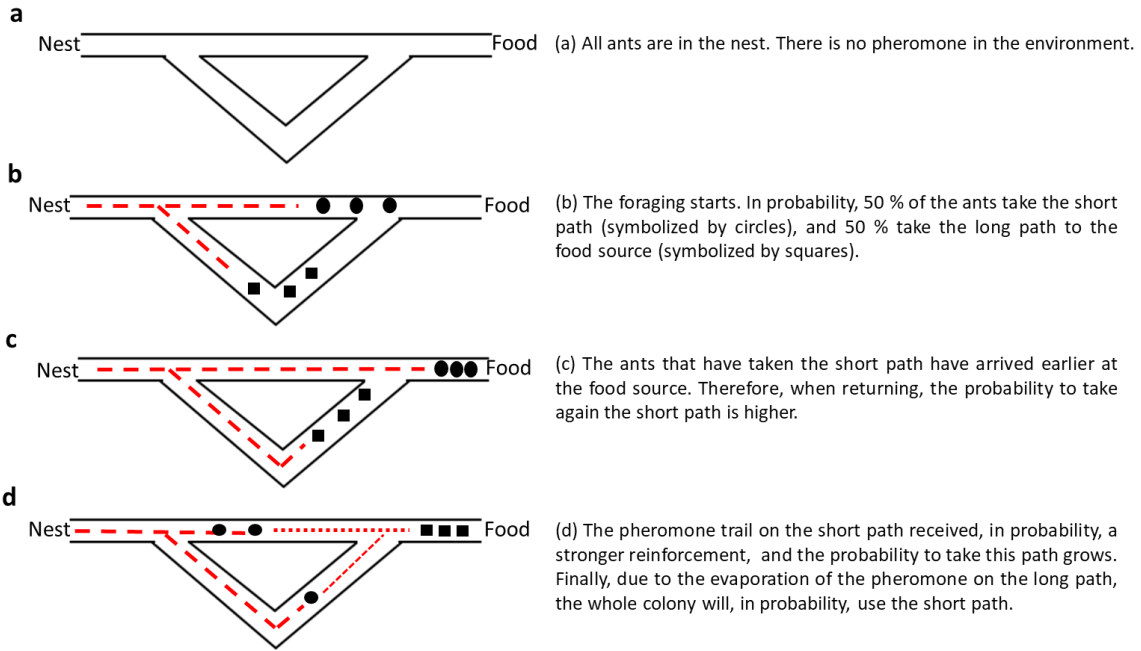


**Figure 9.** The scheme of the experiment demonstrating how ants find the shortest path from their nest to the food source (Blum, 2005).

The ACO algorithm was firstly applied for the well-known traveling salesman problem (TSP) (Dorigo et al., 1996). The purpose of using the ACO algorithm in TSP is to minimize the total distance of the traveling to visit each town only once. The fundamental ACO system is that an ant goes to a town by following a transition rule, which has a distance function and a function of left pheromone on the path. The visited towns are not allowed to visit again, so they are on a tabu list ( $tabu_k$ ). When the mission to visit all towns as one tour is completed, the total pheromone concentration of each tour is considered (Mullen et al., 2009). The concentration of pheromone on trails is calculated following Eq. 25-26. The probability,  $p_{ij}^k(t)$  of the  $k^{\text{th}}$  ant in Eq. 27 makes the transformation between town  $i$  and  $j$  (Mullen et al., 2009).

$$\tau_{ij}(t+n) = (1-\rho)\tau_{ij}(t) + \sum_{k=1}^N \Delta\tau_{ij}^k \quad (25)$$

where  $\tau_{ij}$  is the amount of pheromone on the path between given towns  $i$  and  $j$ ,  $\rho$  is the evaporation rate ( $\rho \in (0,1]$ ),  $N$  represents the number of ants,  $\Delta\tau_{ij}^k$  is the quantity of the pheromone deposited on a path by  $k^{\text{th}}$  ant between time  $t$  and  $t+n$ , and  $n$  is the number of iterations, with the condition below:

$$\Delta\tau_{ij}^k = \begin{cases} \frac{Q}{L_k} & \text{if ant } k \text{ used edge } (i,j) \text{ in its tour} \\ 0 & \text{otherwise} \end{cases} \quad (26)$$

where  $Q$  is a constant and  $L_k$  is the tour length of the  $k^{\text{th}}$  ant.

$$p_{ij}^k(t) = \begin{cases} \frac{[\tau_{ij}(t)]^\alpha [\eta_{ij}]^\beta}{\sum_{k \in allowed_k} [\tau_{ik}(t)]^\alpha [\eta_{ik}]^\beta} & \text{if } j \in allowed_k \\ 0 & \text{otherwise} \end{cases} \quad (27)$$

where  $\eta_{ij}$  is the visibility of edge  $i$  and  $j$  as quantity  $1/d_{ij}$ , ( $d_{ij}$  is the path length between town  $i$  and  $j$ ),  $allowed_k$  represents the unvisited towns, (all towns –  $tabu_k$ ),  $\alpha$  is a parameter to control the influence of  $\tau_{ij}$  and  $\beta$  is a parameter to control the influence of  $\eta_{ij}$ .

The ACO algorithm has been applied for variable or wavelength selection (Shamsipur et al., 2006; Ranzan et al., 2014; Allegrini and Olivieri, 2011). The purpose of using the ACO algorithm in wavelength selection is to find relevant wavelengths correlating to the target responses. The relevant wavelengths are selected based on the high accumulation of pheromone depositing on a variable. Theoretically, these selected wavelengths carry significant information of the data.

## 2.2 Outline

An optimum processing is required in biotechnological industries with the ultimate goal of achieving high productivity and high quality products. In order to achieve this goal, there are many different parameters to be realized and controlled, e.g., physical, chemical and biological aspects of microbial bioprocesses. Microbial cultivations are such a complex process, therefore, reliable and efficient tools are needed for an on-line monitoring to receive as much real-time information as possible, so that the processes can be controlled in time. The main objective for the overall study was to apply a 2D fluorescence spectrometer for the on-line monitoring of a yeast cultivation process in order to follow yeast growth and metabolism in real time. Besides, the process can be controlled as required in time. This study was principally divided into three main research goals.

The primary research plan has been performed to find relevant wavelength combinations corresponding to process variables of the yeast cultivations. They have been selected by three different selection methods: a method based on loadings (Otto, 1999), variable importance in projection (Mehmood et al., 2012) and ant colony optimization (Shamsipur et al., 2006). The selected wavelength combinations from each method were used to predict glucose, ethanol and biomass concentrations of the yeast cultivations via chemometric methods. The selected wavelength combinations, which performed well on the prediction of the target substances, were in the area of NADH, tryptophan, pyridoxine, riboflavin and FAD/FMN. Regarding the results, an on-line monitoring on the relevant biogenic fluorophores under different cultivation conditions has been conducted in the following phase to observe metabolic changes in yeasts.

The different cultivation conditions have been conducted to observe the significant fluorophores due to metabolic changes during yeast cultivations. The metabolic changes due to a glucose spiking in different phases of yeast growth were investigated using a 2D fluorescence spectrometer. According to the results from the previous study, the intracellular fluorophores like NADH, tryptophan, pyridoxine, riboflavin and FAD/FMN were well observed during the yeast cultivations. They are significantly related to several yeast metabolic pathways (Knepper et al., 2008; Pallotta et al., 1998; Bacher et al., 2000; Bafunno et al., 2004; Ishida and Yamada, 2002). Due to the glucose spiking in an ethanol growth phase, the intensity changes of these biogenic fluorophores were obviously recognized by the 2D fluorescence spectrometer, but not in a glucose growth phase. The yeasts instantly switched to grow on glucose instead of ethanol after spiking glucose during the ethanol growth phase. From the results, the 2D fluorescence spectrometer shows potential to detect the metabolic change from growing on ethanol to

glucose. Therefore, it is promising to apply the 2D fluorescence spectroscopy for a process control of yeast cultivations in the next phase of the research project.

This following study has focused on the investigation of a signal, which can determine a metabolic switch between oxidative and oxidoreductive states. The biogenic fluorophores, such as NADH, tryptophan, flavins and pyridoxine, were taken into the examination. The characteristic of the NADH intensity showed the best performance to identify the metabolic switch. Therefore, the NADH fluorescence intensity has been used to control glucose feed rates during the fed-batch cultivations. The objective of a fed-batch cultivation of baker's yeasts is to obtain a high yield of biomass. Thus, overflow metabolism must be avoided by controlling the glucose concentration under a critical value, 0.04-0.07 g/L (Pham et al., 1998; Hantelmann et al., 2006). There is currently no commercial device, which can measure a glucose concentration at the low level of the critical point in real time. Intracellular NADH can be detected as an indirect signal to indicate the critical point of the overflow metabolism. Consequently, the glucose feed rates were controlled with the NADH signal in real time to maintain oxidative metabolism. From this study, it is possible to see if it is promising to build up a specific wavelength fluorescence sensor equipped with light-emitting diodes and photodiodes for yeast cultivations. The sensor would be a cost-effective and miniaturized device for routine analysis (O'Toole and Diamond, 2008).



# **Chapter 3**

## **Publications**

### **3.1 Comparison of methods for wavelength combination selection from multi-wavelength fluorescence spectra for on-line monitoring of yeast cultivations**

By Supasuda Assawajaruwan, Jasmin Reinalter and Bernd Hitzmann.

Published 2017 in **Analytical Bioanalytical Chemistry**.

Volume 409, Pages 707-717

DOI: 10.1007/s00216-016-9823-2



## Comparison of methods for wavelength combination selection from multi-wavelength fluorescence spectra for on-line monitoring of yeast cultivations

Supasuda Assawajaruwan<sup>1</sup> · Jasmin Reinalter<sup>1</sup> · Bernd Hitzmann<sup>1</sup>

Received: 6 May 2016 / Revised: 28 June 2016 / Accepted: 21 July 2016 / Published online: 6 August 2016  
© Springer-Verlag Berlin Heidelberg 2016

**Abstract** The on-line monitoring with two-dimensional (2D) fluorescence spectroscopy of *Saccharomyces cerevisiae* batch cultivations was applied to monitor glucose, ethanol, and biomass concentrations. The measurement of one spectrum by the 2D fluorescence spectrometer has 120 fluorescence intensity values of excitation and emission wavelength combinations (WLCs); scattered light is not considered here. To identify which WLCs of the multi-wavelength fluorescence spectra carry important and relevant information regarding the analyte concentrations, three different methods were compared: a method based on loadings, variable importance in projection, and ant colony optimization. The five selected WLCs for a particular analyte from each method were evaluated by multiple linear regression models to find the most significant variable subsets for predicting the sample concentrations. The most significant WLCs relevant to the three sample properties contained seven different excitation and emission wavelengths, which can combine with each other to have 38 possible wavelength combinations in the fluorescence measurement. Partial least squares (PLS) models were calibrated with the 38 possible variables and the off-line data for the prediction of glucose, ethanol, and biomass concentrations. The best prediction from the PLS models had the percentage of root mean square error of prediction (pRMSEP) in the range of 3.1–6.3 %, which was similar to pRMSEPs of the PLS models with the full variables. Based on these results, it is

promising to build up a specific inexpensive fluorescence sensor for the yeast cultivation process using light-emitting diodes and photodiodes.

**Keywords** Bioprocess monitoring · *Saccharomyces cerevisiae* · 2D fluorescence spectroscopy · Chemometrics · Ant colony optimization · Variable importance in projection

### Introduction

Biological processes are used in various fields of industrial production, such as pharmaceutical, food, and bioenergy industries. To optimize bioprocesses, it is important to receive high productivity and product quality. In microbial bioprocesses, there are many different parameters, e.g., physical, biological, and chemical to be controlled. Due to complex processes of microbial cultivations, efficient and reliable sensors are required to monitor essential substances like cell mass, substrate, and product concentrations. On-line bioprocess monitoring has been studied and developed for many years. In the last years, this process monitoring area was brought into more focus to get more effective progress; for example, in 2004, the US Food and Drug Administration (FDA) launched the Process Analytical Technology (PAT) initiative to be applied in this field [1]. During the past decade, there were many investigations on in-line/on-line monitoring of bioprocesses by using several optical sensors, such as near-infrared (NIR), Raman, and fluorescence spectroscopy [2–5].

Two-dimensional (2D) fluorescence spectroscopy is an effective tool for on-line monitoring of cultivation processes. A non-invasive measurement is an ideal technique for bioprocesses because it will not interfere with microbes or any cells inside a bioreactor. Fluorescence

Published in the topical collection *Process Analytics in Science and Industry* with guest editor Rudolf W. Kessler.

✉ Supasuda Assawajaruwan  
sassawaj@uni-hohenheim.de

<sup>1</sup> Department of Process Analytics and Cereal Science, University of Hohenheim, Garbenstraße 23, 70599 Stuttgart, Germany

sensors have been used almost 30 years for various applications to measure biogenic fluorophores. They are useful and effective, especially, for microorganisms having autofluorescence like yeast. For example, Bhatta et al. 2006 used a fluorescence spectroscopy to detect autofluorescence for differentiating yeast and bacterial cells [6]. The growth and stress responses of the yeast cells were monitored by observing autofluorescence using a fluorescence sensor [7]. However, there was a problem about an overlapping of fluorescence signals which are not able to be identified [8]. For this reason, 2D fluorescence spectroscopy or multi-wavelength fluorescence (MWF) spectroscopy was developed to solve the problem. It can simultaneously measure biogenic fluorophores in a wide range of excitation and emission wavelengths [9, 10]. It was applied in many fields with different microorganisms like *Saccharomyces cerevisiae*, *Claviceps purpurea*, *Streptomyces coelicolor*, and *Escherichia coli* [5, 11–14].

The advantage of using filters in a fluorescence spectroscopy is the lower cost than monochromators. According to Lakowicz 2006, filters are used often rather than monochromators when a known fluorophore's spectral properties has maximum sensitivity. However, using monochromators in a fluorescence sensor can give better spectral resolution than filters [15]. Another important equipment used with a fluorescence spectrometer is a light guide such as optical fibers, which are usually applied for transmitting light from the spectrometer to the object under investigation. The benefit for using optical fibers is that they can simultaneously transmit light of various wavelengths and also in different directions, which is a truly advantage for a 2D fluorescence spectroscopy. Additionally, optical fibers cannot be disturbed by electric and magnetic field; thus, they can give good spectral resolution in harsh locations. Moreover, they can be downsized at low cost. Nevertheless, there are some disadvantages of using optical fibers. For example, they can be interfered with ambient light, but it can be solved by using in the dark environment. Besides, there is feasible photobleaching if indicator phases are applied [16]. Basically, fluorescence sensors built with filters and optical fibers for remote monitoring are effective to detect fluorophores in many processes, such as biotechnological, chemical, food, and environmental processes. In our study, the 2D fluorescence spectroscopy equipped with filters and optical fibers were used for the experiments.

With on-line measuring by a 2D fluorescence sensor, multivariate data are obtained during the whole cultivation process; therefore, chemometric analysis is needed to get significant information out of the data. Chemometric models use statistical or mathematical methods for data analysis and prediction of a process. The chemometric methods can be described into three main parts, such as data preprocessing, qualitative spectral analysis, and

quantitative spectral analysis [17]. The pretreatment of spectral data is applied for reducing unnecessary data or noise in measurements. For example, one method required for fluorescence spectral data of cultivation processes is the technique of spectra subtraction. Due to complex media and metabolic changes, it is better to exclude the media background in order to see clearer changes of fluorescence intensities of processes [9, 17, 18]. Besides, it can reduce variability of batch-to-batch. Principal component analysis (PCA) is a qualitative method for data reduction and evaluation. Not all spectral data from measurements are important; thus, the only significant information is extracted by PCA. It will be described in an easier way like two or more dimensional space called score plots [17, 18]. Methods of quantitative spectral analysis are multiple linear regression (MLR), principal component regression (PCR), and partial least squares (PLS) regression. These methods create the relationship between properties of states variables (e.g., cell mass, substrates, and products) and on-line MWF data. PLS models are most widely used for multivariate data analysis. The purpose of this method is to determine a small number of latent variables or principal components, which can predict target concentrations by using the fluorescence spectra [17]. Presently, there are many publications about research on monitoring of bioprocesses with 2D fluorescence spectroscopy and chemometrics. For example, Haack et al. has done MWF spectroscopy for on-line cell mass monitoring of *S. cerevisiae* cultivations [5]. The 2D fluorescence spectroscopy was also applied for controlling *S. cerevisiae* fed-batch cultivations [14]. Recently, Ödman et al. has done the on-line estimation of biomass, glucose, and ethanol in *S. cerevisiae* cultivations by using 2D fluorescence sensors. The *C. purpurea* bioprocess was the first cultivation of fungi, which has been characterized by chemometric modeling with 2D fluorescence spectroscopy [11]. In addition, there are still others like *Pichia pastoris*, *E. coli*, and *S. coelicolor* which were also on-line monitored with 2D fluorescence sensors and analyzed by chemometric methods [4, 12, 19].

In this study, wavelength combinations (WLCs) or variables of MWF data have been selected which have significant and relevant information on the target substances, such as glucose, ethanol, and biomass of *S. cerevisiae* cultivations. Three methods are examined to choose important WLCs: a method based on loadings, variable importance in projection (VIP) [20], and ant colony optimization (ACO) [21]. Then the results of each approach were compared to have the most significant WLCs related to the important bioprocess variables (glucose, ethanol, and biomass). To have only important WLCs for building up a specific fluorescence sensor for the yeast cultivation would be a promising low-priced device.

**Material and methods**

**Strain and cultivation conditions**

*S. cerevisiae* (fresh baker's yeast, Oma's Ur-Hefe) was used for precultures. Ten grams of fresh baker's yeast was inoculated into 100 mL Schatzmann medium containing 0.34 g L<sup>-1</sup> MgSO<sub>4</sub>·7H<sub>2</sub>O, 0.42 g L<sup>-1</sup> CaCl<sub>2</sub>·2H<sub>2</sub>O, 4.5 g L<sup>-1</sup> (NH<sub>4</sub>)<sub>2</sub>SO<sub>4</sub>, 1.9 g L<sup>-1</sup> (NH<sub>4</sub>)<sub>2</sub>HPO<sub>4</sub>, 0.9 g L<sup>-1</sup> KCl, and 10 g L<sup>-1</sup> glucose [22]. The preculture was shaken for 10 min and then was added into a 3-L stainless steel tank bioreactor (Minifors, Inifors HT, Bottmingen, Switzerland) with a working volume of 1.35 L. The medium used for batch cultivations was the same as the preculture one, but with 1 ml L<sup>-1</sup> trace elements solution (0.015 g L<sup>-1</sup> FeCl<sub>3</sub>·6H<sub>2</sub>O, 9 mg L<sup>-1</sup> ZnSO<sub>4</sub>·7H<sub>2</sub>O, 10.5 mg L<sup>-1</sup> MnSO<sub>4</sub>·2H<sub>2</sub>O, and 2.4 mg L<sup>-1</sup> CuSO<sub>4</sub>·5H<sub>2</sub>O) and 1 ml L<sup>-1</sup> vitamin solution (0.06 g L<sup>-1</sup> myo-inositol, 0.03 g L<sup>-1</sup> Ca-pantothenate, 6 mg L<sup>-1</sup> thiamine HCl, 1.5 mg L<sup>-1</sup> pyridoxine HCl, and 0.03 mg L<sup>-1</sup> biotin). Five batches were operated at a constant temperature at 30 °C and the pH was maintained at 5. The aeration rate and stirrer speed were kept constant at 0.63 vvm (2.5 L min<sup>-1</sup>) and 350 rpm, respectively. Iris software (Inifors HT, Bottmingen, Switzerland) was applied as a process control system for the bioreactor.

**Off-line analysis**

Samples were regularly taken from the bioreactor and put into preweighed and predried microcentrifuge tubes. Cell dry weight (CDW) was determined by centrifugation (Universal 16 R, Hettich Zentrifugen GmbH & Co. KG, Tuttlingen, Germany) of a sample with 1.5 mL (2 times) at 12,000 rpm for 10 min. The samples without the supernatant were let in a drying oven at 103 °C for 24 h. Then they were cooled down for 30 min before weighing.

The supernatant of the samples after the centrifugation were examined by HPLC (ProStar, Variant, Walnut Creek, CA, USA) to determine the concentration of glucose and ethanol. The supernatant was firstly filtrated with pore size filter, 0.45 μm, polypropylene membrane (VWR, Darmstadt, Germany). Subsequently, it was injected 20 μL into a Rezex ROA-organic acid H+ (8 %) column (Phenomenex, Aschaffenburg, Germany) and operated at 70 °C with 5 mM H<sub>2</sub>SO<sub>4</sub> as an eluent at 0.6 mL min<sup>-1</sup> flow rate. The concentrations of glucose and ethanol were calculated by Software Galaxie™ Chromatography (Varian, Walnut Creek, CA, USA). As the number of sampling of the off-line data was lower than the number of measuring of the fluorescence spectra during the cultivation, the theoretical models (Eqs. 1–5) were used to fit to the off-line data, e.g., glucose, ethanol, and cell dry mass,

by using the particle swarm optimization algorithm for estimation [23, 24].

$$\frac{dX}{dt} = \mu_G X + \mu_E X \tag{1}$$

$$\frac{dG}{dt} = -\frac{\mu_G X}{Y_{X/G}} \tag{2}$$

$$\frac{dE}{dt} = \frac{\mu_G X}{Y_{E/G}} - \frac{\mu_E X}{Y_{X/E}} \tag{3}$$

$$\mu_G = \begin{cases} 0 & G = 0 \\ \mu_{G0} & G > 0 \end{cases} \tag{4}$$

$$\mu_E = \begin{cases} 0 & G > 0 \\ \mu_{E0} & G = 0 \end{cases} \tag{5}$$

where *X*, *G*, and *E* are cell mass, glucose, and ethanol concentrations, respectively.  $\mu_G$  and  $\mu_E$  are the specific growth rates on glucose and ethanol, respectively.  $Y_{X/G}$ ,  $Y_{E/G}$ , and  $Y_{X/E}$  are the yield coefficients for glucose with respect to biomass and ethanol and ethanol phase with respect to biomass.

**On-line analysis/2D fluorescence spectroscopy**

The exhaust gas like carbon dioxide (CO<sub>2</sub>) and oxygen (O<sub>2</sub>) was monitored continuously with BlueInOne Cell Sensor (BlueSense gas sensor GmbH, Herten, Germany). During the batch cultivation, it was on-line observed by BlueVis software (BlueSense gas sensor GmbH, Herten, Germany).

A BioView fluorescence spectrometer (DELTA Lights & Optics, Hørsholm, Denmark) was used for measuring multi-wavelength culture fluorescence of the yeast cultivations in range of 270–550 nm excitation (ex) and 310–590 nm emission (em). With increment of 20 nm of these excitation and emission ranges, altogether, there are 120 fluorescence intensity values of WLCs; scattered light is not considered here. The typical bandwidth of a filter is 20 nm. The BioView fluorescence sensor has a xenon flash lamp as a light source for excitation and is equipped with 16 different filters for excitation and emission wavelengths. The excitation light goes via the fiber optic as a guide light into the bioreactor and the fluorescent light, which is emitted in a 180° angle, is monitored after passing the emission filters. Then the emission light is detected by a photomultiplier. The procedure runs continuously until a complete rotation of excitation and emission filters. For the non-invasive monitoring, the fluorescence sensor measured the culture through a quartz window in 25 mm standard port. The measurement for a single scan of the spectrum was performed with in 90 s. The spectrum of one time scanning contains the combinations of excitation and emission wavelengths, which are 120 intensity values of WLCs, and is presented below.

**Selection methods of wavelength combinations**

*A method based on loadings*

The first fluorescence spectrum of each batch after inoculation was subtracted from the following spectra [11, 13]. The resulting spectral data of the five batches were separately operated by PCA with the Unscrambler X® software (Camo, Norway). The loading in PCA represents the projection of the data matrix in the intensity of WLCs on the principal components (PCs). The magnitude of the loading vectors related to the considered PC is an important measure of a WLC for the PC model. Loadings near the center of the coordinate system represent insignificant feature variables. The positive and negative signs of loadings do not indicate high or low, but they indicate directions of the loading vectors. In the method based on loadings, the WLCs with the largest size of loadings on the first three PCs were chosen from each cultivation [25–27].

*VIP*

Variable importance in projection (VIP) technique was used for variable selection [20, 28, 29]. The VIP score on each variable depends on the explained variance of each PLS component which is  $(\mathbf{w}_{ak}/\|\mathbf{w}_a\|^2)$ . The WLC should be taken when threshold of VIP score is more than 1 because the variable is highly influential on the target samples.

$$VIP_k = \sqrt{p \sum_{a=1}^A \left[ (q_a^2 t_a^2) \left( \frac{w_{ak}}{\|\mathbf{w}_a\|^2} \right)^2 \right]} / \sum_{a=1}^A (q_a^2 t_a^2) \tag{6}$$

where  $a$  is a subscription index,  $A$  is the number of latent variables in PLS,  $p$  is the number of different intensity values of the WLCs,  $w_{ak}$  is the loading weight of the  $k^{\text{th}}$  variable in the  $a^{\text{th}}$  component,  $\|\mathbf{w}_a\|$  is the norm of matrix  $\mathbf{w}_a$  and  $\mathbf{t}_a$ ,  $\mathbf{w}_a$ , and  $\mathbf{q}_a$  are the  $a$ th column vectors of  $\mathbf{T}$  (scores of the independent variable matrix),  $\mathbf{W}$  (weight matrix), and  $\mathbf{Q}$  (loading of the dependent variable matrix), respectively [28, 29].

The subtraction spectra with 120 WLCs and the off-line data, e.g., glucose, ethanol, and biomass, from the five batches were firstly operated together with MATLAB PLS Toolbox (MATLAB R2014a) [28]. According to PLS regression,  $\mathbf{T}$ ,  $\mathbf{Q}$ , and  $\mathbf{W}$  were received to be calculated for the VIP score using Eq. 6 to find the important WLCs on each sample. The VIP calculation in Eq. 6 was implemented in MATLAB VIP Toolbox [20].

*ACO*

ACO is a meta-heuristic algorithm, which is characterized from the real ants' behavior. Ants always find a short path between the nest and a food source with the help of pheromone. A typical ACO is based on the accumulation of information in the form of the deposition of pheromone trails. This algorithm was applied for wavelength selection to find the important variables relevant to the estimation of sample concentrations [21, 30]. According to Ranzan et al. 2014, the ACO implementation for the selection of spectrum components used a random factor related to a pheromone density function. Pheromone was deposited on spectrum components by ants as a function of residual error between prediction and measurement [30]. The integration of ACO with multivariate models works in the way that a colony was firstly constructed and then each ant in the colony was evaluated by one method of the multivariate models, such as PLS, PCR, and inverse least squares [21, 31].

The subtraction spectra (120 WLCs) of the five batches with their off-line data were operated by the ACO-based algorithm with PLS regression model (ACO-PLS) in MATLAB with the source code from Ranzan et al. [30]. With this math tool, the spectral data were firstly preprocessed with mean normalization and subsequently run the ACO-PLS (conditions: 120 input variables, 50 iterations, 100 ants,  $10^{-6}$  initial concentration of the pheromone trail, 0.5 evaporation rate of pheromone per trail, and 15 PCs).

**Chemometric analysis and modeling**

*PCA*

According to large data set of on-line MWF data, PCA was used to visualize the best possible data structure. It helps to find out how relationships between objects and features are. The important purpose to use PCA is to quantify the amount of useful information and take out noise which is contained in the data. The process of PCA is to find a direction that carries the most information of the whole data. The direction containing the most of the variance of the data is called the first PC. The second PC carries the maximum variance of the rest data and so on. These PCs are statistically unrelated from each other [25, 26]. The subtraction fluorescence spectra of the five cultivations were used to calculate PCA separately (conditions: mean centering and NIPALS algorithm) by Unscrambler X® software.

The PCs were computed with the fluorescence intensity in each spectrum and the values of the loading vector. To clarify which combinations of excitation and emission wavelengths are significantly related to the considered PC, the percentage sensitivity was calculated using Eq. 7. Firstly, the calculation of the original PC was done by using the data of one measured

spectrum and the loading. Afterwards, one value in this measured spectrum (carrying 120 values in the WLCs) was multiplied by a constant number, i.e., 1.1 and the new PC (=PC') was calculated by the changed spectrum using the original loading. With the new and original PC, the sensitivity can be determined using Eq. 7. From the sensitivity calculation, one can see how the changed intensity value at the WLC effects the considered PC. Therefore, each value of 120 WLCs was changed one by one for computing the new PC to see how every fluorescence intensity value influence the PC.

$$\text{Sensitivity}[\%] = \frac{|\text{PC}-\text{PC}'| \times 100 \%}{\text{PC}} \quad (7)$$

**MLR**

MLR is a regression model to analyze the correlation between dependent and independent variables. The method is based on ordinary least squares regression and the operation of the regression coefficients involves a matrix inversion. Thus, it will bring to the collinearity problems if the predictor variables are linearly dependent [25, 26]. According to the small number of selected WLCs from each selection method, MLR was used to run the models to predict glucose, ethanol, and biomass concentrations by Unscrambler X® software. The leave-one-out cross validation was proceeded for a total of five batches. It means the four batches were run by MLR as a calibration model and the one left was run for a validation set to test the model. To evaluate the calibration and prediction errors of the models, the root mean square error of calibration and prediction (RMSEC/P) was calculated using predicted and measured values (Eq. 8). Additionally, the percentage of the root mean square error of prediction (pRMSEP) was calculated using Eq. 9. The pRMSEPs of the MLR models were compared to get the most significant WLCs relevant to the sample properties.

$$\text{RMSEC/P} = \sqrt{\frac{\sum_{i=1}^n (y'_{i,\text{model}} - y_i)^2}{n}} \quad (8)$$

$$\text{pRMSECP}[\%] = \frac{\text{RMSEP} \times 100}{\max y_{\text{measured}}} \quad (9)$$

where  $y'_i$  is the predicted value of the target analyte for the object  $i$ ,  $y_i$  is the measured value for the object  $i$ ,  $n$  is the number of sample data, and  $\max y_{\text{measured}}$  is the maximum value of the measured off-line data.

**PLS**

The subtraction spectra with all 120 WLCs and the off-line data of the five cultivations were modeled by PLS-1

(Unscrambler X® software, conditions: mean centering, NIPALS algorithm, random segmented cross validation, and 7 PCs). All of the five batches were run in the same procedure as MLR modeling (as mentioned above). For the evaluation of models, RMSEC/P and pRMSEP were calculated as in Eqs. 8 and 9.

For the most significant selected WLCs evaluated by the MLR model, their excitation and emission wavelengths were considered to combine each other for the other possible combinations of wavelengths. For example, if there are two selected WLCs, e.g., ex270/em450 and ex330/em390, the other possible combinations can be ex270/em390 and ex330/em450 for a fluorescence measurement. Thus, there are basically four possible WLCs, which can be used for measuring in the fluorescence sensor. PLS (Unscrambler X® software) was used to create models with the all possible combinations from the most significant selected WLCs and the offline-data. The procedure of the modeling and evaluation was the same as mentioned in the MLR part.

**Results and discussion**

**Characteristics of the cultivations**

The time for running each batch was 9 h as shown in Fig. 1. In the yeast batch cultivation, it contained glucose and ethanol growth phases which have been previously observed by Locher et al. [32]. In Fig. 1, while the glucose was decreasing during the exponential growth, the products, e.g., ethanol and biomass were increasing. At around 2.5 h, the glucose run out and the phase shifted to the ethanol phase. During the decrease of ethanol concentration, the biomass was exponentially increasing.

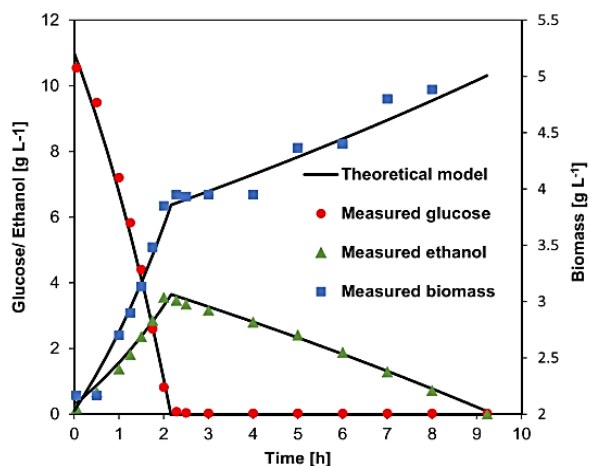
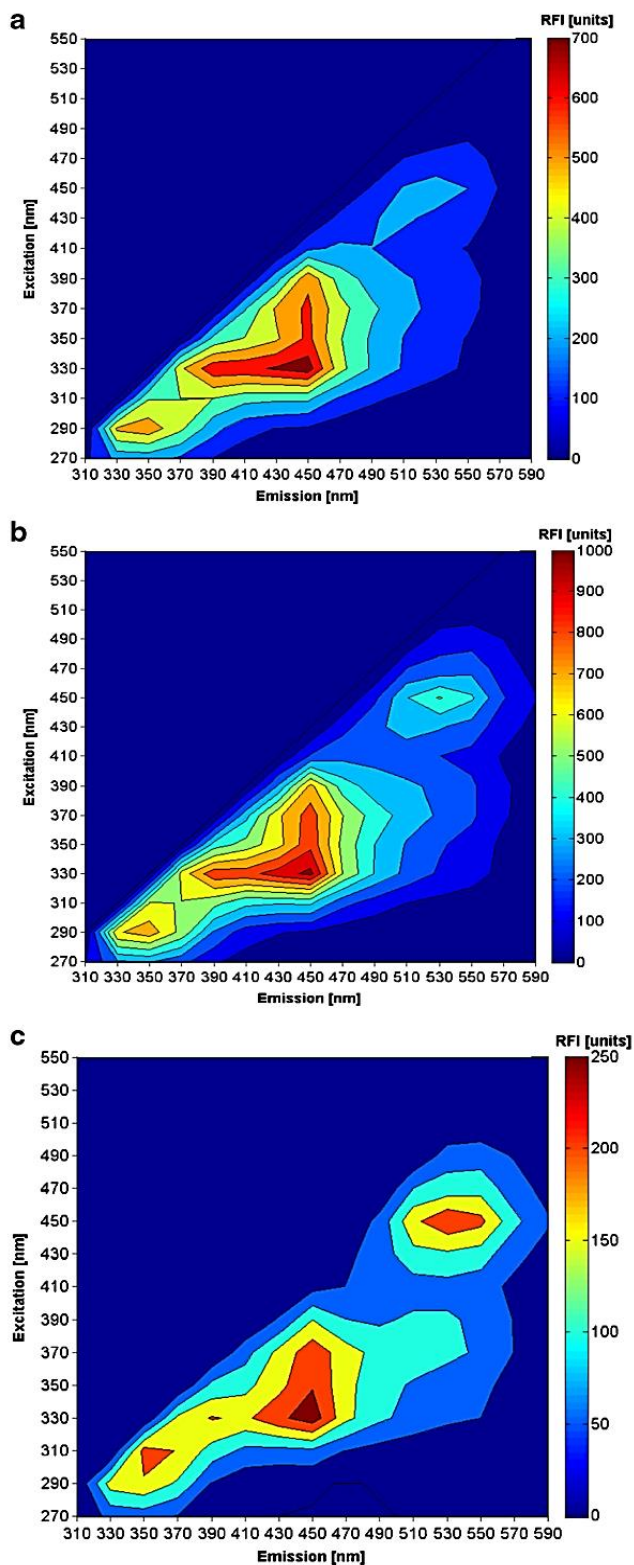


**Fig. 1** The characteristics of the yeast batch cultivation with 10 g L<sup>-1</sup> starting glucose and the theoretical models of the yeast cultivation for glucose, ethanol, and biomass concentrations

**Fig. 2** The fluorescence spectra during the yeast cultivation which clearly show the peak regions of tryptophan (ex290/em350), pyridoxine (ex330/em390), NAD(P)H (ex330, 350/em450), and riboflavin, FMN, FAD (ex450/em530). **a** The spectrum during a glucose phase. **b** The spectrum during an ethanol phase. **c** The difference spectrum of (a) and (b). *RFI* relative fluorescence intensity





The growth parameters were obtained from the theoretical models fitted to the experimental data. Between each batch, the values of parameters had no significant difference (data not shown). The results of the five batches were reproducible. The specific growth rate during the glucose phase was  $0.30 \pm 0.02 \text{ h}^{-1}$  which is higher compared to the ethanol phase ( $0.04 \pm 0.01 \text{ h}^{-1}$ ). During the glucose phase,  $Y_{E/G}$  ( $0.57 \pm 0.03 \text{ g}_{\text{ethanol}} \text{ g}_{\text{glucose}}^{-1}$ ) is higher than,  $Y_{X/G}$  ( $0.18 \pm 0.01 \text{ g}_{\text{biomass}} \text{ g}_{\text{glucose}}^{-1}$ ) as shown in Fig. 1. During the ethanol phase,  $Y_{X/E}$  is  $0.32 \pm 0.09 \text{ g}_{\text{biomass}} \text{ g}_{\text{ethanol}}^{-1}$ . The values of the parameters of the yeast batch cultivations were similar to other studies like Odman et al. [13] and Solle et al. [23].

### On-line fluorescence spectra

The range of the measured fluorescence spectra, as mentioned in the materials and methods part, covers the area of the autofluorescence of the yeast cells. In Fig. 2a, b, the fluorescence spectra of the yeast cultivation during the glucose and ethanol phases are presented. The peak of the protein, cofactor, and vitamin regions were evidently seen, such as tryptophan (ex290/em350), pyridoxine (ex330/em390), NAD(P)H (ex330, 350/em450), and riboflavin, FMN, FAD (ex450/em530) (Fig. 2). In Fig. 2c, it can be observed that the fluorescence intensity in the area of tryptophan, pyridoxine, NAD(P)H, and riboflavin increased from the glucose phase to the ethanol phase. It means that these biogenic fluorophores are related to the yeast growth. Podrazky et al. demonstrated that the autofluorescence of yeast cells can be used to monitor the growth and stress responses of yeast cells [7].

### PCA of the on-line fluorescence data

The fluorescence spectral data from all five batch runs were explored by using PCA to understand the state of the cultivation. For 9 h of running one batch, the sample points were

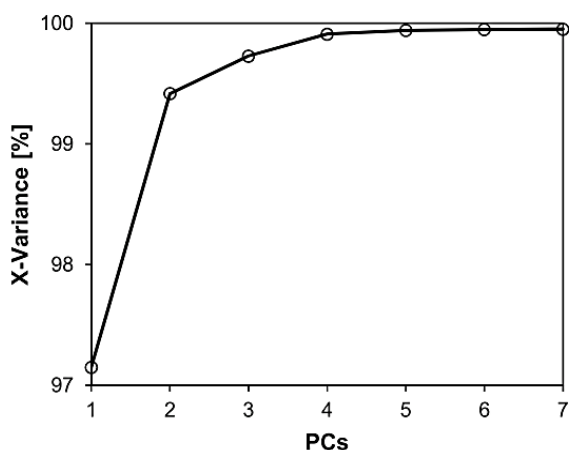


Fig. 3 The explained variance from the batch cultivation by PCA

around 400–430 with 120 variables, a spectral data matrix  $[430 \times 120]$ . The results from PCA modeling consisted of important first three PCs which carried the relevant data of fermentations as shown in Fig. 3. The first PC (PC1) contained the variances which was 97.2 % (Fig. 3). For PC2 and PC3, there were 2.3 and 0.3 %, respectively. According to the observation from the score plots (PC1 vs. PC3) of the five batches, the trajectory of each batch was nearly the same (data not shown). Additionally, the trajectory of the score plot (PC1

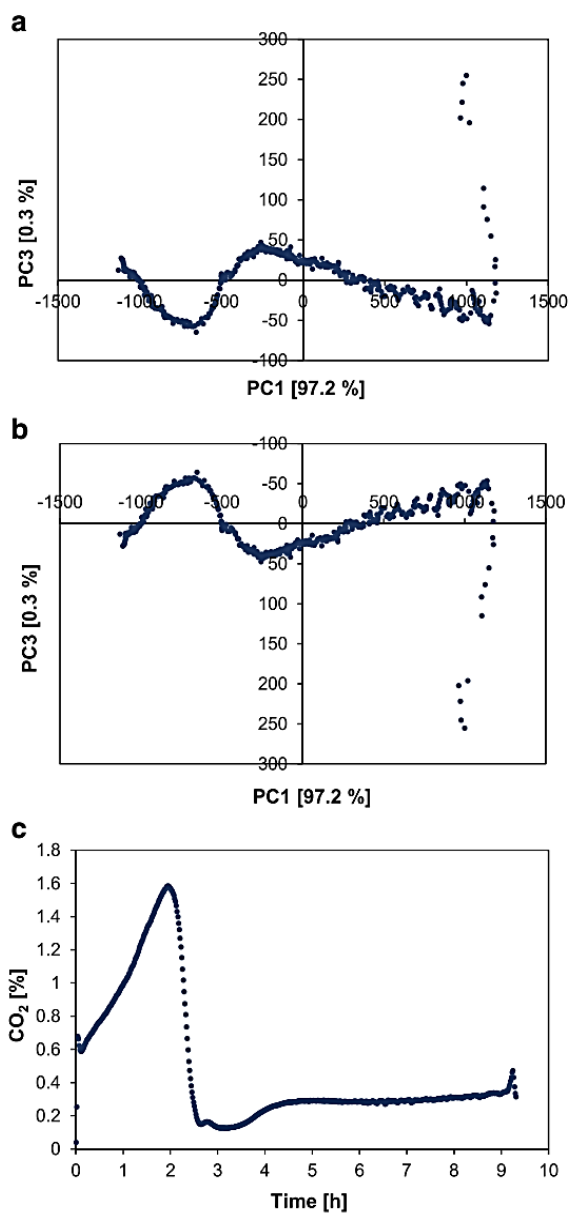


Fig. 4 a A score plot from the yeast batch cultivation by running PCA. b A reversed score plot from (a). c A CO<sub>2</sub> off-gas graph from the yeast cultivation

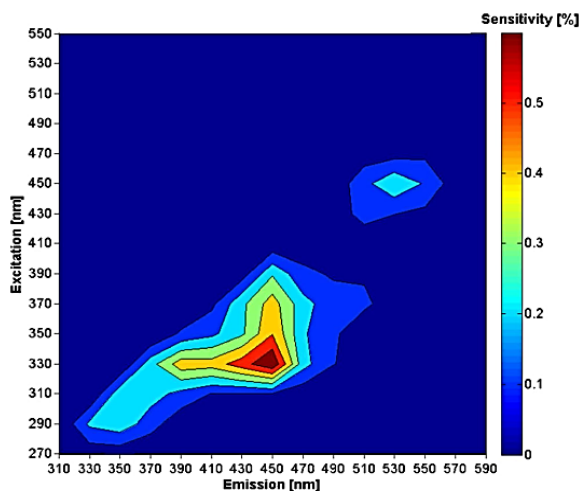


Fig. 5 The sensitivity plot of the fluorescence region in the first PC

vs. PC3) is recognized like the CO<sub>2</sub> off-gas graph, particularly the reversed score plot as shown in Fig. 4a–c.

According to the sensitivity calculation (Fig. 5), it can be obviously seen that in the first PC, the fluorescence area of tryptophan, pyridoxine, NAD(P)H, and riboflavin has the strong sensitivity. From the result, the areas in the spectrum corresponding to these biogenic fluorophores play a significant role to the first PC.

**The selected WLCs by the three selection methods**

Although we know the important area of the fluorescence spectra which effects significantly on the yeast growth, there are still many variables (WLCs) in these areas and all of them might be not specific on every state variable. Therefore, the methods of selection variables are needed. To receive the more information from the fluorescence data, the variables with the magnitude of the elements of the loading vectors are considered [12, 27]. Guo et al. 2002 [27] showed the high consensus by the PC loading for a feature selection method. With the method based on loadings, there were simply five different

WLCs selected for the three analytes as shown in Table 1. These five WLCs are in the important spectral regions which are correlated to the metabolism of the yeast growth like NAD(P)H (ex330/em450 and ex350/em450), tryptophan (ex290/em350), riboflavin, FMN, FAD (ex450/em530), and pyridoxine (ex330/em390) [9]. Each biogenic fluorophore plays the different role in the yeast growth, so it means that they are correlated to the different sample properties. Horvath et al. showed that tryptophan had a better correlation to cell mass than NAD(P)H [33]. The changes of the NAD(P)H and flavins (FAD and FMN) concentrations have a correlation to the metabolism changes from the oxidative to oxidoreductive [14]. Therefore, these selected WLCs seem to carry the relevant information to predict the glucose, ethanol, and biomass concentrations. Although it is promising that they have correlations to the yeast metabolism, they had to be validated by MLR modeling.

The VIP and ACO methods chose WLCs relevant to a particular sample from all 120 WLCs, which is not like the method based on loadings that can select only the same set of WLCs for all three process variables. Therefore, these two methods might be more advantageous because multivariate prediction models should be built from variables containing high-quality analyte-specific information [34]. For the VIP method, the first five WLCs with the highest VIP scores were selected (Table 1). Some of the chosen WLCs by VIP are also in the area of NAD(P)H, riboflavin, FMN, FAD, and pyridoxine. However, the selected WLCs were not exactly the same as the selected ones by the method based on loadings. The ACO method selected the first five highest pheromone concentrations on WLCs (Table 1). Some of the five selected WLCs by ACO are also in the important yeast metabolism area like NAD(P)H, pyridoxine, and riboflavin. Even though there are some selected WLCs of the three methods identical, it is not easy to decide which set of the five selected WLCs from which method is the most relevant to the sample properties. For this reason, each set of the five selected WLCs of the analytes was further modeled by MLR.

**Table 1** Five selected WLCs by the method based on loadings, VIP, and ACO

Selection method	Analyte	Selected WLCs (excitation/emission)				
PC loadings	Glucose	290/350	330/390	330/450	350/450	450/530
	Ethanol					
	Biomass					
VIP	Glucose	270/310	270/350	330/390	330/450	390/450
	Ethanol	270/350	330/450	350/450	450/530	450/550
	Biomass	330/430	330/450	350/450	370/450	450/530
ACO	Glucose	270/350	270/370	270/390	290/330	310/350
	Ethanol	270/350	270/370	310/350	330/490	370/530
	Biomass	270/430	270/450	310/350	310/370	310/390

**Table 2** MLR models with different sets of five selected WLCs from the three selection methods

Selection method	Analyte	RMSEP (g L <sup>-1</sup> )	R <sup>2</sup> <sub>PredModel</sub>	pRMSEP (%)
PC loadings	Glucose	0.32 ± 0.05	0.99 ± 0.00	3.2
	Ethanol (GP)	0.22 ± 0.03	0.97 ± 0.01	6.3
	Ethanol (EP)	0.20 ± 0.05	0.96 ± 0.02	6.2
	Biomass (GP)	0.25 ± 0.10	0.93 ± 0.05	6.9
	Biomass (EP)	0.29 ± 0.07	0.79 ± 0.12	6.3
VIP	Glucose	0.40 ± 0.14	0.98 ± 0.01	3.9
	Ethanol (GP)	0.25 ± 0.06	0.96 ± 0.02	7.3
	Ethanol (EP)	0.28 ± 0.10	0.90 ± 0.11	8.7
	Biomass (GP)	0.22 ± 0.07	0.95 ± 0.03	6.0
	Biomass (EP)	0.18 ± 0.04	0.92 ± 0.02	3.9
ACO	Glucose	0.44 ± 0.11	0.98 ± 0.01	3.6
	Ethanol (GP)	0.22 ± 0.03	0.97 ± 0.01	5.2
	Ethanol (EP)	0.25 ± 0.11	0.94 ± 0.04	6.2
	Biomass (GP)	0.20 ± 0.08	0.96 ± 0.03	4.4
	Biomass (EP)	0.19 ± 0.09	0.90 ± 0.08	3.4

The values in the table are mean value ± standard deviation

GP glucose phase, EP ethanol phase, CalModel calibration model, PredModel prediction model

### Modeling using 120 WLCs of the fluorescence spectra

The 120 variables of subtraction fluorescence spectra and simulated data by the theoretical models fitted to the off-line data were modeled by PLS. The results of the models, i.e., PCs, RMSEC/Ps, and R<sup>2</sup> were calculated for the mean values, as shown in Table 3. These PLS models for glucose, ethanol, and biomass concentrations were separately modeled with the optimum number of PCs in the glucose and ethanol phases. The number of PCs influences on the effectiveness of modeling. When the numbers of them are too small, there is not adequate information to make a good model. On the contrary, if there are

many PCs, the model will be overfitting and less robust [12]. For the PLS models of glucose and ethanol in the glucose phase, the optimum number of PCs was only one used for creating the models. However, the results of the calibration models had the low RMSEC and high coefficient of determination (R<sup>2</sup><sub>CalModel</sub>) values. It showed that the first PC contained sufficient significant information to glucose and ethanol concentrations (in GP). Basically, RMSEC shows how good a calibration model fits to the measured data. For the low RMSEC and high R<sup>2</sup><sub>CalModel</sub> values of other models (Table 3), it also showed that the models using all 120 WLCs of fluorescence spectra provided a good fit to the measured data. The coefficient of

**Table 3** PLS models for glucose, ethanol, and biomass concentrations using all 120 WLCs and the possible 38 WLCs from the selected WLCs

Model	Analyte	Mean PCs	RMSEC (g L <sup>-1</sup> )	R <sup>2</sup> <sub>CalModel</sub>	RMSEP (g L <sup>-1</sup> )	R <sup>2</sup> <sub>PredModel</sub>	pRMSEP (%)
PLS	Glucose	1.0 ± 0.0	0.34 ± 0.02	0.99 ± 0.00	0.32 ± 0.14	0.99 ± 0.01	3.2
	Ethanol (GP)	1.0 ± 0.0	0.14 ± 0.02	0.98 ± 0.01	0.22 ± 0.04	0.97 ± 0.01	6.4
	Ethanol (EP)	2.6 ± 0.8	0.14 ± 0.02	0.98 ± 0.01	0.22 ± 0.07	0.95 ± 0.03	6.7
	Biomass (GP)	2.6 ± 1.0	0.08 ± 0.01	0.98 ± 0.00	0.19 ± 0.07	0.96 ± 0.02	5.2
	Biomass (EP)	4.0 ± 0.0	0.07 ± 0.00	0.97 ± 0.00	0.24 ± 0.07	0.85 ± 0.09	5.0
PLS*	Glucose	2.0 ± 0.0	0.31 ± 0.00	0.99 ± 0.02	0.32 ± 0.16	0.99 ± 0.01	3.1
	Ethanol (GP)	1.8 ± 0.4	0.13 ± 0.01	0.98 ± 0.00	0.22 ± 0.03	0.97 ± 0.01	6.3
	Ethanol (EP)	2.8 ± 0.4	0.14 ± 0.00	0.98 ± 0.02	0.18 ± 0.05	0.97 ± 0.01	5.4
	Biomass (GP)	3.0 ± 0.9	0.08 ± 0.00	0.98 ± 0.01	0.20 ± 0.08	0.95 ± 0.03	5.4
	Biomass (EP)	4.4 ± 0.8	0.07 ± 0.00	0.97 ± 0.01	0.22 ± 0.07	0.87 ± 0.08	4.7

PLS\* the PLS models using 38 WLCs

determination in the prediction models ( $R^2_{\text{PredModel}}$ ) of glucose concentration was indeed high. For the prediction of ethanol and biomass concentrations, the  $R^2_{\text{PredModel}}$  were also relatively high, but the prediction model of biomass in EP had  $R^2_{\text{PredModel}}$  lower than others. The models to predict glucose, ethanol, and biomass concentrations in GP had pRMSEPs of 3.2, 6.4, and 5.2 %, respectively. For ethanol and biomass concentrations in EP, pRMSEPs were 6.7 and 5.0 %, respectively (as shown in Table 3). With the low pRMSEP and high  $R^2_{\text{PredModel}}$  values, the models had good statistical power to predict the glucose, ethanol, and biomass concentrations.

### Modeling using the significant selected WLCs

According to the small number of selected WLCs of each selection method, MLR was applied for creating models to predict the process variables. The prediction models of analytes were also separately modeled during the glucose and ethanol phases. The results can be seen in Table 2. The RMSEPs of the MLR models for the three analytes were analyzed of significant differences using *t* test. However, no significant difference could be detected. Thus, it means that the selected WLCs from the three selection methods do not show significant difference. According to the low RMSEP and high  $R^2_{\text{PredModel}}$  as shown in Table 2, the three selection methods can effectively choose the important variables in the yeast cultivation process. In each method, some WLCs are contained, which are in the same area (or almost in the same area), such as NAD(P)H, tryptophan, and riboflavin region as presented in Table 1. Therefore, the selected WLCs carry the information relevant to three analyte concentrations.

From the all significant selected WLCs, there were 7 different excitation wavelengths (e.g., 270, 290, 310, 330, 350, 370, and 450 nm) and 7 emission wavelengths (e.g., 350, 370, 390, 430, 450, 490, and 530 nm). These different excitation and emission wavelengths are able to be combined each other for having 38 WLCs. To use these 38 WLCs, PLS models were calculated to predict the process variables.

The RMSEC values and  $R^2_{\text{CalModel}}$  of the PLS models with all 120 variables and the PLS models with 38 WLCs (Table 3) were similar to each other. For the prediction models, the pRMSEPs and  $R^2_{\text{PredModel}}$  showed no significant difference (based on *t* test). The pRMSEPs of the PLS models with the 38 WLCs for the glucose, ethanol, and biomass prediction (in GP and EP) were in the range of 3.1–6.3 %, as shown in Table 3. In Fig. 6, the PLS predicted concentrations as well as the measured ones are presented. With 120 WLCs, 32 filters are used. For the measure of the 38 WLCs, only 14 filters are applied. Thus, the specific fluorescence sensor for the yeast

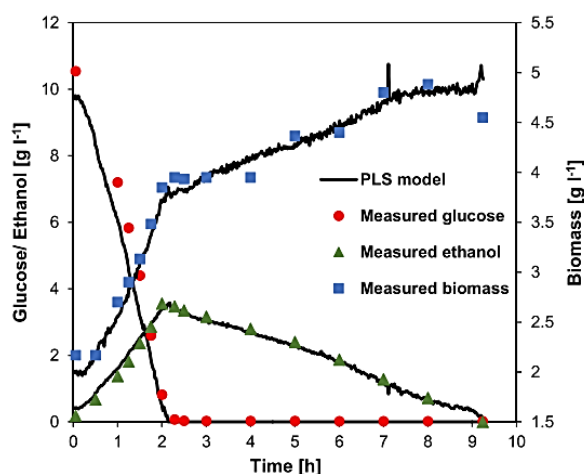


Fig. 6 Correlation between PLS predicted data from the 38 WLCs and the measured off-line data

cultivation could be built with only a small amount of filters, which would be an inexpensive device.

### Conclusions

In this study, a comparison of three methods for selecting relevant and important wavelength combinations is presented, such as a method based on loadings, VIP, and ACO. The selected WLCs from these three methods were modeled by MLR and evaluated with the RMSEP and  $R^2$ . From the results, the five selected WLCs from the three selection methods had a good predictive performance on glucose, ethanol, and biomass concentrations. All three selection methods performed in a good way. It could be because these three methods have chosen the WLCs, mostly in the same regions of the biogenic fluorophores, which are related to the yeast metabolism, such as NAD(P)H, tryptophan, pyridoxine, and riboflavins. When the computing time of each process is considered, the calculating process of the method based on loadings and VIP spend less time than ACO. As the computing process in ACO, it has to be done with many iterations. With 7 filters for excitation and emission wavelengths, there were 38 possible WLCs. The PLS models with 120 as well as 38 WLCs were calculated. The results of their pRMSEPs had no significant difference. Thus, it is promising to build a specific economical fluorescence sensor using light-emitting diodes and photodiodes for the yeast cultivation process.

**Compliance with ethical standards** The research does not contain any studies with human participants or animals performed by any of the authors. Written informed consent was obtained from all individual participants included in the study.

**Conflict of interest** The authors declare that they have no conflict of interest.

References

1. Junker BH, Wang HY. Bioprocess monitoring and computer control: key roots of the current PAT initiative. *Biotechnol Bioeng.* 2006;95(2):226–61.
2. Eliasson C, Macleod NA, Jayes LC, Clarke FC, Hammond SV, Smith MR, et al. Non-invasive quantitative assessment of the content of pharmaceutical capsules using transmission Raman spectroscopy. *J Pharm Biomed Anal.* 2008;47(2):221–9.
3. Sarragaça MC, Paulo A, Alves MM, Dias AMA, Lopes JA, Ferreira EC. Quantitative monitoring of an activated sludge reactor using on-line UV-visible and near-infrared spectroscopy. *Anal Bioanal Chem.* 2009;395(4):1159–66.
4. Odman P, Johansen CL, Olsson L, Germaey KV, Lantz AE. Sensor combination and chemometric variable selection for online monitoring of *Streptomyces coelicolor* fed-batch cultivations. *Appl Microbiol Biotechnol.* 2010;86(6):1745–59.
5. Haack MB, Eliasson A, Olsson L. On-line cell mass monitoring of *Saccharomyces cerevisiae* cultivations by multi-wavelength fluorescence. *J Biotechnol.* 2004;114(1–2):199–208.
6. Bhatta H, Goldys EM, Learmonth RP. Use of fluorescence spectroscopy to differentiate yeast and bacterial cells. *Appl Microbiol Biotechnol.* 2006;71(1):121–6.
7. Podrazky O, Kuncova G, Krasowska A, Sigler K. Monitoring the growth and stress responses of yeast cells by two-dimensional fluorescence spectroscopy: first results. *Folia Microbiol.* 2003;48:189–92.
8. Scheper T, Schügerl K. Characterization of bioreactors by in-situ fluorometry. *J Biotechnol.* 1986;3:221–9.
9. Marose S, Lindemann C, Scheper T. Two-dimensional fluorescence spectroscopy: a new tool for on-line bioprocess monitoring. *Biotechnol Prog.* 1998;14(1):63–74.
10. Lindemann C, Marose S, Nielsen H, Scheper T. 2-dimensional fluorescence spectroscopy for on-line bioprocess monitoring. *Sens Actuators B Chem.* 1998;51(1–3):273–7.
11. Boehl D, Solle D, Hitzmann B, Scheper T. Chemometric modelling with two-dimensional fluorescence data for *Claviceps purpurea* bioprocess characterization. *J Biotechnol.* 2003;105(1–2):179–88.
12. Rhee JI, Kang T. On-line process monitoring and chemometric modeling with 2D fluorescence spectra obtained in recombinant *E. coli* fermentations. *Process Biochem.* 2007;42(7):1124–34.
13. Odman P, Johansen CL, Olsson L, Germaey KV, Lantz AE. On-line estimation of biomass, glucose and ethanol in *Saccharomyces cerevisiae* cultivations using in-situ multi-wavelength fluorescence and software sensors. *J Biotechnol.* 2009;144(2):102–12.
14. Hantelmann K, Kollecker M, Hüll D, Hitzmann B, Scheper T. Two-dimensional fluorescence spectroscopy: a novel approach for controlling fed-batch cultivations. *J Biotechnol.* 2006;121(3):410–7.
15. Lakowicz JR (ed). *Principles of fluorescence spectroscopy [Instrumentation for Fluorescence Spectroscopy]*; 2006.
16. Marazuela D, Moreno-Bondi MC. Fiber-optic biosensors—an overview. *Anal Bioanal Chem.* 2002;372(5–6):664–82.
17. Lourenço ND, Lopes JA, Almeida CF, Sarragaça MC, Pinheiro HM. Bioreactor monitoring with spectroscopy and chemometrics: a review. *Anal Bioanal Chem.* 2012;404(4):1211–37.
18. Faassen SM, Hitzmann B. Fluorescence spectroscopy and chemometric modeling for bioprocess monitoring. *Sensors (Basel).* 2015;15(5):10271–91.
19. Surribas A, Geissler D, Gierse A, Scheper T, Hitzmann B, Montesinos JL, et al. State variables monitoring by in situ multi-wavelength fluorescence spectroscopy in heterologous protein production by *Pichia pastoris*. *J Biotechnol.* 2006;124(2):412–9.
20. Mehmood T, Liland KH, Snipen L, Sæbø S. A review of variable selection methods in partial least squares regression. *Chemom Intell Lab Syst.* 2012;118:62–9.
21. Shamsipur M, Zare-Shahabadi V, Hemmateenejad B, Akhond M. Ant colony optimisation: a powerful tool for wavelength selection. *J Chemometr.* 2006;20(3–4):146–57.
22. Schatzmann H. *Anaerobes Wachstum von Saccharomyces cerevisiae*. Dissertation, ETH Zürich No.5504 1975.
23. Solle D, Geissler D, Stärk E, Scheper T, Hitzmann B. Chemometric modelling based on 2D-fluorescence spectra without a calibration measurement. *Bioinformatics.* 2003;19(2):173–7.
24. Grote B, Jinu MJ, Hitzmann B. Erschließen von Prozesswissen für das Monitoring und die Regelung von Fermentationsprozessen. *Systeme und Anwendungen der Messtechnik.* 2011;78(12):569–78.
25. CAMO Process AS. *The Unscrambler tutorials 2006*.
26. Otto, M. *Chemometrics: statistics and computer application in analytical chemistry*. WILEY-VCH; 1999.
27. Guo Q, Wu W, Massart D, Boucon C, de Jong S. Feature selection in principal component analysis of analytical data. *Chemom Intell Lab Syst.* 2002;61(1–2):123–32.
28. Wold S, Sjostrom M, Eriksson L. PLS-regression: a basic tool of chemometrics. *Chemom Intell Lab Syst.* 2001;58:109–30.
29. Gosselin R, Rodrigue D, Duchesne C. A bootstrap-VIP approach for selecting wavelength intervals in spectral imaging applications. *Chemom Intell Lab Syst.* 2010;100(1):12–21.
30. Ranzan C, Strohm A, Ranzan L, Trierweiler LF, Hitzmann B, Trierweiler JO. Wheat flour characterization using NIR and spectral filter based on ant colony optimization. *Chemom Intell Lab Syst.* 2014;132:133–40.
31. Allegrini F, Olivieri AC. A new and efficient variable selection algorithm based on ant colony optimization. Applications to near infrared spectroscopy/partial least-squares analysis. *Anal Chim Acta.* 2011;699(1):18–25.
32. Locher G, Hahnemann U, Sonnleitner B, Fiechter A. Automatic bioprocess control. 4. A prototype batch of *Saccharomyces cerevisiae*. *J Biotechnol.* 1993;29(1–2):57–74.
33. Horvath JJ, Glazier SS, Spangler CJ. In situ fluorescence cell mass measurements of *Saccharomyces cerevisiae* using cellular tryptophan. *Biotechnol Prog.* 1993;9:666–70.
34. Swierenga H, Wülfert F, de Noord OE, de Weijer AP, Smilde AK, Buydens L. Development of robust calibration models in near infrared spectrometric applications. *Anal Chim Acta.* 2000;411(1–2):121–35.

## **3.2 On-line monitoring of relevant fluorophores of yeast cultivations due to glucose addition during the diauxic growth**

By Supasuda Assawajaruwan, Philomena Eckard and Bernd Hitzmann

Published 2017 in **Process Biochemistry**.

Volume 58, Pages 51-59

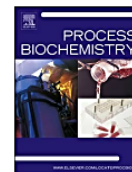
DOI: [doi.org/10.1016/j.procbio.2017.05.007](https://doi.org/10.1016/j.procbio.2017.05.007)



Contents lists available at ScienceDirect

Process Biochemistry

journal homepage: [www.elsevier.com/locate/procbio](http://www.elsevier.com/locate/procbio)



## On-line monitoring of relevant fluorophores of yeast cultivations due to glucose addition during the diauxic growth



Supasuda Assawajaruwan\*, Philomena Eckard, Bernd Hitzmann

Department of Process Analytics and Cereal Science, University of Hohenheim, Garbenstraße 23, 70599 Stuttgart, Germany

### ARTICLE INFO

#### Keywords:

On-line monitoring  
*Saccharomyces cerevisiae*  
Biogenic fluorophores  
2D Fluorescence spectroscopy  
Principal component analysis

### ABSTRACT

The relevant fluorophores in cells can be a key component to understanding cellular activities, which in turn explains states of cultivation processes. The autofluorescence inside microorganisms can be measured by 2D fluorescence spectroscopy which is an effective and non-invasive device for an on-line monitoring of bioprocesses. We detected the following intrinsic fluorophores which are part of metabolic pathways for yeast growth during fermentation in real-time: tryptophan, pyridoxine, NADH, riboflavin, FAD, and FMN. The changes of these intrinsic fluorophores were observed from the yeast cultivations under three conditions: (i) normal batch, (ii) glucose addition during glucose growth phase, and (iii) glucose addition during ethanol growth phase after a diauxic shift. The glucose addition during ethanol growth phase demonstrated the correlative changes of the fluorophores, which was a key component in the metabolic switch from ethanol to glucose growth phase. Additionally, the quantification of conversion between tryptophan and NADH was shown as a proportional factor. It was calculated from the ratio of the area of NADH and tryptophan fluorescence intensity after the glucose addition until depletion. The proportional factor was independent on various glucose concentrations with the coefficient of determination,  $R^2 = 0.999$ .

### 1. Introduction

An optimum processing is needed in the field of food, pharmaceutical, and biotechnological industry with the ultimate goal of achieving high productivity and high quality products. In order to achieve this goal, there are many different parameters to be realized and controlled, e.g., physical, chemical, and biological aspects of microbial bioprocesses. Microbial cultivations are such a complex process, therefore, reliable and efficient tools are required for an on-line monitoring to receive as much real-time information as possible, so that the processes can be controlled in time. On-line bioprocess monitoring has been studied and developed for many years. In 2002, the US Food and Drug Administration (FDA) launched the Process Analytical Technology (PAT) initiative to be applied in the process monitoring and effectively drove progresses in this field [1–5]. During the past decade, there were many investigations on in-line/on-line monitoring of bioprocesses by using various optical technologies, such as in situ microscopy, near-infrared (NIR), Raman, and fluorescence spectroscopy [6–15].

Fluorescence spectroscopy is one of the potential techniques for an on-line monitoring without any interfering processes, which reduces the risk of contamination in a bioreactor. Besides, it provides real-time information and bypasses the need to sampling data [15–20]. The

fluorescence sensor is particularly effective for monitoring the autofluorescence inside cells. Two-dimensional (2D) or multi-wavelength fluorescence spectroscopy was developed to be able to measure biogenic fluorophores in a wider range of excitation and emission wavelengths [17,21,22]. Thus, the non-identified overlapping peaks and the quenching of different fluorophores can be detected by the 2D fluorescence spectroscopy. The sensor is not only applied in monitoring cultivation processes of *Saccharomyces cerevisiae*, but also in many different microorganisms, such as *Claviceps purpurea*, *Streptomyces coelicolor*, and *Escherichia coli* [14,23–26]. The on-line monitoring using 2D fluorescence spectroscopy can enhance the understanding of the diversity in biological systems. For example, Bhatta et al., 2006 applied fluorescence spectroscopy to differentiate species between yeast and bacteria and also between different strains of yeasts [27]. Another study used a fluorescence sensor to monitor growth and stress responses of yeast cells by observing changes of autofluorescence [28]. The fluorescence sensor cannot directly measure glucose and ethanol concentrations because they are not fluorescent. However, it can monitor the fluorescent molecules relating to cellular activities, such as nicotinamide-adenine dinucleotide (NADH), tryptophan, pyridoxine (vitamin B<sub>6</sub>), riboflavin (vitamin B<sub>2</sub>), flavin-adenine dinucleotide (FAD), and flavin mononucleotide (FMN) [15,16]. Many studies investigated the

\* Corresponding author.

E-mail address: [sassawaj@uni-hohenheim.de](mailto:sassawaj@uni-hohenheim.de) (S. Assawajaruwan).

<http://dx.doi.org/10.1016/j.procbio.2017.05.007>

Received 9 February 2017; Received in revised form 3 April 2017; Accepted 8 May 2017

Available online 10 May 2017

1359-5113/© 2017 Elsevier Ltd. All rights reserved.

relation between intrinsic fluorophores and products or substrates. Then they used the fluorophores to estimate concentrations of cell mass, glucose, ethanol, and other products [14–25,29,30].

Cellular metabolism occurring in living microorganisms contains several metabolic pathways, such as glycolysis, the citric acid cycle (TCA cycle), and the electron transport chain. The intracellular fluorophores are key metabolic components for the metabolic pathways [22]. In different fermentation systems or conditions, the behavior of each biogenic fluorophore is different. Therefore, it is necessary to understand and recognize the change of intrinsic fluorophores during each phase of cultivations in order to find a relevant indicator of the metabolic switches. These significant indicators could be used to predict state variables and improve the cultivation process.

The objective of this study was to investigate relevant fluorophores under the three different cultivation conditions. The biogenic fluorophores, such as NADH, tryptophan, pyridoxine, riboflavin, FAD, and FMN, were monitored to observe their behaviors in different operations during the cultivations.

## 2. Materials and methods

### 2.1. Yeast strain, culture and fermentation conditions

*S. cerevisiae* (fresh baker's yeast, Oma's Ur-Hefe) was pre-cultivated before fermentation. 10 g fresh baker's yeast was inoculated into 100 mL Schatzmann medium, which consists of 0.34 g/L  $MgSO_4 \cdot 7H_2O$ , 0.42 g/L  $CaCl_2 \cdot 2H_2O$ , 4.5 g/L  $(NH_4)_2SO_4$ , 1.9 g/L  $(NH_4)_2HPO_4$ , and 0.9 g/L KCl [31]. The preculture was shaken for 10 min (180 rpm) and then was pumped into a 3-L stainless steel tank bioreactor (Minifors, Inifors HT, Bottmingen, Switzerland) with a working volume of 1.35 L. The medium used for the cultivations was the same as the one for the preculture, but with 10 g/L glucose, 1 mL/L trace elements solution (0.015 g/L  $FeCl_3 \cdot 6H_2O$ , 9 mg/L  $ZnSO_4 \cdot 7H_2O$ , 10.5 mg/L  $MnSO_4 \cdot 2H_2O$ , and 2.4 mg/L  $CuSO_4 \cdot 5H_2O$ ), 1 mL/L vitamin solution (0.06 g/L myoinositol, 0.03 g/L Ca-pantothenate, 6 mg/L thiamine HCl, 1.5 mg/L pyridoxine HCl, and 0.03 mg/L biotin), and 200  $\mu$ L/L antifoam. The yeast cultivations under three different conditions were run in triplicate. The first cultivation condition was a normal batch (Fig. 1A). The second condition was a cultivation with the glucose addition during the glucose growth phase at ca. 1.5 h. For the last condition, the glucose solution was also added, but during the ethanol growth phase at ca. 6 h. A 10 mL sample was regularly taken. Before the glucose addition at ca. 1.5 h, 4 samplings were taken as shown in Fig. 1B. Then 30 mL glucose feed solution was pumped into the bioreactor with the concentration of  $1.35 \times 10^2$  g/L. Hence, the glucose concentration in the cultivation after feeding increased around 3.0 g/L. In the case of the glucose addition at ca. 6 h, 12 samplings were taken before adding as demonstrated in Fig. 1C. 30 mL of the glucose feed solution was pumped in as well, but with the different required glucose concentrations, i.e., 1.5, 3.0, 4.5, and 6.0 g/L, in the total medium. Thus, the glucose feed solution was provided with the various concentrations of 63,  $1.26 \times 10^2$ ,  $1.89 \times 10^2$ , and  $2.52 \times 10^2$  g/L, respectively. To realize the biomass and ethanol concentrations, 30 mL increasing from the remaining volume is less than 3%, therefore, the dilution factor was not considered in the theoretical models (in chapter 2.4). All cultivations were operated at a constant temperature, 30 °C and a maintained pH 5. The aeration and agitation rates were kept constant at 3.5 L/min and 430 rpm, respectively. Iris software (Inifors HT, Bottmingen, Switzerland) was applied as a process control system for the bioreactor.

### 2.2. Off-line analysis

Samples for analyzing concentrations of biomass, glucose, and ethanol were regularly taken from the bioreactor and put into pre-weighed and predried microcentrifuge tubes. Cell dry weight was determined by centrifugation (Universal 16 R, Hettich Zentrifugen GmbH & Co. KG, Tuttlingen, Germany) of a sample with 1.5 mL (2 times)

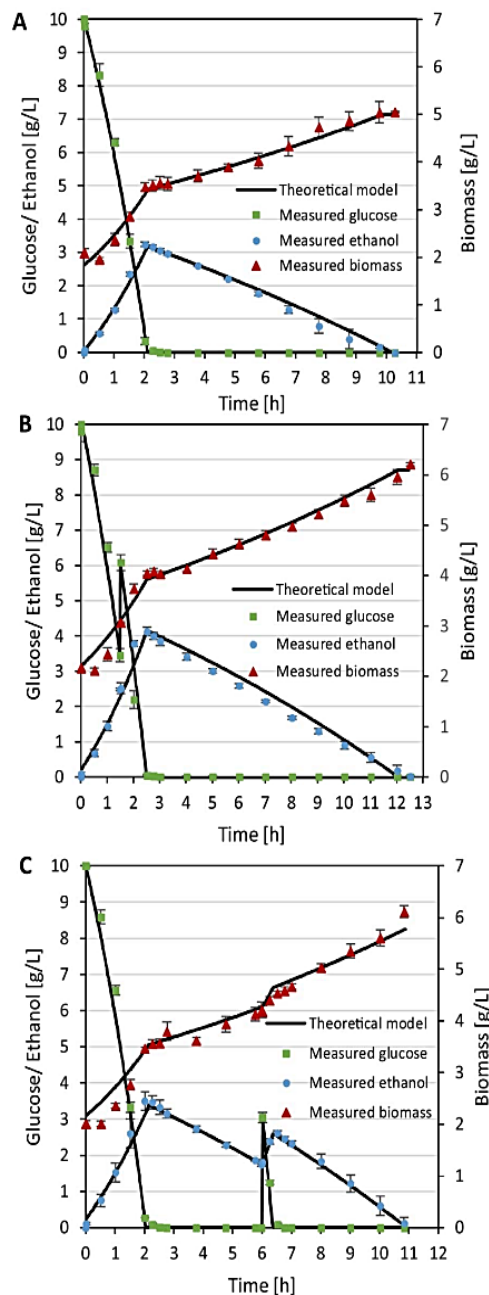


Fig. 1. The characteristics of the yeast cultivation with 10 g/L starting glucose and the theoretical models of the yeast cultivation in different conditions. (A) Normal batch. (B) Cultivation with glucose addition during GP and (C) during EP.

at 14,000 rpm for 10 min at 4 °C. The wet cells were let in a drying oven at 103 °C for 24 h. Subsequently, they were cooled down for 30 min before weighing. The supernatant of the samples after the centrifugation was examined by HPLC (ProStar, Variant, Walnut Creek, CA, USA) to determine the glucose and ethanol concentrations. Firstly, the supernatant was filtrated with pore size filter, 0.45  $\mu$ m, polypropylene membrane (VWR, Darmstadt, Germany), then 20  $\mu$ L was injected into a Rezex ROA-organic acid H+ (8%) column (Phenomenex, Aschaffenburg, Germany) and operated at 70 °C with 5 mM  $H_2SO_4$  as an eluent at 0.6 mL/min flow rate. The concentrations of glucose and ethanol were calculated by Galaxie software (Varian, Walnut Creek, CA, USA).



### 2.3. On-line monitoring/analysis

Carbon dioxide (CO<sub>2</sub>) and oxygen (O<sub>2</sub>) as an off-gas from the yeast fermentation were monitored continuously with BlueInOne Cell sensor (BlueSense gas sensor GmbH, Herten, Germany). During the cultivation, they were on-line evaluated by BlueVis software (BlueSense gas sensor GmbH, Herten, Germany).

Relative fluorescence intensity of the relevant fluorophores during the cultivations was monitored by BioView fluorescence spectrometer (DELTA Lights & Optics, Hørsholm, Denmark). It can measure multi-wavelength fluorescence in range of 270–550 nm excitation (Ex) and 310–590 nm emission (Em) with increment of 20 nm of these excitation and emission ranges. The scattered light is not considered in this work. BioView fluorescence sensor has a xenon flash lamp as a light source for excitation and is equipped with 15 different filters for excitation and emission wavelengths. The excitation light is guided via the fiber optic into the bioreactor and the fluorescent light, which is emitted in a 180° angle, is monitored after passing the emission filters. Then the fluorescent light is detected by a photomultiplier. A full spectrum is acquired if a complete rotation of excitation and emission filters is performed. The fluorescence sensor measured the culture through a quartz window in 25 mm standard port as a non-invasive monitoring. The measurement for a single scan of the spectrum was achieved within 90 s. The spectrum contains the combinations of excitation and emission wavelengths.

### 2.4. Mathematical models for yeast growth

The theoretical model (Eqs. (1)–(5)) was applied to fit to the measured data of glucose, ethanol, and cell dry mass concentrations by the particle swarm optimization algorithm [15,32]. Particle swarm optimization algorithm works by improving a population of candidate solutions called particles, which are the parameters in the following mathematical models. The particles are flying through the search space and the velocity of each particle is determined by the position of its best-known performance as well as the position of the overall swarm's best known performance. The swarm iteratively moves to the best solution. A more detailed description can be found in the literature [33]. The growth parameters of the yeast cultivations were estimated by using the following model.

$$\frac{dX}{dt} = \mu_G X + \mu_E X \quad (1)$$

$$\frac{dG}{dt} = -\frac{\mu_G X}{Y_{X/G}} \quad (2)$$

$$\frac{dE}{dt} = \frac{\mu_G X}{Y_{E/G}} - \frac{\mu_E X}{Y_{X/E}} \quad (3)$$

$$\mu_G = \begin{cases} 0 & G = 0 \\ \mu_{G0} & G > 0 \end{cases} \quad (4)$$

$$\mu_E = \begin{cases} 0 & G > 0 \\ \mu_{E0} & G = 0 \end{cases} \quad (5)$$

where  $X$ ,  $G$ , and  $E$  are cell mass, glucose, and ethanol concentrations, respectively.  $\mu_G$  and  $\mu_E$  are the specific growth rates on glucose and ethanol, respectively.  $Y_{X/G}$ ,  $Y_{E/G}$ , and  $Y_{X/E}$  are the yield coefficients for glucose with respect to biomass and ethanol, and for ethanol with respect to biomass.

According to the Chapter 2.1, the concentration of the glucose feed solution has been considered for the increased glucose concentration in the theoretical models. For the concentration of biomass and ethanol, the changing volume is less than 3%, therefore, it has not been considered in the model.

### 2.5. Calibration of NADH and tryptophan concentrations and their fluorescence intensities

In order to calibrate the fluorescence intensity with the concentrations of biogenic fluorophores, powdery NADH (GERBU Biotechnik GmbH, Gaiberg, Germany) and L-tryptophan (Sigma-Aldrich, St. Louis, USA) were prepared for various concentrations, such as 1.25, 2.5, 5.0, 10, 30, and 50 mg/L. They were dissolved in distilled water and then measured by BioView sensor to observe the linear correlation between their fluorescence intensities and concentrations. One solution was measured three times by the sensor.

### 2.6. Principle component analysis (PCA)

Before running PCA, the first fluorescence spectrum (after inoculation) of each batch was subtracted from the following spectra of itself [15,16,23,25]. In PCA, the score data was computed from the subtraction fluorescence spectra. According to the large on-line data set, PCA transforms the raw data into a new coordinate system for visualizing the best possible data structure. It provides relevant and useful information to represent states of fermentation processes. The important purpose to use PCA is to quantify the amount of useful information and take out noise which is contained in the data [34,35]. The subtraction spectra of each cultivation were used to calculate PCA (conditions: mean centering and NIPALS algorithm) by Unscrambler X<sup>®</sup> software (Camo, Norway).

### 2.7. Calculation of the proportional area of NADH and tryptophan fluorescence intensity

The area of the NADH and tryptophan fluorescence intensity after the glucose addition during ethanol growth phase until the added glucose depletion was calculated as a proportional factor (Eq. (6)). The noticed point of the glucose depletion is the fluorescence intensity of NADH and tryptophan coming back to the normal state of ethanol growth phase.

$$\text{Proportional factor} = \frac{\text{Area of NADH fluorescence intensity [units}_{\text{NADH}}^* \text{h}]}{\text{Area of tryptophan fluorescence intensity [units}_{\text{tryptophan}}^* \text{h}]} \quad (6)$$

The area under or above a linear trend function was integrated, which will be demonstrated in Chapter 3.6.

## 3. Results and discussion

### 3.1. Cultivation and growth characteristics of baker's yeast

In the first condition of the cultivations, the fermentation process took 10 h as shown in Fig. 1A. The products, e.g., ethanol and biomass were increasing, while the glucose was decreasing during the exponential growth. The diauxic shift was noticed at around 2 h. The glucose concentration was exhausted and then the phase shifted to grow on ethanol, which have been formerly observed by Locher et al. [36]. During the ethanol consumption, the biomass was exponentially increasing (Fig. 1A). The growth characteristics of yeasts in the second condition are demonstrated in Fig. 1B. After the glucose addition at around 1.5 h, the glucose concentration was rising directly. In this process, the trend of the diagram of ethanol and biomass concentrations is similar to the first condition, but the concentrations of them are higher and the diauxic shift was postponed to approximately 2.5 h. As shown in Fig. 1B, the glucose addition does not disturb the steady state of the glucose growth phase. The yeast cells have two major glucose receptors for a low and high glucose level to generate an intracellular glucose signal and their mechanisms can control the different glucose levels [37–39]. Consequently, the glucose addition during glucose growth phase (GP) is not detected as an adulterated situation for the cells and the cellular activity is able to keep functioning as usual. In

**Table 1**  
Growth parameters of the yeast cultivations in different conditions.

Cultivation condition	Starting glucose [g/L]	Glucose addition [g/L]	$\mu_G$ [ $\text{h}^{-1}$ ]	$\mu_E$ [ $\text{h}^{-1}$ ]	$Y_{X/G}$ [ $\text{g}_{\text{biomass}}/\text{g}_{\text{glucose}}$ ]	$Y_{E/G}$ [ $\text{g}_{\text{ethanol}}/\text{g}_{\text{glucose}}$ ]	$Y_{X/E}$ [ $\text{g}_{\text{biomass}}/\text{g}_{\text{ethanol}}$ ]
Normal <sup>a</sup>	10	–	$0.28 \pm 0.01$	$0.05 \pm 0.01$	$0.15 \pm 0.01$	$0.49 \pm 0.02$	$0.45 \pm 0.02$
GP <sup>b</sup>	10	3	$0.26 \pm 0.02$	$0.04 \pm 0.01$	$0.14 \pm 0.01$	$0.47 \pm 0.03$	$0.51 \pm 0.01$
EP <sup>c</sup>	10	3	$0.27 \pm 0.02$	$0.05 \pm 0.01$	$0.15 \pm 0.01$	$0.48 \pm 0.03$	$0.47 \pm 0.05$

<sup>a</sup> Normal condition is the normal batch.

<sup>b</sup> GP condition means the cultivation with glucose addition during glucose growth phase.

<sup>c</sup> EP condition means the cultivation with glucose addition during ethanol growth phase. The values in the table are mean value  $\pm$  standard deviation.

Fig. 1C, 3 g/L glucose increasing during ethanol growth phase (EP) can be observed. The glucose, ethanol and biomass concentrations look nearly the same as the first condition prior to the glucose addition at around 6 h (Fig. 1A and C). After adding the glucose solution, the ethanol and biomass concentrations were obviously increasing when comparing with the first condition at 7 h. Due to a glucose signal, yeasts growing on ethanol promptly switch to grow on glucose. As known, glucose is a primary carbon source for yeast cells and other eukaryotic cells as well [37–39].

The growth parameters of each cultivation condition are shown in Table 1. These parameters were obtained from fitting theoretical model to the experimental data. Between three repeated batches at the same condition, the value of parameters has no significant difference due to the low standard deviation. It indicates that these cultivations provide reproducible results. Between different conditions, the growth parameters like  $\mu_G$ ,  $\mu_E$ ,  $Y_{X/G}$ ,  $Y_{E/G}$ , and  $Y_{X/E}$  show no significant difference as well (Table 1). It shows that the yeast cells have regulatory mechanisms to be able to balance the cellular activity, although there are disturbances. For all cultivation conditions,  $\mu_G$  is higher than  $\mu_E$  as presented in Table 1. During the glucose growth phase of all conditions,  $Y_{E/G}$  is higher than  $Y_{X/G}$ , which can be seen in Fig. 1A–C. When yeasts grow on ethanol, the biomass yield is higher than growing on glucose owing to the ethanol production as shown in Table 1, which is corresponding to the results by Locher et al. [36].

### 3.2. Monitoring of exhaust gas

The trend of CO<sub>2</sub> off-gas evolution under the first and second cultivation conditions is similar, but the amount of CO<sub>2</sub> produced in the second condition is higher by reason of more glucose in total as demonstrated in Fig. 2A. Furthermore, the diauxic shift of the second condition came circa 30 min after the one of the first condition. Fig. 2B illustrates the CO<sub>2</sub> evolution by varying the concentrations of the glucose addition during EP (i.e., 1.5, 3.0, 4.5, and 6.0 g/L). The maximum CO<sub>2</sub> evolution rate (CER) has a correlation to the concentrations of the glucose addition with the coefficient of determination,  $R^2 = 0.979$  (Fig. 2C). From the results, the trajectories of CO<sub>2</sub> exhaust gas evolution can interpret the characteristics of the yeast growth [36].

### 3.3. Standard curves of NADH and tryptophan

The provided concentrations of NADH and tryptophan in mg/L were converted to mol/L to be compared at the same molar concentration as shown on the abscissa in Fig. 3A and B. The standard curve of NADH (Ex370/Em450) shows the linear correlation between the fluorescence intensity and the concentrations until  $4.5 \times 10^{-5}$  mol/L NADH as illustrated in Fig. 3A (with the blue dotted line). It means that when the concentration of NADH is higher than  $4.5 \times 10^{-5}$  mol/L, it cannot be proportionally measured to the fluorescence intensity by BioView sensor. For the tryptophan (Ex290/Em370) standard curve, the linear correlation between the fluorescence intensity and the concentrations is until  $4.9 \times 10^{-5}$  mol/L as shown in Fig. 3B. The maximal intensity of NADH and tryptophan, which correlates linearly with their concentrations, is around 1400 and 800 units, respectively. At an equal molar

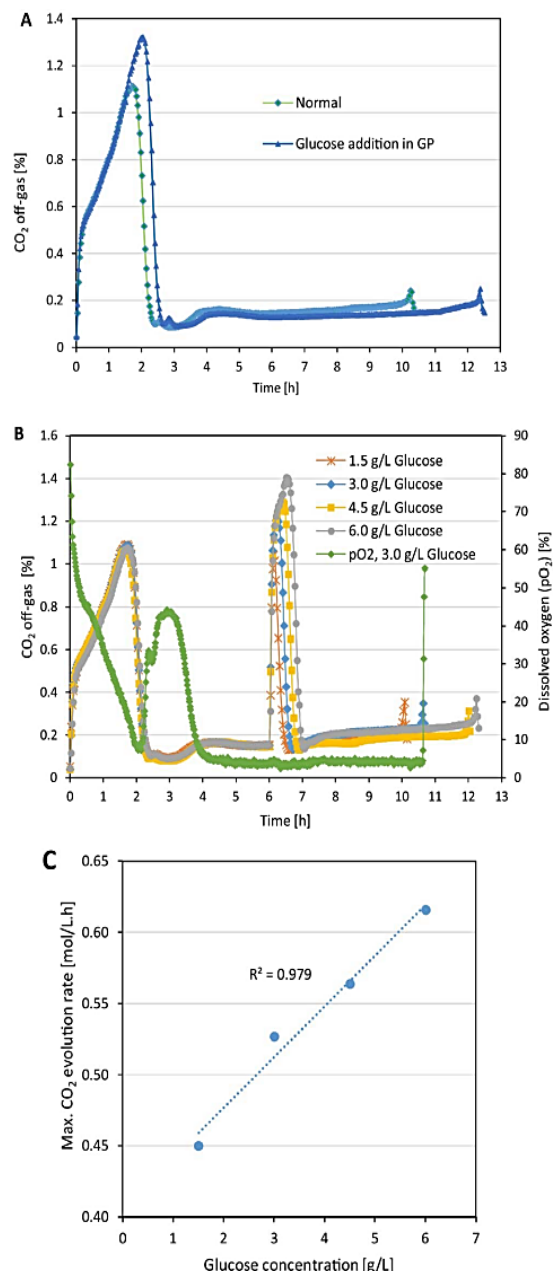


**Fig. 2.** CO<sub>2</sub> exhaust gas in different conditions. (A) Normal batch and glucose addition during GP. (B) Glucose addition during EP with various concentrations of glucose and dissolved oxygen (pO<sub>2</sub>) in the condition with 3 g/L glucose addition. (C) Correlation between maximum CER due to the glucose addition and the various glucose concentrations.

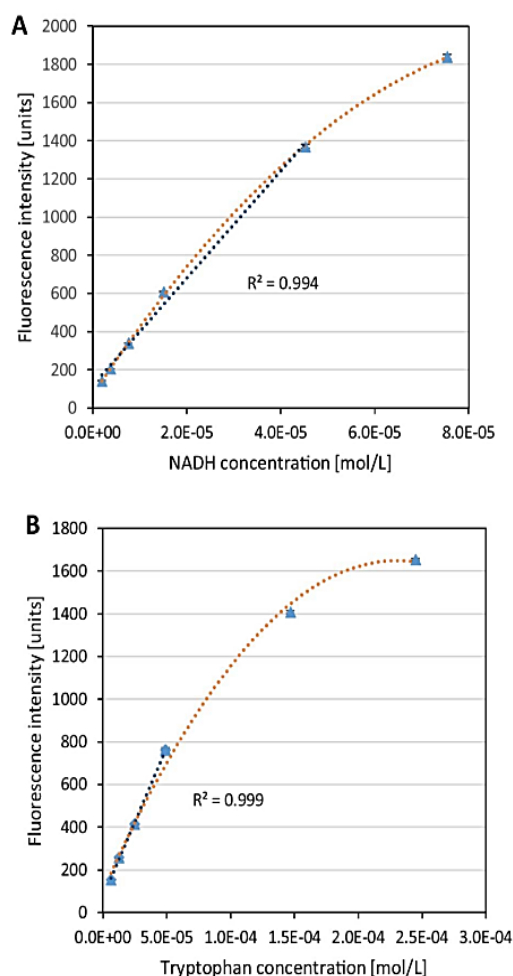


Fig. 3. Calibration curves of NADH (Ex370/Em450) and tryptophan (Ex290/Em370). (A) The standard curve (the blue dotted line) of NADH and (B) tryptophan with  $R^2 = 0.994$  and  $0.999$ , respectively. (For interpretation of the references to color in this figure legend, the reader is referred to the web version of this article.)

concentration, the NADH fluorescence intensity is higher than the tryptophan intensity (Fig. 3A and B). From the calibration curves, the increased fluorescence intensity corresponds to the increased concentration of the biogenic fluorophores. However, the behavior of the fluorescence intensity of each molecule is different. The range of the original fluorescence intensity (not subtraction spectra) of NADH and tryptophan during the cultivations were around 300–1200 and 200–550 units, respectively. It means that their fluorescence intensities during the cultivations are not over the maximum range of the linearity.

### 3.4. Monitoring of yeast cultivations using PCA

The score plot (PC1 vs. PC3) of the first cultivation condition has similarity to the one of the second condition as demonstrated in Fig. 4A and B, respectively. These two score plots have the trajectory similar to their reversed graphs of CO<sub>2</sub> off-gas evolution (Fig. 2A) [15]. In Fig. 4A and B at  $t = 2.2$  h and  $t = 2.6$  h, respectively, the tight coil in each score plot is recognized that they occur at the same time as the diauxic shifts in their CO<sub>2</sub> exhaust gas evolutions and growth characteristics. According to the trajectory of PC3 scores, it reflects the characteristics of the CO<sub>2</sub> exhaust gas evolution. As also shown in Fig. 4C, the trajectory of PC3 scores of the cultivation in the third condition looks similar to its reversed graph of CO<sub>2</sub> exhaust gas evolution. It can be

particularly seen in Fig. 4C that the direction of the score plot changes directly after the glucose addition (ca.  $t = 6.0$  h) like the diagram of the CO<sub>2</sub> off-gas evolution. Another observation is that the score plot and its CO<sub>2</sub> off-gas evolution (3 g/L glucose) demonstrate the same time point of glucose depletion (Figs. 4C and 2B). All score plots in Fig. 4A–C show the same characteristics of the increase in the PC1 scores from the beginning until the end, which indicates like the cell growth. Fig. 4D (i–iii) represents the correlation between the simulated values of biomass by the theoretical models and the PC1 scores of the three different cultivation conditions with  $R^2$ , 0.962, 0.970, and 0.979, respectively. According to the score plots, PCA provides relevant information of the yeast cultivations and can represent shifted states of the fermentation processes.

### 3.5. Monitoring of the relevant fluorophores' changes using 2D fluorescence spectroscopy

The significant fluorophores, which were monitored during the fermentation processes, are tryptophan (Ex290/Em370), pyridoxine (Ex330/Em390), NADH (Ex370/Em450), riboflavin (Ex370/Em530) and FAD, FMN (Ex450/Em530). The fluorescence spectra of these fluorophores, shown in Fig. 5, are the subtraction spectra obtained from subtracting the first fluorescence spectrum. In Fig. 5A and B, the tendency of the relevant fluorophores under the first and second cultivation conditions looks similar as well as the diagrams of their growth characteristics (Fig. 1A and B), CO<sub>2</sub> exhaust gas evolutions (Fig. 2A), and score plots (Fig. 4A and B). The glucose addition during GP did not disrupt the steady state of the constant increase of the fluorophore intensities (Fig. 5B). As mentioned in chapter 3.1, the yeast cells can regulate different levels of glucose concentrations [37–39]. The glucose addition might be detected as a normal glucose signal. Hence, the cellular metabolism, such as glycolysis and TCA cycle, keeps performing normally. The small differences between the first and second conditions are the different time point of the diauxic shift and the period of the cultivations, which match with other aforementioned diagrams. Besides, the intensity of these five biogenic fluorophores of the second condition is higher than the ones of the first condition due to the more given total amount of glucose. In the third condition before adding glucose, all of the fluorophores show the same time point of the diauxic shift as the ones of the first condition (Fig. 5C). The interesting point of the third condition is the explicit changing of the five fluorophores after the glucose addition at ca. 6 h. The fluorescence intensity of NADH and riboflavin was instantly increasing, but the intensity of tryptophan, pyridoxine and FAD, FMN was decreasing. Around 30 min after adding glucose (3 g/L), the fluorescence intensity of all fluorophores came back to the normal state of EP and kept increasing normally until the end of the cultivation like the first two conditions. Thus, it shows that the metabolization of 3 g/L glucose takes around 30 min. After the glucose depletion, the intrinsic fluorophores of the cellular activities were regulated to the normal EP state again.

As mentioned in the introduction part, NADH, tryptophan, pyridoxine (vitamin B<sub>6</sub>), riboflavin (vitamin B<sub>2</sub>), FAD, and FMN are related to cellular activities inside cells. In Fig. 5A–C, at the end of the yeast cultivations, the instant changes of the fluorescence intensity of NADH, FAD, FMN, and riboflavin can be explicitly seen. The fluorescence intensity of NADH was immediately and dramatically decreasing after the last carbon source depletion. The result is corresponding to the cellular activity inside the yeast cells. Owing to the running out of carbon sources, the catabolism stops functioning and then the dissolved oxygen increases as illustrated in Fig. 2B. With the existence of oxygen, the oxidative phosphorylation functions and then NADH (reduced form) is oxidized to NAD<sup>+</sup> (oxidized form). Therefore, the signal of the NADH intensity immediately drops as shown in all three diagrams (Fig. 5A–C). Conversely, the FAD fluorescence intensity was increasing after the last carbon source depletion as shown in Fig. 5A–C. In TCA

## CHAPTER 3.2. ON-LINE MONITORING OF RELEVANT FLUOROPHORES OF YEAST CULTIVATIONS DUE TO GLUCOSE ADDITION DURING THE DIAUXIC GROWTH

S. Assawajaruwan et al.

Process Biochemistry 58 (2017) 51–59

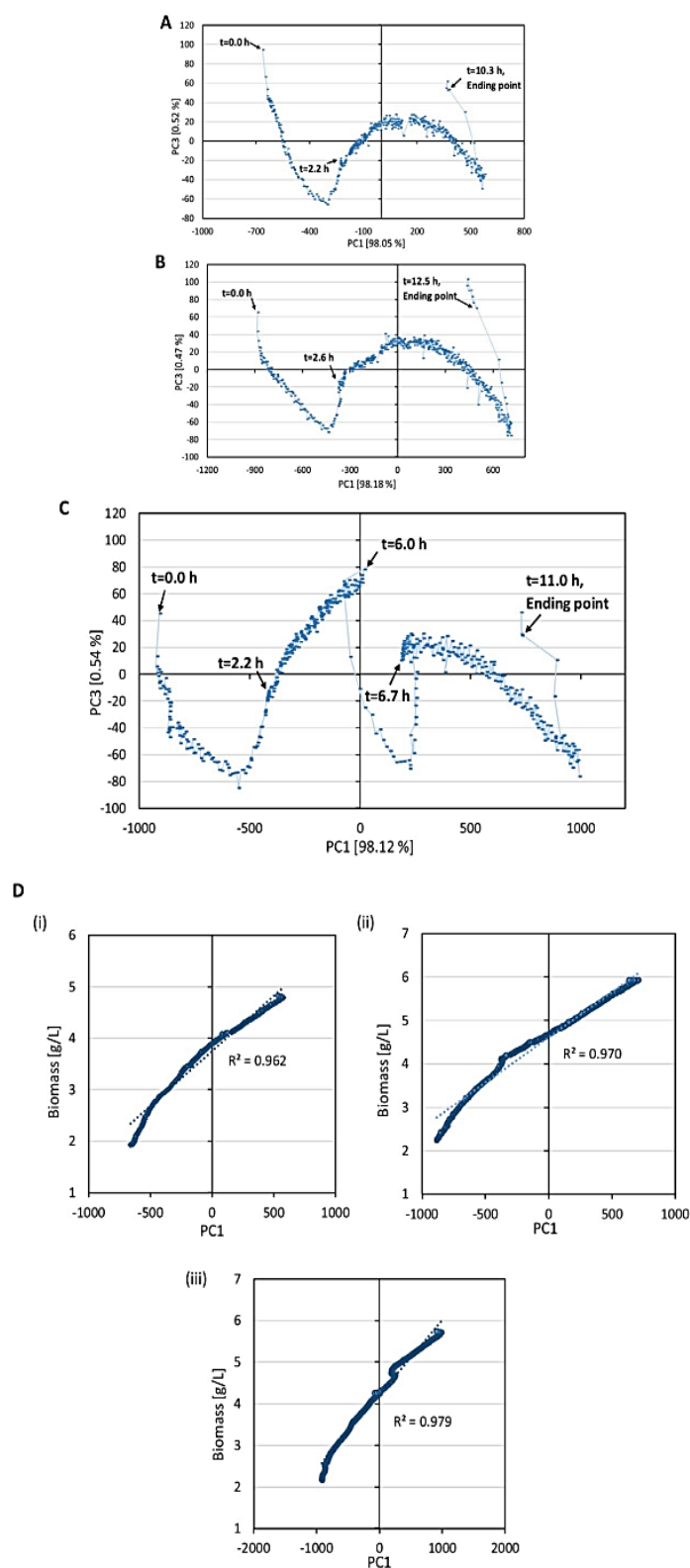


Fig. 4. Score plots of PC1 versus PC3 in different cultivation conditions. (A) Normal batch. (B) Cultivation with glucose addition during GP and (C) during EP (3 g/L glucose). (D) Correlation between biomass (theoretical models) and PC1 score in different cultivation conditions. (i) Normal batch. (ii) Cultivation with glucose addition during GP and (iii) during EP.

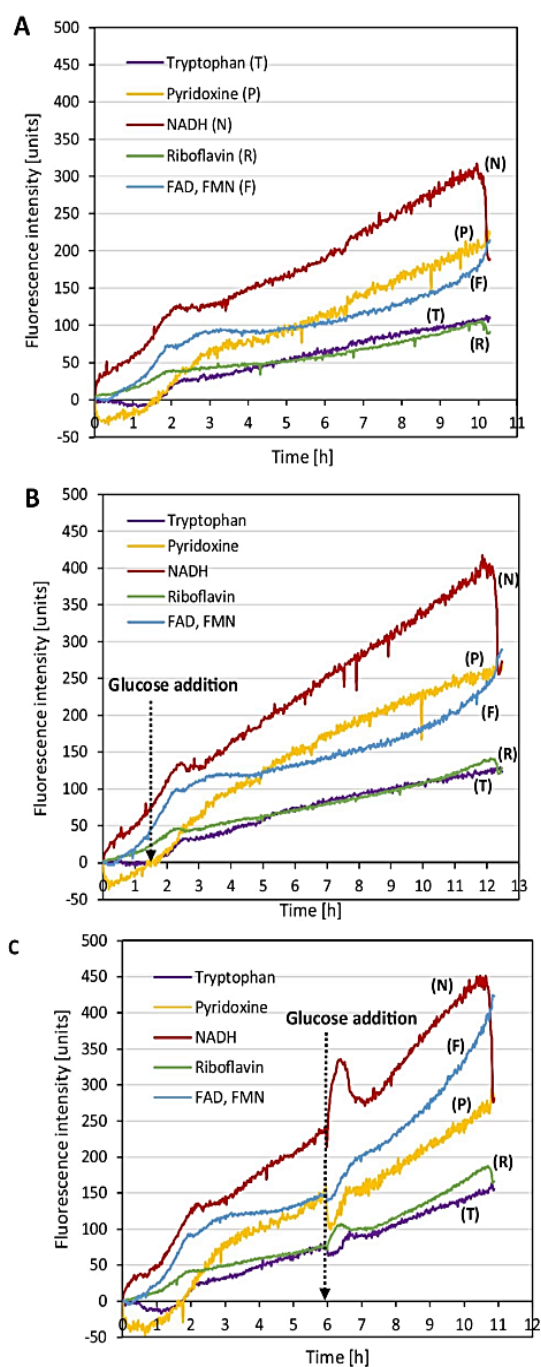


Fig. 5. Subtraction spectra of the biogenic fluorophores, such as tryptophan (Ex290/Em370), pyridoxine (Ex330/Em390), NADH (Ex370/Em450), riboflavin (Ex370/Em530) and FAD, FMN (Ex450/Em530), of the different cultivation conditions. (A) Normal batch. (B) Cultivation with glucose addition during GP (ca. 1.5 h) and (C) during EP (ca. 6 h, 3 g/L glucose).

cycle, the electrons are transferred to FAD (oxidized form) and then FAD becomes FADH<sub>2</sub> (reduced form) as the electron carriers like NADH [40,41]. When the TCA cycle does not occur, FAD will not be converted to FADH<sub>2</sub>. For this reason, FAD is accumulating after the last carbon source running out. Another interesting point, the fluorescence intensity of riboflavin was slightly decreasing at the end of yeast cultivations (Fig. 5A–C). During the yeast cultivations, the riboflavin fluorescence

intensity kept slightly rising. It demonstrates that riboflavin can be synthesized by yeasts, which is also mentioned by Bacher et al. [42]. The biosynthesis of one molecule of riboflavin requires one molecule of guanosine 5-triphosphate (GTP) and two molecules of ribulose 5-phosphate [42]. The ribulose 5-phosphate is an intermediate product of the pentose phosphate pathway [40]. Apart from biosynthesizing riboflavin, yeasts can use riboflavin for synthesizing FAD [43,44]. The slight increase of riboflavin during the cultivations might be because some riboflavin is used for FAD synthesis. Besides, it is assumed that the decrease of riboflavin at the end of the cultivation might be because of the riboflavin turning to be FAD and no more produced after the depletion of the last carbon source. For the fluorescence intensity of tryptophan and pyridoxine, they were not recognized any obvious change at the end of the yeast cultivations. According to the results, NADH, FAD, and riboflavin are sensitive to the changes of the cellular metabolism after the last carbon source running out.

Fig. 5C illustrates the sudden increase of the NADH fluorescence intensity due to the glucose addition during EP. It shows that the yeast metabolism switches from the ethanol growth phase to metabolize glucose when the primary carbon source exists. The NADH primarily produced from glycolysis and TCA cycle is oxidized to NAD<sup>+</sup> in the electron transport chain because yeast cells need the energy from the electrons to produce adenosine triphosphate (ATP) [40,41]. Then NAD<sup>+</sup> is further used for accepting more electrons from glycolysis and TCA cycle to keep cellular process going [40,41]. In this case, there was low oxygen supplied during EP as shown in Fig. 2B. The oxidative phosphorylation in the electron transport chain needs oxygen as an electron acceptor [40,41]. With insufficient oxygen, the oxidative phosphorylation might not be able to take place or function. Although NADH is still produced by catabolic pathways, it is not able to be oxidized to NAD<sup>+</sup> due to inadequate oxygen for the oxidative phosphorylation [40,41,45]. As yeast cells require NAD<sup>+</sup> to keep process going, tryptophan might be used as a main precursor for synthesizing NAD<sup>+</sup> by the de novo pathway [46–50]. Tryptophan is converted to quinolinic acid and then the quinolinic acid as an intermediate is converted to NAD<sup>+</sup> under either aerobic or anaerobic condition [47,48]. Apart from the de novo biosynthetic pathway, NAD<sup>+</sup> also can be synthesized from the recycled metabolites, such as nicotinamide and nicotinic acid, by the salvage pathway [46–48]. According to Sporty et al., the de novo pathway plays less role when the salvage pathway functions [50]. It means tryptophan is taken only in the beginning for the NAD<sup>+</sup> synthesis. Afterwards, the intermediates from the conversion of tryptophan to NAD<sup>+</sup> are recycled to synthesize NAD<sup>+</sup> by the salvage pathway. According to the mentioned studies, the slight decrease of the tryptophan fluorescence intensity might be just used for the NAD<sup>+</sup> synthesis at the start.

The fluorescence intensity of FAD was moderately declining by cause of the glucose addition during EP (Fig. 5C). As discussed above, FAD as an electron acceptor is reduced to FADH<sub>2</sub> to carry electrons in cellular metabolism [40,41]. The glucose addition re-initiates the cellular activity, such as glycolysis and TCA cycle, therefore, FAD is required as an electron acceptor. The pentose phosphate pathway, caused by the glucose addition, could explain the small increase of the riboflavin fluorescence intensity. For the reason that ribulose 5-phosphate is produced, which is an important substrate for the biosynthesis of riboflavin as discussed above [42]. Additionally, it is assumed that the FAD fluorescence intensity decreased only a little and then slowly upturned with the help of compensation from produced riboflavin, which is used for FAD biosynthesis. For this reason, it also supports that the fluorescence intensity of riboflavin just fairly increased and diminished.

Pyridoxine is a vital co-factor in several enzymatic reactions, which are necessarily related to amino acid metabolism, and therefore is essential to all living organisms [40,51–53]. If they cannot synthesize by themselves, they have to intake from nutrients [51]. The Schatzman medium contains pyridoxine for growing yeasts. From the observation

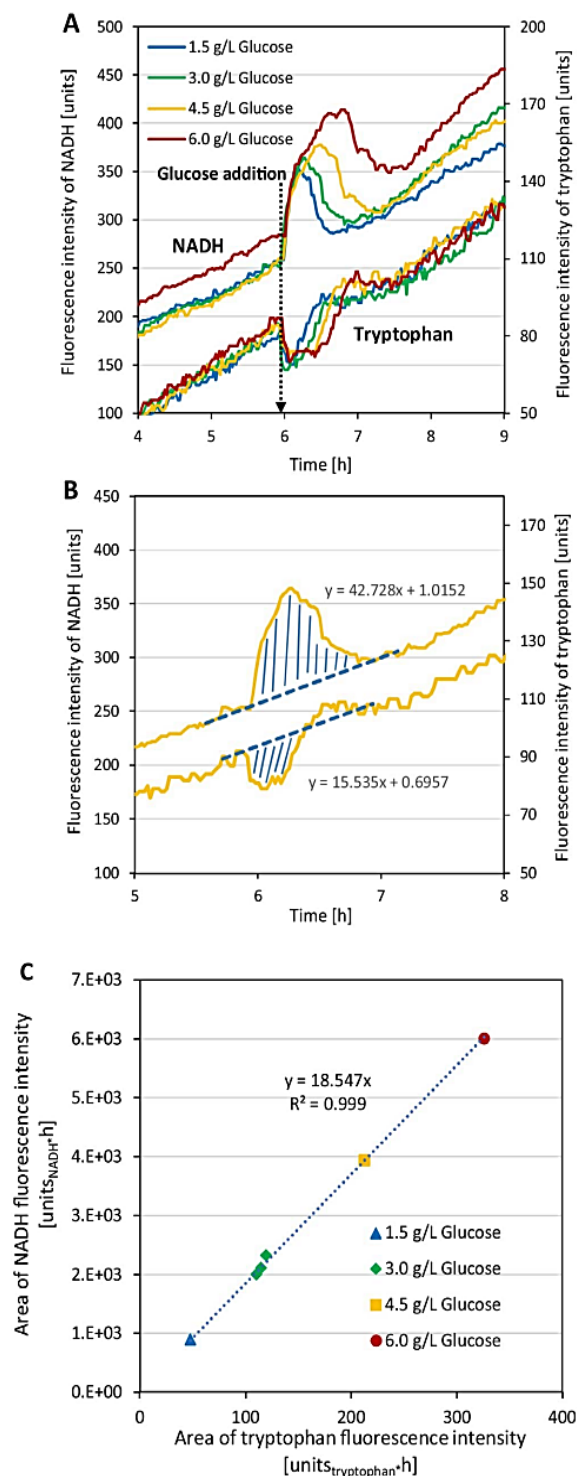


Fig. 6. (A) Correlative and proportional changes of NADH and tryptophan fluorescence intensity with various glucose concentrations, 1.5, 3.0, 4.5, and 6.0 g/L. (B) Calculated area of the conversion of tryptophan and NADH fluorescence intensity after the glucose addition until depletion (4.5 g/L glucose addition). (C) Correlation between the area of NADH and tryptophan fluorescence intensity with  $R^2 = 0.999$ .

of the prompt decrease of the pyridoxine fluorescence intensity at the beginning, after inoculation (in Fig. 5A–C), it represents that the yeast cells require pyridoxine for their cellular activities. Pyridoxine might be applied by the yeast cells as a co-factor for enzyme reactions because there are several enzymes required in cellular metabolism, such as glycolysis and TCA cycle. Afterwards, the fluorescence intensity of pyridoxine was slowly increasing as shown in Fig. 5A–C. It demonstrates that yeasts can biosynthesize pyridoxine [53,54]. In Fig. 5C, the pyridoxine fluorescence intensity was immediately declining after the glucose addition, which has the same trend at the start of the yeast cultivations. As a result, pyridoxine might be used in the same reason.

### 3.6. Proportional and correlative changes of the area of NADH and tryptophan fluorescence intensity

As mentioned in chapter 3.5, NADH and tryptophan have a correlative conversion which has  $\text{NAD}^+$  as an intermediate product. Fig. 6A illustrates that the curves of the NADH and tryptophan fluorescence intensity, due to the glucose addition during EP, are getting more pronounced with the higher concentration of glucose. The area under and above curves, between the glucose addition and depletion, was found by integration. The depletion point is the point at which the fluorescence intensity of these fluorophores returns to the normal EP state. Fig. 6B presents the area of the NADH and tryptophan fluorescence intensity under and above the curves to the linear trend functions. According to the integrated area of these two fluorophores, the proportional factor was calculated using Eq. (6). Fig. 6C demonstrates the proportional factor of the conversion between tryptophan and NADH, which is 18.5 ( $\text{units}_{\text{NADH}}\cdot\text{h}/\text{units}_{\text{tryptophan}}\cdot\text{h}$ ). The factor is independent on different concentrations of the glucose addition. The proportional change between the area of the NADH and tryptophan fluorescence intensity, due to the different concentrations of the added glucose, are correlated with the coefficient of determination,  $R^2 = 0.999$  (Fig. 6C). From the result, it shows the potentiality of the 2D fluorescence spectroscopy, which can be used to monitor the quantitative change of the fluorescence intensity.

## 4. Conclusion

According to the results, 2D fluorescence spectroscopy can effectively monitor the real-time changes of the relevant fluorophores, such as tryptophan, pyridoxine, NADH, riboflavin, FAD, and FMN. The glucose pulse during EP can be clearly seen in the fluorescence spectra. However, there is a limitation to detect the glucose pulse during GP. In this case, the longer glucose growth phase and the increased fluorescence intensity of the fluorophores demonstrate the glucose addition during GP. The different states of fermentation processes, particularly the glucose pulse during EP, can be recognized and identified from the on-line fluorescence spectra by using PCA. Furthermore, the related change between the tryptophan and NADH intensity can be quantified as a proportional factor. Anyhow, the on-line monitoring of the glucose addition during GP by using only PCA seems not possible. In case of a pure batch fermentation, an on-line monitoring of glucose, ethanol, and biomass concentrations seems achievable.

### Conflict of interest

The authors declare that they have no conflict of interest.

### Ethical misconduct

The research does not contain any studies with human participants or animals performed by any of authors.

## CHAPTER 3.2. ON-LINE MONITORING OF RELEVANT FLUOROPHORES OF YEAST CULTIVATIONS DUE TO GLUCOSE ADDITION DURING THE DIAUXIC GROWTH

S. Assawajarwan et al.

Process Biochemistry 58 (2017) 51–59

### References

- [1] B.H. Junker, H.Y. Wang, Bioprocess monitoring and computer control: key roots of the current PAT initiative, *Biotechnol. Bioeng.* 95 (2006) 226–261.
- [2] P. Biechele, C. Busse, D. Solle, T. Scheper, K. Reardon, Sensor systems for bioprocess monitoring, *Eng. Life Sci.* 15 (2015) 469–488.
- [3] J. Classen, F. Aupert, K.F. Reardon, D. Solle, T. Scheper, Spectroscopic sensors for in-line bioprocess monitoring in research and pharmaceutical industrial application, *Anal. Bioanal. Chem.* 409 (2017) 651–666.
- [4] S.M. Mercier, B. Diepenbroek, M.C.F. Dalm, R.H. Wijffels, M. Streefland, Multivariate data analysis as a PAT tool for early bioprocess development data, *J. Biotechnol.* 167 (2013) 262–270.
- [5] N.D. Lourenco, J.A. Lopes, C.F. Almeida, M.C. Sarraçuca, H.M. Pinheiro, Bioreactor monitoring with spectroscopy and chemometrics: a review, *Anal. Bioanal. Chem.* 404 (2012) 1211–1237.
- [6] I. Havlik, P. Lindner, T. Scheper, K.F. Reardon, On-line monitoring of large cultivations of microalgae and cyanobacteria, *Trends Biotechnol.* 31 (2013) 406–414.
- [7] D. Marquard, A. Enders, G. Roth, U. Rinas, T. Scheper, P. Lindner, In situ microscopy for online monitoring of cell concentration in *Pichia pastoris* cultivations, *J. Biotechnol.* 234 (2016) 90–98.
- [8] R. Schalk, D. Geoerg, J. Staubach, M. Raedle, F.-J. Methner, T. Beuermann, Evaluation of a newly developed mid-infrared sensor for real-time monitoring of yeast fermentations, *J. Biosci. Bioeng.* 123 (2017) 651–657.
- [9] M. Clavaud, Y. Roggo, R. von Daeniken, A. Liebler, J.-O. Schwabe, Chemometrics and in-line near infrared spectroscopic monitoring of a biopharmaceutical Chinese hamster ovary cell culture: prediction of multiple cultivation variables, *Talanta* 111 (2013) 28–38.
- [10] M.C. Sarraçuca, A. Paulo, M.M. Alves, A.M.A. Dias, J.A. Lopes, E.C. Ferreira, Quantitative monitoring of an activated sludge reactor using on-line UV-vis and near-infrared spectroscopy, *Anal. Bioanal. Chem.* 395 (2009) 1159–1166.
- [11] C. Eliasson, N.A. Macleod, L.C. Jayes, F.C. Clarke, S.V. Hammond, M.R. Smith, P. Matousek, Non-invasive quantitative assessment of the content of pharmaceutical capsules using transmission Raman spectroscopy, *J. Pharm. Biomed. Anal.* 47 (2008) 221–229.
- [12] G.P. Singh, S. Goh, M. Canzoneri, R.J. Ram, Raman spectroscopy of complex defined media. Biopharmaceutical applications, *J. Raman Spectrosc.* 46 (2015) 545–550.
- [13] B.N. Berry, T.M. Dobrowsky, R.C. Timson, R. Kshirsagar, T. Ryll, K. Wiltberger, Quick generation of Raman spectroscopy based in-process glucose control to influence biopharmaceutical protein product quality during mammalian cell culture, *Biotechnol. Prog.* 32 (2016) 224–234.
- [14] M.B. Haack, A. Eliasson, L. Olsson, On-line cell mass monitoring of *Saccharomyces cerevisiae* cultivations by multi-wavelength fluorescence, *J. Biotechnol.* 114 (2004) 199–208.
- [15] S. Assawajarwan, J. Reinalter, B. Hitzmann, Comparison of methods for wavelength combination selection from multi-wavelength fluorescence spectra for on-line monitoring of yeast cultivations, *Anal. Bioanal. Chem.* 409 (2017) 707–717.
- [16] S.M. Faassen, B. Hitzmann, Fluorescence spectroscopy and chemometric modeling for bioprocess monitoring, *Sensors (Basel)* 15 (2015) 10271–10291.
- [17] S. Marose, C. Lindemann, T. Scheper, Two-dimensional fluorescence spectroscopy: a new tool for on-line bioprocess monitoring, *Biotechnol. Prog.* 14 (1998) 63–74.
- [18] J.J. Horvath, S.A. Glazier, C.J. Spangler, In situ fluorescence cell mass measurements of *Saccharomyces cerevisiae* using cellular tryptophan, *Biotechnol. Prog.* 9 (1993) 666–670.
- [19] X. Zhang, S.-T. Yang, An online, non-invasive fluorescence probe for immobilized cell culture process development, *Process Biochem.* 46 (2011) 2030–2035.
- [20] T. Ladner, M. Beckers, B. Hitzmann, J. Buchs, Parallel online multi-wavelength (2D) fluorescence spectroscopy in each well of a continuously shaken microtiter plate, *Biotechnol. J.* 11 (2016) 1605–1616.
- [21] C. Lindemann, S. Marose, H. Nielsen, T. Scheper, 2-Dimensional fluorescence spectroscopy for on-line bioprocess monitoring, *Sens. Actuators B: Chem.* 51 (1998) 273–277.
- [22] J.K. Li, E.C. Asali, A.E. Humphrey, J.J. Horvath, Monitoring cell concentration and activity by multiple excitation fluorometry, *Biotechnol. Prog.* 7 (1991) 21–27.
- [23] D. Boehl, D. Solle, B. Hitzmann, T. Scheper, Chemometric modelling with two-dimensional fluorescence data for *Claviceps purpurea* bioprocess characterization, *J. Biotechnol.* 105 (2003) 179–188.
- [24] J.I. Rhee, T.-H. Kang, On-line process monitoring and chemometric modeling with 2D fluorescence spectra obtained in recombinant *E. coli* fermentations, *Process Biochem.* 42 (2007) 1124–1134.
- [25] P. Odman, C.L. Johansen, L. Olsson, K.V. Gernaey, A.E. Lantz, On-line estimation of biomass, glucose and ethanol in *Saccharomyces cerevisiae* cultivations using in-situ multi-wavelength fluorescence and software sensors, *J. Biotechnol.* 144 (2009) 102–112.
- [26] K. Hantelmann, M. Kollerker, D. Hull, B. Hitzmann, T. Scheper, Two-dimensional fluorescence spectroscopy: a novel approach for controlling fed-batch cultivations, *J. Biotechnol.* 121 (2006) 410–417.
- [27] H. Bhatta, E.M. Goldys, R.P. Learmonth, Use of fluorescence spectroscopy to differentiate yeast and bacterial cells, *Appl. Microbiol. Biotechnol.* 71 (2006) 121–126.
- [28] O. Podrazky, G. Kuncova, A. Krasowska, K. Sigler, Monitoring the growth and stress responses of yeast cells by two-dimensional fluorescence spectroscopy: first results, *Folia Microbiol.* 48 (2003) 189–192.
- [29] A. Eliasson Lantz, P. Jorgensen, E. Poulsen, C. Lindemann, L. Olsson, Determination of cell mass and polymyxin using multi-wavelength fluorescence, *J. Biotechnol.* 121 (2006) 544–554.
- [30] S. Srivastava, S. Harsh, A.K. Srivastava, Use of NADH fluorescence measurement for on-line biomass estimation and characterization of metabolic status in bioreactor cultivation of plant cells for azadirachtin (a biopesticide) production, *Process Biochem.* 43 (2008) 1121–1123.
- [31] H. Schatzmann, Anaerobes Wachstum Von Saccharomyces, Dissertation, ETH No. 5504, (1975).
- [32] D. Solle, D. Geissler, E. Stärk, T. Scheper, B. Hitzmann, Chemometric modelling based on 2D-fluorescence spectra without a calibration measurement, *Bioinformatics* 19 (2003) 173–177.
- [33] G.-G. Wang, A. Hossein Gandomi, X.-S. Yang, A. Hossein Alavi, A novel improved accelerated particle swarm optimization algorithm for global numerical optimization, *Eng. Comput.* 31 (2014) 1198–1220.
- [34] M. Otto, Chemometrics: Statistics and Computer Application in Analytical Chemistry, Weinheim, 1999.
- [35] CAMO Process AS, The Unscrambler Tutorials, (2006).
- [36] G. Locher, U. Hahnemann, B. Sonnleitner, A. Fiechter, Automatic bioprocess control. 4. A prototype batch of *Saccharomyces cerevisiae*, *J. Biotechnol.* 29 (1993) 57–74.
- [37] S. Ozcan, J. Dover, A.G. Rosenwald, S. Wolf, M. Johnston, Two glucose transporters in *Saccharomyces cerevisiae* are glucose sensors that generate a signal for induction of gene expression, *Proc. Natl. Acad. Sci. U. S. A.* 93 (1996) 12428–12432.
- [38] M. Johnston, Feasting, fasting and fermenting. Glucose sensing in yeast and other cells, *Trends Genet.* 15 (1999) 29–33.
- [39] K.J. Verstrepen, D. Iserentant, P. Malcorps, G. Derdelinckx, P. van Dijk, J. Winderickx, I.S. Pretorius, J.M. Thevelein, F.R. Delvaux, Glucose and sucrose: hazardous fast-food for industrial yeast? *Trends Biotechnol.* 22 (2004) 531–537.
- [40] H.F. Gilbert, Basic Concepts in Biochemistry. A Student's Survival Guide, McGraw-Hill, Health Professions Division, New York, 2000.
- [41] Harper's Illustrated Biochemistry, in: R.K. Murray, D. Bender, K.M. Botham, P.J. Kennelly, V.W. Rodwell, P.A. Weil (Eds.), 29th edition, McGraw-Hill Medical, 2012.
- [42] A. Bacher, S. Eberhardt, M. Fischer, K. Kis, G. Richter, Biosynthesis of vitamin B2 (riboflavin), *Annu. Rev. Nutr.* 20 (2000) 153–167.
- [43] V. Bafunno, T.A. Giancaspero, C. Brizio, D. Bufano, S. Passarella, E. Boles, M. Barile, Riboflavin uptake and FAD synthesis in *Saccharomyces cerevisiae* mitochondria: involvement of the Flx1p carrier in FAD export, *J. Biol. Chem.* 279 (2004) 95–102.
- [44] M.L. Pallotta, C. Brizio, A. Fratianni, C. de Virgilio, M. Barile, S. Passarella, *Saccharomyces cerevisiae* mitochondria can synthesize FMN and FAD from externally added riboflavin and export them to the extramitochondrial phase, *FEBS Lett.* 428 (1998) 245–249.
- [45] W.B. Armiger, J.F. Forro, L.M. Montalvo, J.F. Lee, D.W. Zabriskie, The interpretation of on-line process measurements of intracellular NADH in fermentation process, *Chem. Eng. Commun.* 45 (1986) 197–206.
- [46] A. Rongvaux, F. Andris, F. van Gool, O. Leo, Reconstructing eukaryotic NAD metabolism, *Bioessays* 25 (2003) 683–690.
- [47] F. Ahmad, A.G. Moat, Nicotinic acid biosynthesis in prototrophs and tryptophan auxotrophs of *Saccharomyces cerevisiae*, *J. Biol. Chem.* 241 (1966) 775–780.
- [48] A. Knepper, M. Schleicher, M. Klauke, D. Weuster-Botz, Enhancement of the NAD (P)(H) pool in *Saccharomyces cerevisiae*, *Eng. Life Sci.* 8 (2008) 381–389.
- [49] C. Panozzo, M. Nawara, C. Suski, R. Kucharczyka, M. Skoneczny, A.-M. Becam, J. Rytko, C.J. Herbert, Aerobic and anaerobic NAD<sup>+</sup> metabolism in *Saccharomyces cerevisiae*, *FEBS Lett.* 517 (2002) 97–102.
- [50] J. Sporty, S.-J. Lin, M. Kato, T. Ognibene, B. Stewart, K. Turteltaub, G. Bench, Quantitation of NAD<sup>+</sup> biosynthesis from the salvage pathway in *Saccharomyces cerevisiae*, *Yeast* 26 (2009) 363–369.
- [51] P. Bilski, M.Y. Li, M. Ehrenschaft, M.E. Daub, C.F. Chignell, Vitamin B (pyridoxine) and its derivatives are efficient singlet oxygen quenchers and potential fungal antioxidants, *Photochem. Photobiol.* 71 (2000) 129–134.
- [52] T. Tanaka, Y. Tateno, T. Gojobori, Evolution of vitamin B6 (pyridoxine) metabolism by gain and loss of genes, *Mol. Biol. Evol.* 22 (2005) 243–250.
- [53] K. Tazuya, Y. Adachi, K. Masuda, K. Yamada, H. Kumaoka, Origin of the nitrogen atom of pyridoxine in *Saccharomyces cerevisiae*, *Biochim. Biophys. Acta* 1244 (1995) 113–116.
- [54] S. Ishida, K. Yamada, Biosynthesis of pyridoxine in *Saccharomyces cerevisiae* —origin of the pyridoxine nitrogen atom differs under anaerobic and aerobic conditions-, *J. Nutr. Sci. Vitaminol.* 48 (2002) 448–452.

### **3.3 Feedback-control based on NADH fluorescence intensity for *Saccharomyces cerevisiae* cultivations**

By Supasuda Assawajaruwan, Fiona Kuon, Matthias Funke and Bernd Hitzmann

Published 2018 in **Bioresources and Bioprocessing**.

Volume 5, Pages 1-9

DOI: [doi.org/10.1186/s40643-018-0210-z](https://doi.org/10.1186/s40643-018-0210-z)



RESEARCH

Open Access



# Feedback control based on NADH fluorescence intensity for *Saccharomyces cerevisiae* cultivations

Supasuda Assawajaruwan\*, Fiona Kuon, Matthias Funke and Bernd Hitzmann

## Abstract

**Background:** A glucose concentration is an important factor for a fed-batch process of *Saccharomyces cerevisiae*. Therefore, it is necessary to be controlled under a critical concentration to avoid overflow metabolism and to gain high productivity of biomass. In the study, 2D fluorescence spectroscopy was applied for an online monitoring and controlling of the yeast cultivations to attain the pure oxidative metabolism.

**Results:** The characteristic of the NADH intensity can effectively identify the metabolic switch between oxidative and oxidoreductive states. Consequently, the feed rate was regulated using the single signal based on the fluorescence intensity of NADH. With this closed-loop control of the glucose concentration, a biomass yield was obtained at 0.5  $g_{\text{biomass}}/g_{\text{glucose}}$ . In addition, ethanol production could be avoided during the controlled feeding phase.

**Conclusions:** The fluorescence sensor with a single signal of the NADH fluorescence intensity has potential to control a glucose concentration under the critical value in real time. Therefore, this achievement of the feedback control is promising to build up a compact and economical fluorescence sensor with the specific wavelength using light-emitting diodes and photodiodes. The sensor could be advantageous to the bioprocess monitoring because of a cost-effective and miniaturized device for routine analysis.

**Keywords:** Bioprocess monitoring, Fluorescence spectroscopy, Closed-loop control, *Saccharomyces cerevisiae*, NADH

## Background

The fundamental purpose of a fed-batch process is to achieve a high production yield at the low cost. The objective of the fed-batch cultivation of baker's yeast is to obtain a high yield of biomass. The main factor, which is considered in the fed-batch cultivation, is a glucose concentration, because it plays a pivotal role in regulating yeast metabolism. When the glucose concentration in a yeast cultivation is above a critical value, it leads to oxidoreductive metabolism and ethanol is produced as an overflow metabolite under an aerobic condition (Walker 1998). Due to the ethanol production, the yeast cultivation gains a lower biomass yield (Pham et al. 1998). This phenomenon has been known as the Crabtree effect caused by a limited respiratory capacity (Sonnleitner

and Käppeli 1986). A critical glucose concentration is in the range between 0.04 and 0.07 g/L depending on yeast strains, media components, and operation systems (Pham et al. 1998; van Hoek et al. 1998; Hantelmann et al. 2006). In industries, the oxidoreductive growth of yeasts is necessarily avoided to reach a high biomass yield. Consequently, the substrate feed rate is controlled under the critical glucose concentration to maintain oxidative metabolism. Literally, the yield coefficient ( $Y_{X/G}$ ) of an oxidative growth of yeasts attains in the range of 0.47–0.50  $g_{\text{biomass}}/g_{\text{glucose}}$  (Sonnleitner and Käppeli 1986; Pham et al. 1998; Hantelmann et al. 2006). Many studies have investigated effective approaches, such as the feed rate control with models or online measurements during a fed-batch process (Hantelmann et al. 2006; Henes and Sonnleitner 2007; Klockow et al. 2008; Craven et al. 2014; Mears et al. 2017; Vann and Sheppard 2017).

\*Correspondence: [sassawaj@uni-hohenheim.de](mailto:sassawaj@uni-hohenheim.de)  
 Department of Process Analytics and Cereal Science, University of Hohenheim, Garbenstraße 23, 70599 Stuttgart, Germany

To manipulate the glucose concentration under the critical value, an online measurement device is required to detect overflow metabolism. Two-dimensional (2D) fluorescence spectroscopy is an effective tool for online monitoring of cultivation processes (Biechele et al. 2015; Faassen and Hitzmann 2015). It was developed for measuring fluorescent molecules in a wide range of excitation and emission wavelengths to detect non-identified overlapping peaks and quenching of different fluorophores (Marose et al. 1998). Besides, it is possible to perform a non-invasive measurement without interfering an inner system of cultivation processes. The fluorescence sensor has been applied in many studies for online bioprocess monitoring and the fluorescence data can be used for quantification of fluorescence substances, particularly proteins, and for estimation of cell mass, glucose and ethanol concentrations (Haack et al. 2004; Rhee and Kang 2007; Srivastava et al. 2008; Odman et al. 2009; Rossi et al. 2012; Almqvist et al. 2016; Assawajaruwan et al. 2017a). Furthermore, 2D fluorescence spectroscopy can recognize metabolic changes during yeast cultivations (Hantelmann et al. 2006; Assawajaruwan et al. 2017b).

There is currently no commercial device, which can measure a glucose concentration at the low level of the critical point in real time. For this reason, a 2D fluorescence spectroscopy was applied in the study to investigate a signal, which can determine a metabolic switch between oxidative and oxidoreductive states. The biogenic fluorophores, such as NADH, tryptophan, flavins, and pyridoxine, were taken into consideration of the investigation because they are significantly related to the growth characteristics of yeasts (Marose et al. 1998; Hantelmann et al. 2006; Assawajaruwan et al. 2017b). The fluorescence intensity, which can greatly indicate the metabolic switch, was chosen and applied as a metabolic signal to control the glucose feed rate. In addition, it is possible to see from the study if it is promising to build up a specific-wavelength fluorescence sensor equipped with light-emitting diodes and photodiodes for yeast cultivations. The sensor will be a cost-effective and miniaturized device for routine analysis (O'Toole and Diamond 2008).

## Methods

### Yeast strain and cultivation conditions

The fed-batch cultivations were operated in a 2.5-L stainless steel tank bioreactor (Minifors, Inifors HT, Bottmingen, Switzerland) with an initial volume of 1.35 L. The amount of 2.5-g dry baker's yeast or *S. cerevisiae* (SAF Instant Red, S.I.Lesaffre, Marcq, France) was pre-cultivated in 100 mL Schatzmann medium, which consists of 0.34 g/L  $MgSO_4 \cdot 7H_2O$ , 0.42 g/L  $CaCl_2 \cdot 2H_2O$ , 4.5 g/L  $(NH_4)_2SO_4$ , 1.9 g/L  $(NH_4)_2HPO_4$ , and 0.9 g/L

KCl (Schatzmann 1975). The pre-culture was shaken for 30 min at 180 rpm and was then pumped into the bioreactor. The medium for the yeast cultivations was the same as for the pre-culture, but with glucose, 1 mL/L trace elements solution (0.015 g/L  $FeCl_3 \cdot 6H_2O$ , 9 mg/L  $ZnSO_4 \cdot 7H_2O$ , 10.5 mg/L  $MnSO_4 \cdot 2H_2O$ , and 2.4 mg/L  $CuSO_4 \cdot 5H_2O$ ), 1 mL/L vitamin solution (0.06 g/L myo-inositol, 0.03 g/L Ca-pantothenate, 6 mg/L thiamine HCl, 1.5 mg/L pyridoxine HCl, and 0.03 mg/L biotin), and 200  $\mu$ L/L antifoam agent. The fed-batch cultivations to test relevant fluorescence signals of the metabolic switch were performed with 1.5 g/L initial glucose concentration. For the fed-batch cultivations with the feedback control, the initial glucose concentration was reduced to 1.0 g/L for minimizing time of the batch phase in the beginning. The yeast cultivations were conducted in triplicate. The glucose concentration of the feed solution was 15 g/L in Schatzmann medium with trace elements and vitamin solutions. All fed-batch cultivations were performed with a maintained temperature and pH at 30 °C and 5, respectively. The aeration and agitation rates were kept constant at 4 L/min and 450 rpm, respectively. Iris software (Inifors HT, Bottmingen, Switzerland) was applied as a process control system for the bioreactor.

### Bioprocess setup and control

#### Manual control

A peristaltic pump (Ismatec MCP Process, Cole-Parmer GmbH, Wertheim, Germany) was connected to the bioreactor and computer. For the investigation of significant fluorescence signals, the feed rate was calculated based on Eq. 1, which is referred from a mathematical model of a fed-batch cultivation process (Rode Kristensen 2003; Henes and Sonnleitner 2007):

$$F_0 = \frac{\mu}{Y_{x/s}(S_f - S_0)} V_0 X_0 e^{\mu t_0} \quad (1)$$

$$t_p = \frac{1}{\mu_p} < \frac{1}{\mu_{\max \text{ on glucose}}} \quad (2)$$

$$F(t) = F_0 e^{\frac{t}{t_p}}, \quad (3)$$

where  $F_0$  and  $F(t)$  are the feed rate at the beginning and at time  $t$ , respectively.  $\mu$  is the maximum specific growth rate of yeasts on glucose.  $V_0$  is the volume of the culture broth at the start of feeding.  $X_0$  is the biomass concentration at the start of feeding.  $Y_{x/s}$  is the yield coefficient for biomass with respect to glucose.  $S_f$  and  $S_0$  are the glucose concentration of the feed solution and the cultivation at the start of feeding, respectively.  $t_0$  is the time at the start of feeding.  $t_p$  is a time constant converted from the specific growth rate ( $h^{-1}$ ), which is considered to be

higher than the maximum specific growth rate on glucose ( $\mu_p > \mu_{\max \text{ on glucose}}$ ) to drive the metabolism from a state of pure oxidative glucose consumption to an oxidoreductive mode.

After the initial glucose in the batch phase was depleted, the glucose feed solution was pumped with the starting feed rate ( $F_0$ ) at 0.87 mL/min to maintain an oxidative consumption of glucose. When the steady state of an oxidative phase was reached, the feed solution was exponentially pumped into the bioreactor based on Eq. 3. The feed rate was manually controlled via MATLAB (R2015b).

#### Closed-loop control

For the fed-batch cultivations with the feedback control, the feed rate was also calculated based on Eqs. 1–3, but it was regulated with the online measured fluorescence spectral data from the fluorescence spectrometer (BioView, DELTA Lights & Optics, Hørsholm, Denmark). The computer connecting to BioView collected the measured spectra and sent the spectra to another computer, which was connected to the pump, as illustrated in Fig. 1a.

The feed rate was manipulated based on the NADH intensity (ex330/em450) according to its intensity change referred to the metabolic switch from oxidative to oxidoreductive states. The signal of the metabolic change to an oxidoreductive state is detected as a noise signal in the oxidative metabolism. For this reason, the Savitzky–Golay filter for derivative of signal curves was applied to pronounce the peak of the metabolic change. The NADH spectra were first smoothed with the three-point median filter to reduce regular noises occurring from the turbidity of the culture and the device itself, not from the metabolic change. Then the median-smoothed NADH spectra were processed with the Savitzky–Golay filter for first derivative (quadratic, five-point size) as in Eq. 4 (Gorry 2002). These derivative values were named as a metabolic signal. The metabolic signal was used to indicate the metabolic switch between oxidative and oxidoreductive states:

$$N'_j = (-2 \times N_{j-2} - 1 \times N_{j-1} + 0 \times N_j + 1 \times N_{j+1} + 2 \times N_{j+2}) \times \frac{1}{10\Delta t}, \quad (4)$$

where  $N_j$  and  $N'_j$  are the median-smoothed NADH intensities and its derivative at the central point of each subset, respectively.  $j$  is an index presenting the data point of the NADH measurement and  $\Delta t$  is the time interval between each measurement of the NADH intensity, which is 1.5 min.

The glucose feed solution was being pumped with the starting feed rate ( $F_0$ ) into the fermenter when the initial

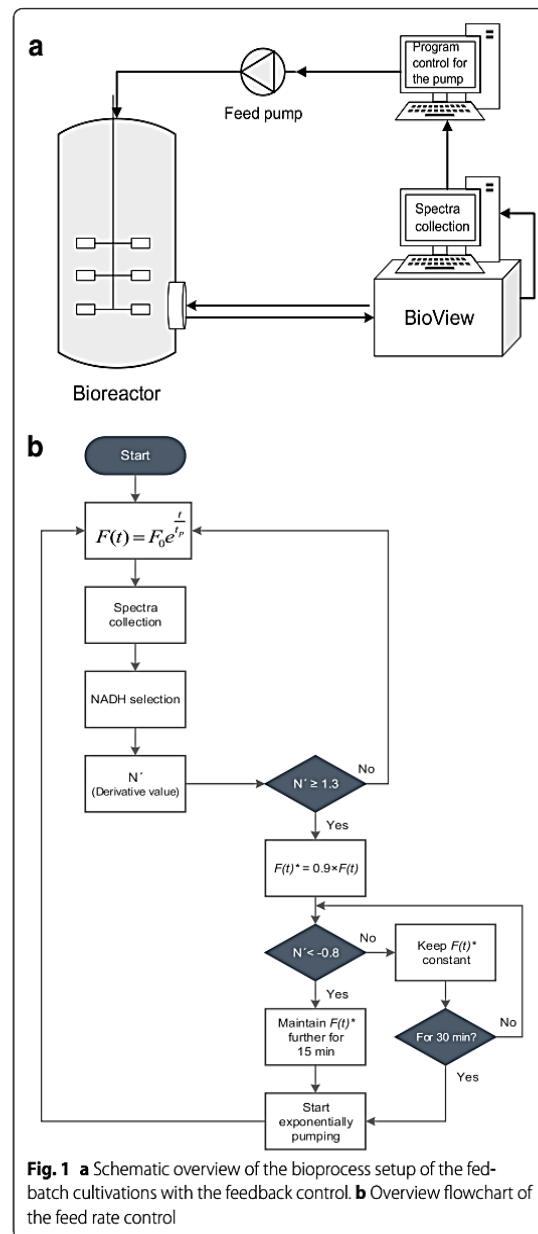


**Fig. 1** a Schematic overview of the bioprocess setup of the fed-batch cultivations with the feedback control. b Overview flowchart of the feed rate control

glucose in the batch phase ran out. Then, the feed solution was exponentially pumped into the bioreactor as the function shown in Eq. 3 after reaching the steady state of an oxidative phase. The feed rate was manipulated under the program control by MATLAB (R2015b) as shown in Fig. 1b. As illustrated in the scheme, the current feed rate at that time point will be 10% reduced when the derivative value is more than or equal to the upper threshold signal ( $N' \geq 1.3$  rel. unit/min). Then, the 10%–reduced

feed rate ( $F(t)^* = 0.9F(t)$ ) will be kept pumping for 30 min or till the lower threshold signal is achieved, which is  $-0.8$  rel. unit/min. In the latter case, the 10%—reduced feed rate will be constantly pumped further for 15 min. After 15 min, it will start pumping the feed solution with the exponential rate from the 10%—reduced feed rate as demonstrated in Fig. 1b.

#### Online monitoring/analysis

Relative fluorescence intensity of relevant fluorophores, such as NADH, tryptophan, pyridoxine, and flavins, was online monitored during the yeast cultivations by the BioView fluorescence spectrometer (Marose et al. 1998; Haack et al. 2004; Hantelmann et al. 2006; Faassen and Hitzmann 2015). The device is equipped with 15 different filters for excitation and emission wavelengths. The multi-wavelength fluorescence in range of 270–550 nm excitation (ex) and 310–590 nm emission (em) with increment of 20 nm were measured during the cultivations. The BioView fluorescence sensor has a xenon flash lamp as a light source for exciting molecules. The excitation light goes via the fiber optic as a guide light into the bioreactor, and the fluorescent light, which is emitted in a  $180^\circ$  angle, is monitored after passing the emission filters. Then, the fluorescent light is detected by a photomultiplier. The process runs continuously until a complete rotation of excitation and emission filters. The fluorescence sensor measured the yeast culture through a quartz window in 25-mm standard port as a non-invasive monitoring. The measurement for a single scan of the spectrum was achieved within 1.5 min. The spectrum of a scanning contains the combinations of excitation and emission wavelengths.

Dissolved oxygen was monitored continuously with OxyFerm DO sensor (Hamilton Bonaduz AG, Bonaduz, Switzerland). The online measurements of the dissolved oxygen were observed during the cultivations with the Iris Software (Inifors HT, Bottmingen, Switzerland).

#### Offline analysis

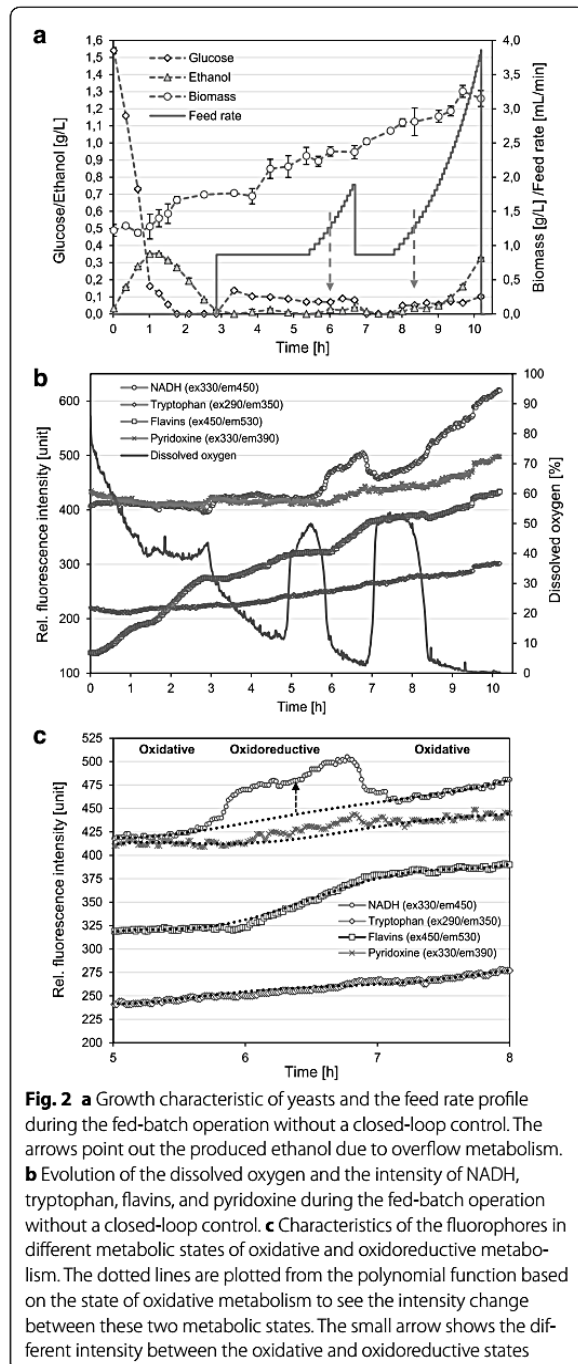
Offline samples were regularly taken from the bioreactor and put into preweighed and predried microcentrifuge tubes for analyzing biomass, glucose, and ethanol concentrations in triplicate. Dry cell mass was determined by centrifugation (Mega Star 600R, VWR International BVBA, Haasrode, Belgium) of a sample with 1.5 mL (two times) at 14,000 rpm for 10 min at  $4^\circ\text{C}$ . The wet cells were put in a drying oven at  $100^\circ\text{C}$  for 24 h. Subsequently, they were cooled down for 30 min before weighing. The supernatant of the samples after the centrifugation was examined by HPLC (ProStar, Variant, Walnut Creek, CA, USA) to determine glucose and ethanol concentrations. The supernatant was firstly filtrated with pore size filter,

0.2  $\mu\text{m}$ , polypropylene membrane (VWR, Darmstadt, Germany). Then, the filtrate was injected 20  $\mu\text{L}$  into a Rezex ROA-organic acid H+ (8%) column (Phenomenex, Aschaffenburg, Germany) and operated at  $70^\circ\text{C}$  with 5 mM  $\text{H}_2\text{SO}_4$  as an eluent at 0.6 mL/min flow rate. The concentrations of glucose and ethanol were calculated by Software Galaxie™ Chromatography (Varian, Walnut Creek, CA, USA).

## Results and discussion

### Investigation of fluorescence signals corresponding to the metabolic change

The biogenic fluorophores, which were examined during the fed-batch process, are the peak intensity in NADH (ex330/em450), tryptophan (ex290/em350), flavins (ex450/em530), and pyridoxine (ex330/em390) regions. These fluorophores were regularly mentioned in several studies that they are related to some important metabolic pathways of yeast cells, e.g., glycolysis and TCA cycle (Marose et al. 1998; Hantelmann et al. 2006; Assawajaruwan et al. 2017b). According to an increase of the dissolved oxygen at approximately 3 h, the glucose feed solution was being pumped into the bioreactor as illustrated in Fig. 2a, b. The slight increase of the dissolved oxygen at around 3 h was assumed that glucose and ethanol substrates in the batch phase were depleted, which can be seen in Fig. 2a. After pumping the glucose feed solution, the dissolved oxygen was immediately decreasing. The feed solution was constantly pumped at the minimum rate for around 2.5 h. The dissolved oxygen dramatically increased at about 5 h and then kept slightly increasing as demonstrated in Fig. 2b. From this evolution of the dissolved oxygen between roughly 3 and 5 h, it was presumed that the cells were starving and tried to adapt themselves with the feed condition. Due to the slight increase of the dissolved oxygen after 5 h, it was assumed that the yeasts slowly maintained the steady state of oxidative metabolism. In addition, it was also assumed that there was no produced ethanol after the increment of the dissolved oxygen. If there is ethanol in the system, the dissolved oxygen would be lower, because yeasts consume more oxygen during the metabolization of ethanol (Henes and Sonnleitner 2007). It means that the metabolism after about 5 h was in a complete oxidative mode due to no production of ethanol, which can be seen in Fig. 2a. Subsequently, the feed solution was exponentially pumped until the dissolved oxygen was decreasing almost to zero, as shown in Fig. 2b. Then, the feed rate was manually set back to the minimum rate and kept constant till the dissolved oxygen increased and reached the steady state again (Fig. 2a, b). Afterwards, the feed rate was exponentially pumped again until the depletion of the dissolved oxygen. In Fig. 2a, the ethanol



was slightly produced after the feed rate was exponentially increasing (see arrows), which is corresponding to the decrease of the dissolved oxygen. Besides, the ethanol was rapidly produced, since about 9 h, because there was the lack of oxygen in the cultivation (Fig. 2a, b).

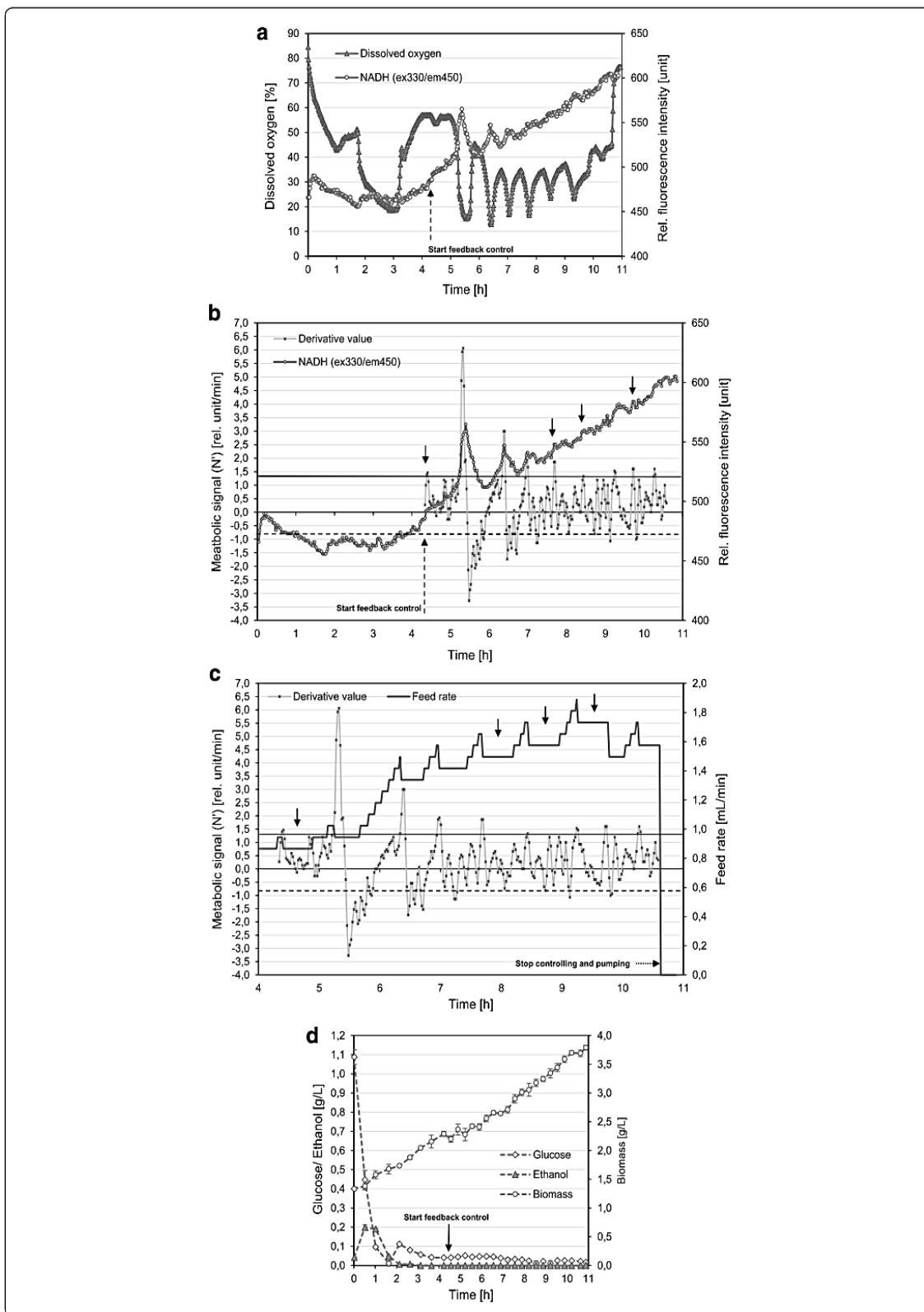
The characteristics of NADH, tryptophan, flavins, and pyridoxine intensities during the fed-batch operation were presented in Fig. 2b, c. During the exponential feeding of glucose, the NADH intensity instantly and distinctly increased comparing to other fluorophores. When the feed rate was reduced to the minimum rate and kept constant, the NADH intensity was later dropping to the oxidative state as demonstrated in Fig. 2b, c. The oxidative state can be proved from the completely consumed ethanol at about 7 h in Fig. 2a. The phenomenon of the NADH intensity has a reverse correlation with the evolution of the dissolved oxygen. The change of their fluorescence intensities between the oxidative and oxidoreductive metabolism is quantified using the polynomial function based on the oxidative state as presented in Fig. 2c. It is clear to see the increased intensity of NADH from the oxidative state, which is around 40 rel. fluorescence units in average. For other three fluorophores, the difference of their intensities from their polynomial functions is less than the half of the increased intensity of NADH, as illustrated in Fig. 2c. Regarding the results, the metabolic switch between oxidative and oxidoreductive states is recognizable from the NADH intensity, but it is not obvious to see from tryptophan, flavins, and pyridoxine. Although the intensity of flavins was slowly increasing after 6 h, it responded to the overflow metabolism slower than NADH did. Furthermore, it cannot be recognized when the oxidative mode returns.

NADH/NAD<sup>+</sup> as redox carriers are prerequisite for catabolic and anabolic reactions, particularly, for providing cells with energy in the form of ATP. Due to the overflow metabolism, NADH is accumulated as shown in Fig. 2c and yeast cells need to maintain their cellular redox balance or metabolic homeostasis of NADH/NAD<sup>+</sup> ratio. Therefore, the accumulation of NADH due to high glycolytic fluxes leads to the formation of byproducts, such as ethanol and glycerol (Vemuri et al. 2007; Chen et al. 2014). Then, these fermentation products, e.g., ethanol and glycerol, are further oxidized through the TCA cycle and the oxidative phosphorylation for generating ATP to reach the requirement of growth (Brauer et al. 2005).

#### Online controlling of the feed rate using the metabolic signal

The NADH intensity was applied as a single signal for the feed control in real time. The evolution of the NADH intensity during the fed-batch process is illustrated in Fig. 3a. The feedback control started functioning at the same time as starting exponential feed rates (see an arrow in Fig. 3a). After approximately 5 h, the NADH intensity significantly increased, whereas the dissolved oxygen declined. As mentioned above that the NADH intensity

# CHAPTER 3.3. FEEDBACK-CONTROL BASED ON NADH FLUORESCENCE INTENSITY FOR *SACCHAROMYCES CEREVISIAE* CULTIVATIONS



(See figure on previous page)

**Fig. 3** **a** Evolution of the dissolved oxygen and the NADH intensity during the fed-batch operation with the closed-loop control. **b** Evolution of the NADH intensity and its derivative as a metabolic signal during the fed-batch operation with the closed-loop control. The arrows show the points that the upper threshold was reached, but it might be because of the noise of the NADH intensity. **c** Metabolic signals and the feed rate profile during the controlled feeding phase. The arrows refer to the time that the lower threshold signal was not reached. **d** Glucose, ethanol, and biomass concentrations during the fed-batch operation with the closed-loop control

drops back to the same gradient of the linear rate, which indicates a state of oxidative metabolism, when the feed rate was reduced and kept constant. Besides, no matter how high the incline of the NADH peak is, the intensity will decrease to the same state of an oxidative phase (Fig. 3a). This phenomenon is observed empirically during the fed-batch cultivations. Due to the reduction of the dissolved oxygen, it can be presumed that more substrate was applied as shown in Figs. 2b and 3a. However, it is not clear to see which level of the dissolved oxygen indicates the overflow metabolism.

The NADH intensity obtained in real time during the fed-batch operation was computationally converted to the metabolic signal. The metabolic signals or derivative values during the controlled feeding phase are demonstrated in Fig. 3b, c. The upper and lower threshold signals were illustrated with the solid and dashed lines, respectively (Fig. 3b, c). The level of the threshold signals was determined from experiments by trial and error. However, they were realized based on outside noise area, which was between these two lines. For the upper threshold ( $N' \geq 1.3$  rel. unit/min), the level was not set too high from the noise area to deter reaching overflow metabolism in time. The lower threshold ( $N' < -0.8$  rel. unit/min) was also not set too low from the noises, because, if the lower threshold is not reached, it will take too long to maintain the constant reduced feed rate. Then, the glucose substrate might be too low for the yeast cells to reach an optimum growth. Although the lower threshold is achieved, the reduced feed rate is still maintained constant for a short while to make sure that the metabolism turns back to an oxidative state (Fig. 3b, c). There were a few times that the lower threshold was not reached after the upper threshold arrived (see arrows in Fig. 3c). In this case, the reduced feed rate will be maintained constant for 30 min before exponential feeding (Fig. 1b). The pause time to maintain the constant reduced feed rate was determined based on experiments. In some cases of reaching the upper threshold, it might be due to the noise intensity of NADH, as shown in Fig. 3b, with the small arrows. It could be also the reason why the lower threshold was sometimes not reached. In Fig. 3c, the feed rate at about 10 h was more reduced after the pause time, because the upper threshold was reached right away after 30 min. However, as shown in Fig. 3b, it might be because of the noise of the NADH intensity (see

the arrow between 9 and 10 h). According to the results, the feed rate was decently regulated with the metabolic signals based on the NADH intensity.

#### Growth characteristics of yeasts under the feedback control

The growth characteristics of yeasts during the fed-batch process with the feedback control are demonstrated in Table 1 and Fig. 3d. The batch phase took almost 2 h until the concentration of glucose and ethanol was depleted. The yield coefficient ( $Y_{X/G}$ ) during the batch phase is  $0.31 \text{ g}_{\text{biomass}}/\text{g}_{\text{glucose}}$ , which shows a characteristic of an oxidoreductive growth (Woehrer and Roehr 1981; Hantelmann et al. 2006). After all substrates in the batch phase ran out, the glucose feed solution was pumped into the cultivations, as can be seen at around 2 h in Fig. 3d. During 3–4 h, the fed-batch process became steady and the glucose concentrations were approximately 0.04–0.05 g/L, which are in the range of the critical value (Pham et al. 1998; van Hoek et al. 1998; Hantelmann et al. 2006). Thus, the feed solution was pumped with the exponential rate and the feedback control also started functioning. During the controlled feeding phase, the feed rate was continuously regulated in real time to keep the glucose concentrations in the range or under the range of the critical value, as shown in Fig. 3d. Furthermore, there was no production of ethanol during the controlled feeding phase, which indicates the state of oxidative metabolism. The yield coefficient during the controlled feeding phase reached  $0.49 \text{ g}_{\text{biomass}}/\text{g}_{\text{glucose}}$ , which shows the sign of a pure oxidative growth of yeasts (Sonnleitner and Käppli 1986; Pham et al. 1998; Hantelmann et al. 2006). For the entire cultivation, the yield coefficient is reduced due to the oxidoreductive growth during the batch phase, as presented in Table 1.

**Table 1** Yield coefficients during the fed-batch process of the yeast cultivations in triplicate

Cultivation phase	$Y_{X/G}$ ( $\text{g}_{\text{biomass}}/\text{g}_{\text{glucose}}$ )
Batch phase	$0.31 \pm 0.01$
Controlled feeding phase	$0.49 \pm 0.01$
Entire cultivation	$0.46 \pm 0.02$

The values in the table are mean value  $\pm$  standard deviation

The starting time of the controlled feeding phase is shown in Fig. 3d

According to the achievement of the typical high yield coefficient during the controlled phase, the 2D fluorescence spectrometer using the single signal of the NADH intensity has great potential to detect the metabolic change within 1.5 min and delivers instantaneous results to control the feed rate in real time. Although a conventional approach for the fed-batch control by off-gas analysis as respiratory quotient (RQ) is robust and widely used in industries, there is still the problem regarding a certain time delay comparing with the control by the NADH signal (Claes and van Impe 2000; Jobé et al. 2003). Besides, the cost of the fluorescence sensor with the specific wavelength equipped with light-emitting diodes and photodiodes will be more effective in comparison with off-gas analyzers (O'Toole and Diamond 2008; Yang et al. 2009). Another concern is the comparison between the potential of a direct and indirect measurement of the critical glucose concentration. Although it seems more reliable to measure directly the glucose concentration from the broth, there is a concern in a time delay and certain errors at the low critical concentration of glucose (Shimizu et al. 1988; Arndt and Hitzmann 2004).

### Conclusions

In this contribution, we proposed a control of the feed rate based on the fluorescence intensity of NADH, which was selected over tryptophan, flavins, and pyridoxine. The signal of the NADH intensity showed the best performance to determine the metabolic switch between oxidative and oxidoreductive states. Under the feedback control, the glucose concentration was capably maintained under the range of the critical value. Accordingly, the glucose was oxidatively metabolized by the cells during the controlled feeding phase. From the results, the fluorescence sensor shows great potential not only for the applications in process monitoring, but also in the process control. However, there is still a challenging task for the scale-up fermentation process using the fluorescence sensor based on the NADH signal. There are many technical issues to be considered concerning transferring the bench scale to the larger scale cultivations, i.e., pilot and production scales (Formenti et al. 2014). The critical issues of the scale-up process can be basically categorized into biological, chemical, and physical impacts. The production strains should be fundamentally robust enough to withstand changing environmental conditions in the large scale, such as new media components, substrate, pH, temperature, and oxygen inhomogeneities (Takors 2012). These changing conditions make microorganisms stressed during the cultivations and affect metabolic activities in cells, particularly, the product yield and productivity. A scale-down tool, which is principally used as a lab test simulation of large-scale conditions, is based

on the monitoring of metabolic responses (Takors 2012). Without doubt, the fluorescence sensor is the one of the powerful tools to detect the metabolic change in real time. Particularly, the NADH-based measurement can provide significant information about metabolic states of the yeast cells.

### Authors' contributions

SA designed research and experiments, analyzed data, and wrote the article under the guidance of BH. MF carried out the experiments for the part of "Investigation of fluorescence signals corresponding to the metabolic change". FK performed the experiments of the feedback control of the yeast cultivations. SA reviewed the results and edited the manuscript under the guidance of BH. All authors read and approved the final manuscript.

### Acknowledgements

Not applicable.

### Competing interests

The authors declare that they have no competing interests.

### Availability of data and materials

All data sets are presented in the main paper.

### Consent for publication

Not applicable.

### Ethics approval and consent to participate

The research does not contain any studies with human participants or animals performed by any of the authors.

### Publisher's Note

Springer Nature remains neutral with regard to jurisdictional claims in published maps and institutional affiliations.

Received: 26 March 2018 Accepted: 19 May 2018

Published online: 24 May 2018

### References

- Almqvist H, Pateraki C, Alexandri M, Koutinas A, Lidén G (2016) Succinic acid production by *Actinobacillus succinogenes* from batch fermentation of mixed sugars. *J Ind Microbiol Biotechnol* 43:1117–1130. <https://doi.org/10.1007/s10295-016-1787-x>
- Arndt M, Hitzmann B (2004) Kalman filter based glucose control at small set points during fed-batch cultivation of *Saccharomyces cerevisiae*. *Biotechnol Prog* 20:377–383. <https://doi.org/10.1021/bp034156p>
- Assawajaruwan S, Reinalter J, Hitzmann B (2017a) Comparison of methods for wavelength combination selection from multi-wavelength fluorescence spectra for on-line monitoring of yeast cultivations. *Anal Bioanal Chem* 409:707–717. <https://doi.org/10.1007/s00216-016-9823-2>
- Assawajaruwan S, Eckard P, Hitzmann B (2017b) On-line monitoring of relevant fluorophores of yeast cultivations due to glucose addition during the diauxic growth. *Process Biochem* 58:51–59. <https://doi.org/10.1016/j.procbio.2017.05.007>
- Biechele P, Busse C, Solle D, Scheper T, Reardon K (2015) Sensor systems for bioprocess monitoring. *Eng Life Sci* 15:469–488. <https://doi.org/10.1002/elsc.201500014>
- Brauer MJ, Saldanha AJ, Dolinski K, Botstein D (2005) Homeostatic adjustment and metabolic remodeling in glucose-limited yeast cultures. *Mol Biol Cell* 16:2503–2517
- Chen X, Li S, Liu L (2014) Engineering redox balance through cofactor systems. *Trends Biotechnol* 32:337–343. <https://doi.org/10.1016/j.tibtech.2014.04.003>



- Claes JE, van Impe JF (2000) Combining yield coefficients and exit-gas analysis for monitoring of the baker's yeast fed-batch fermentation. *Bioprocess Eng* 22:195–200
- Craven S, Whelan J, Glennon B (2014) Glucose concentration control of a fed-batch mammalian cell bioprocess using a nonlinear model predictive controller. *J Process Control* 24:344–357. <https://doi.org/10.1016/j.jproc.ont.2014.02.007>
- Faassen SM, Hitzmann B (2015) Fluorescence spectroscopy and chemometric modeling for bioprocess monitoring. *Sensors (Basel)* 15:10271–10291. <https://doi.org/10.3390/s150510271>
- Formenti LR, Nørrgaard A, Bolic A, Hernandez DQ, Hagemann T, Heins A, Larsson H, Mears L, Mauricio-Iglesias M, Krühne U, Gernaey KV (2014) Challenges in industrial fermentation technology research. *Biotechnol J* 9:727–738. <https://doi.org/10.1002/biot.201300236>
- Gorry PA (2002) General least-squares smoothing and differentiation by the convolution (Savitzky–Golay) method. *Anal Chem* 62:570–573. <https://doi.org/10.1021/ac00205a007>
- Haack MB, Eliasson A, Olsson L (2004) On-line cell mass monitoring of *Saccharomyces cerevisiae* cultivations by multi-wavelength fluorescence. *J Biotechnol* 114:199–208. <https://doi.org/10.1016/j.jbiotec.2004.05.009>
- Hantelmann K, Kollecker M, Hüll D, Hitzmann B, Scheper T (2006) Two-dimensional fluorescence spectroscopy: a novel approach for controlling fed-batch cultivations. *J Biotechnol* 121:410–417. <https://doi.org/10.1016/j.jbiotec.2005.07.016>
- Henes B, Sonnleitner B (2007) Controlled fed-batch by tracking the maximal culture capacity. *J Biotechnol* 132:118–126. <https://doi.org/10.1016/j.jbiotec.2007.04.021>
- Jobé AM, Herwig C, Surzyn M, Walker B, Marison I, von Stockar U (2003) Generally applicable fed-batch culture concept based on the detection of metabolic state by on-line balancing. *Biotechnol Bioeng* 82:627–639. <https://doi.org/10.1002/bit.10610>
- Klockow C, Hüll D, Hitzmann B (2008) Model based substrate set point control of yeast cultivation processes based on FIA measurements. *Anal Chim Acta* 623:30–37. <https://doi.org/10.1016/j.aca.2008.06.011>
- Kristensen NR (2003) Fed-batch process modelling for state estimation and optimal control: a stochastic grey-box modelling framework, [1. oplag]. Department of Chemical Engineering, Technical University of Denmark, Lyngby
- Marose S, Lindemann C, Scheper T (1998) Two-dimensional fluorescence spectroscopy: a new tool for on-line bioprocess monitoring. *Biotechnol Prog* 14:63–74. <https://doi.org/10.1021/bp970124o>
- Mears L, Stocks SM, Sin G, Gernaey KV (2017) A review of control strategies for manipulating the feed rate in fed-batch fermentation processes. *J Biotechnol* 245:34–46. <https://doi.org/10.1016/j.jbiotec.2017.01.008>
- Odman P, Johansen CL, Olsson L, Gernaey KV, Lantz AE (2009) On-line estimation of biomass, glucose and ethanol in *Saccharomyces cerevisiae* cultivations using in situ multi-wavelength fluorescence and software sensors. *J Biotechnol* 144:102–112. <https://doi.org/10.1016/j.jbiotec.2009.08.018>
- O'Toole M, Diamond D (2008) Absorbance based light emitting diode optical sensors and sensing devices. *Sensors* 8:2453–2479
- Pham HTB, Larsson G, Enfors S (1998) Growth and energy metabolism in aerobic fed-batch cultures of *Saccharomyces cerevisiae*: simulation and model verification. *Biotechnol Bioeng* 60:474–482. [https://doi.org/10.1002/\(SICI\)1097-0290\(19981120\)60:4%3C474:AID-BIT9%3E3.0.CO;2-J](https://doi.org/10.1002/(SICI)1097-0290(19981120)60:4%3C474:AID-BIT9%3E3.0.CO;2-J)
- Rhee JI, Kang T (2007) On-line process monitoring and chemometric modeling with 2D fluorescence spectra obtained in recombinant *E. coli* fermentations. *Process Biochem* 42:1124–1134. <https://doi.org/10.1016/j.procbio.2007.05.007>
- Rossi DM, Solle D, Hitzmann B, Ayub MAZ (2012) Chemometric modeling and two-dimensional fluorescence analysis of bioprocess with a new strain of *Klebsiella pneumoniae* to convert residual glycerol into 1,3-propanediol. *J Ind Microbiol Biotechnol* 39:701–708. <https://doi.org/10.1007/s10295-011-1075-8>
- Schatzmann H (1975) Anaerobes Wachstum von *Saccharomyces*. Dissertation, ETH No. 5504
- Shimizu K, Marikawa M, Mizutanil S, Iijima S, Matsubara M, Konayashi T (1988) Comparison of control techniques for baker's yeast culture using an automatic glucose analyzer. *J Chem Eng Japan* 21:113–117. <https://doi.org/10.1252/jcej.21.113>
- Sonnleitner B, Käppli O (1986) Growth of *Saccharomyces cerevisiae* is controlled by its limited respiratory capacity: formulation and verification of a hypothesis. *Biotechnol Bioeng* 28:927–937
- Srivastava S, Harsh S, Srivastava AK (2008) Use of NADH fluorescence measurement for on-line biomass estimation and characterization of metabolic status in bioreactor cultivation of plant cells for azadirachtin (a biopesticide) production. *Process Biochem* 43:1121–1123. <https://doi.org/10.1016/j.procbio.2008.06.008>
- Takors R (2012) Scale-up of microbial processes: impacts, tools and open questions. *J Biotechnol* 160:3–9. <https://doi.org/10.1016/j.jbiotec.2011.12.010>
- van Hoek P, van Dijken JP, Pronk JT (1998) Effect of specific growth rate on fermentative capacity of baker's yeast. *Appl Environ Microbiol* 64:4226–4233
- Vann L, Sheppard J (2017) Use of near-infrared spectroscopy (NIRs) in the biopharmaceutical industry for real-time determination of critical process parameters and integration of advanced feedback control strategies using MIDUS control. *J Ind Microbiol Biotechnol* 44:1589–1603. <https://doi.org/10.1007/s10295-017-1984-2>
- Vemuri GN, Eiteman MA, McEwen JE, Olsson L, Nielsen J (2007) Increasing NADH oxidation reduces overflow metabolism in *Saccharomyces cerevisiae*. *Proc Natl Acad Sci USA* 104:2402–2407. <https://doi.org/10.1073/pnas.0607469104>
- Walker GM (1998) Yeast physiology and biotechnology. Wiley, Chichester
- Woehrer W, Roehr M (1981) Regulatory aspects of baker's yeast metabolism in aerobic fed-batch cultures. *Biotechnol Bioeng* 23:567–581
- Yang F, Pan J, Zhang T, Fang Q (2009) A low-cost light-emitting diode induced fluorescence detector for capillary electrophoresis based on an orthogonal optical arrangement. *Talanta* 78:1155–1158. <https://doi.org/10.1016/j.talanta.2009.01.033>

Submit your manuscript to a SpringerOpen® journal and benefit from:

- Convenient online submission
- Rigorous peer review
- Open access: articles freely available online
- High visibility within the field
- Retaining the copyright to your article

Submit your next manuscript at ► [springeropen.com](http://springeropen.com)

# **Chapter 4**

## **Conclusion and final remarks**

## 4.1 Conclusion

On-line bioprocess monitoring has been studied and developed for many years (Biechele et al., 2015; Claßen et al., 2017). For the time being, it still plays an important role in bioprocesses and it is being continuously developed. Bioprocesses are complex systems, therefore, potential and effective devices are needed to monitor, control and optimize the processes. 2D fluorescence spectroscopy is one of the potential techniques for an on-line monitoring without any interfering processes, which reduces the risk of contamination in a bioreactor. Besides, it provides real-time information and bypasses the need to sampling data (Faassen and Hitzmann, 2015; Claßen et al., 2017). Biogenic fluorophores inside cells can be monitored in real time via 2D fluorescence spectroscopy (Lindemann et al., 1998; Marose et al., 1998; Rhee and Kang, 2007). For this reason, a 2D fluorescence spectroscopy was chosen for the research.

A 2D fluorescence spectrometer, which was applied in the study, is the BioView fluorescence spectrometer. The device is equipped with 15 different filters for excitation and emission wavelengths. The measurement of one spectrum using the BioView spectrometer has 120 fluorescence intensity variables of excitation and emission wavelength combinations (WLCs); scattered light is not considered here. The three selection methods, such as (1) method based on loadings, (2) variable importance in projection (VIP) and (3) ant colony optimization (ACO), have been performed to choose relevant and significant WLCs on target substances of yeast cultivations. The five selected WLCs from each selection method were used to predict the analytes by MLR and the MLR models were evaluated with the RMSEP and  $R^2$ . Regarding the results of the MLR models, all selected WLCs had a good predictive performance on glucose, ethanol and biomass concentrations, so the three selection methods apparently performed in a good way. It could be because these three methods have chosen WLCs, mostly in the same regions of biogenic fluorophores, such as NADH, tryptophan, pyridoxine and flavins. However, the calculating process of the method based on loadings and VIP spent less time than ACO. From all selected WLCs, there were seven different excitation and emission wavelengths. These different excitation and emission wavelengths were combined each other to have 38 WLCs. The PLS models with 120 as well as 38 WLCs were implemented to compare their predictive performance. Their pRMSEPs had no significant difference, regarding the results. Thus, it is promising to build a fluorescence sensor with only 14 filters for monitoring yeast cultivations.

The 2D fluorescence spectrometer cannot directly measure glucose and ethanol concentrations because they are not fluorescent. However, it can monitor the fluorescent molecules relating to cellular activities, such as NADH, tryptophan, pyridoxine, riboflavin and

FAD/FMN. Biogenic fluorophores inside cells are key metabolic components to understanding cellular activities, which in turn explains states of cultivation processes (Li et al., 1991). The three different conditions of yeast cultivations, i.e., batch, fed-batch with the glucose pulse during the glucose growth phase (GP) and fed-batch with the glucose pulse during the ethanol growth phase (EP), have been conducted to observe the behavior of intracellular fluorophores in real time. A change of fluorescence intensities in the spectra of the fed-batch cultivations with the glucose pulse during GP was not recognized. Their fluorescence spectra looked similar to the ones of the batch cultivations, but their intensities were higher and their glucose growth phase took longer. The glucose addition might be detected as a normal glucose signal during GP. On the contrary, the glucose pulse during EP can be clearly seen in the fluorescence spectra. The different states of yeast fermentation processes, particularly the glucose pulse during EP, can be recognized and identified from the on-line fluorescence spectra by PCA. Due to the glucose pulse during EP, the change of NADH, tryptophan, pyridoxine, riboflavin and FAD/FMN intensities was not in the same direction. The fluorescence intensity of NADH and riboflavin increased, but the intensity of tryptophan, pyridoxine and FAD/FMN decreased. The relation between tryptophan and NADH in the yeast metabolism has been studied by Knepper et al., 2008. The change of their intensities can be quantified as a proportional factor, corresponding to various glucose concentrations with the coefficient of determination,  $R^2 = 0.999$ .

According to the previous results, 2D fluorescence spectroscopy can effectively monitor the real-time changes of the relevant fluorophores, such as tryptophan, pyridoxine, NADH, riboflavin and FAD/FMN. The signal of the NADH intensity showed the best performance to determine the metabolic switch between oxidative and oxidoreductive states. Therefore, a control of glucose feed rates was based on the fluorescence intensity of NADH, which was selected over tryptophan, flavins and pyridoxine. Under the feedback control, the glucose concentration was capably maintained under the range of the critical value. Accordingly, ethanol production could be avoided and glucose was purely metabolized by yeasts during the controlled feeding phase. With this closed-loop control of the glucose concentration, a biomass yield was obtained at  $0.5 \text{ g}_{\text{biomass}}/\text{g}_{\text{glucose}}$ . According to the achievement of the typical high yield coefficient during the controlled feeding phase, the 2D fluorescence spectrometer using the NADH intensity has great potential to detect the metabolic change within 1.5 min and delivers instantaneous results to control the feed rates in real time. Although a conventional approach for the fed-batch control by off-gas analysis as respiratory quotient (RQ) is robust and widely used in industries, there is still the problem regarding a certain time delay comparing with the

control by the NADH signal (Claes and van Impe, 2000; Jobé et al., 2003). Besides, the cost of a fluorescence sensor with specific wavelengths equipped with light-emitting diodes and photodiodes will be more effective in comparison with off-gas analyzers (O'Toole and Diamond, 2008; Yang et al., 2009). Another concern is the comparison between the potential of a direct and indirect measurement of the critical glucose concentration. Although it seems more reliable to measure directly a glucose concentration from the broth, there is a concern in a time delay and certain errors at the low critical concentration of glucose (Shimizu et al., 1988; Arndt and Hitzmann, 2004). Without doubt, the fluorescence sensor is one of the powerful tools to detect the metabolic change in real time. Regarding the results of the overall study, the 2D fluorescence spectrometer shows great potential not only for the application in a process monitoring, but also in a process control.

## 4.2 Final remarks

In the study, 2D fluorescence spectroscopy has been applied not only for an on-line monitoring, but also for a process control of the yeast cultivations. It showed great potential to provide informative data of the yeast cultivations in real time. Even though the target substances like glucose and ethanol are not fluorescent, the performance of their predictions based on the fluorescence spectral data, particularly, from NADH, tryptophan, pyridoxine, riboflavin and FAD/FMN, showed a high correlation. Through the on-line monitoring of these relevant intracellular fluorophores, metabolic states during the yeast cultivations can be recognized at the proper time.

Using fresh and dry baker's yeasts for the cultivations was conveniently prepared, but there was an issue from time to time about the unreproducible results of the cultivations. As a result of the commercial yeast products, it was not easy to have the same lot number for the experiments. When the identical input is not well controlled, it will be troublesome to achieve reproducible results. Therefore, utilization of a pure strain of *S. cerevisiae* would be a good solution for future experiments.

The application of the single pair of NADH (ex330/em450) for the feedback control effectively performed to maintain the glucose concentration under the critical point. However, there was occasionally misinterpretation of the metabolic signal due to the noise in the NADH intensity. Thus, it could be more effective to apply the entire region of NADH as a metabolic signal. Then all wavelength pairs in NADH area will be processed using PCA to reduce their non-informative data and noise.

Lastly, the increased glucose feed rate during the cultivations can be recognized through the dissolved oxygen. Consequently, a working combination of a fluorescence sensor and a dissolved oxygen probe could be a promising technique for controlling a substrate feed rate.

## Bibliography

- Ahmed F, Moat AG. 1966. Nicotinic acid biosynthesis in prototrophs and tryptophan auxotrophs of *Saccharomyces cerevisiae*. *The Journal of Biological Chemistry*:775–780.
- Albani RJ. 2007. *Principles and Applications of Fluorescence Spectroscopy*.
- Allegrini F, Olivieri AC. 2011. A new and efficient variable selection algorithm based on ant colony optimization. Applications to near infrared spectroscopy/partial least-squares analysis. *Analytica chimica acta* 699:18–25.
- Arndt M, Hitzmann B. 2004. Kalman filter based glucose control at small set points during fed-batch cultivation of *Saccharomyces cerevisiae*. *Biotechnology progress* 20:377–383.
- Bacher A, Eberhardt S, Fischer M, Kis, K. and Richter, G. 2000. Biosynthesis of vitamin B2 (Riboflavin). *Annual Review of Nutrition*:153–167.
- Bafunno V, Giancaspero TA, Brizio C, Bufano D, Passarella S, Boles E, Barile M. 2004. Riboflavin uptake and FAD synthesis in *Saccharomyces cerevisiae* mitochondria: involvement of the Flx1p carrier in FAD export. *The Journal of Biological Chemistry* 279:95–102.
- Barnett JA. 1992. The taxonomy of the genus *Saccharomyces meyen ex reess*: A short review for non-taxonomists. *Yeasts* 8:1–23.
- Bass D. 2000. *An Introduction to Fluorescence Spectroscopy*.
- Biechele P, Busse C, Solle D, Scheper T, Reardon K. 2015. Sensor systems for bioprocess monitoring. *Eng. Life Sci.* 15:469–488.
- Blum C. 2005. Ant colony optimization: Introduction and recent trends. *Physics of Life Reviews* 2:353–373.
- Boekhout T, Kurtzman CP. 1996. Principles and Methods Used in Yeast Classification, and an Overview of Currently Accepted Yeast Genera. *Nonconventional Yeasts in Biotechnology*:1–81.
- Brauer MJ, Saldanha AJ, Dolinski, K. and Botstein, D. 2005. Homeostatic Adjustment and Metabolic Remodeling in glucose-limited Yeast cultures. *Molecular Biology of the Cell*:2503–2517.
- CAMO Process AS. 2006. *The Unscrambler Tutorials*.
- Chen X, Li S, Liu L. 2014. Engineering redox balance through cofactor systems. *Trends in biotechnology* 32:337–343.
- Claes JE, van Impe JF. 2000. Combining yield coefficients and exit-gas analysis for monitoring of the baker's yeast fed-batch fermentation. *Bioprocess Engineering*:195–200.

- Claßen J, Aupert F, Reardon KF, Solle D, Scheper T. 2017. Spectroscopic sensors for in-line bioprocess monitoring in research and pharmaceutical industrial application. *Analytical and bioanalytical chemistry* 409:651–666.
- Dorigo M, Maniezzo V, Colomi A. 1996. Ant system: optimization by a colony of cooperating agents. *IEEE Transactions on Systems, Man, and Cybernetics, Part B (Cybernetics)* 26:29–41.
- Faassen SM, Hitzmann B. 2015. Fluorescence spectroscopy and chemometric modeling for bioprocess monitoring. *Sensors (Basel, Switzerland)* 15:10271–10291.
- Gorry PA. 2002. General least-squares smoothing and differentiation by the convolution (Savitzky-Golay) method. *Anal. Chem.* 62:570–573.
- Gosselin R, Rodrigue D, Duchesne C. 2010. A Bootstrap-VIP approach for selecting wavelength intervals in spectral imaging applications. *Chemometrics and Intelligent Laboratory Systems* 100:12–21.
- Grote B, Jinu MJ, Hitzmann B. 2011. Erschließen von Prozesswissen für das Monitoring und die Regelung von Fermentationsprozessen. *Systeme und Anwendungen der Messtechnik* 78:569–578.
- Guo Q, Wu W, Massart D, Boucon C, Jong S de. 2002. Feature selection in principal component analysis of analytical data. *Chemometrics and Intelligent Laboratory Systems* 61:123–132.
- Haack MB, Eliasson A, Olsson L. 2004. On-line cell mass monitoring of *Saccharomyces cerevisiae* cultivations by multi-wavelength fluorescence. *Journal of Biotechnology* 114:199–208.
- Hantelmann K, Kollecker M, Hüll D, Hitzmann B, Scheper T. 2006. Two-dimensional fluorescence spectroscopy: a novel approach for controlling fed-batch cultivations. *Journal of Biotechnology* 121:410–417.
- Havlik I, Lindner P, Scheper T, Reardon KF. 2013. On-line monitoring of large cultivations of microalgae and cyanobacteria. *Trends in biotechnology* 31:406–414.
- Ishida S, Yamada K. 2002. Biosynthesis of pyridoxine in *Saccharomyces cerevisiae* -Origin of the pyridoxine nitrogen atom differs under anaerobic and aerobic conditions. *Journal of Nutritional Science and Vitaminology*:448–452.
- Jobé AM, Herwig C, Surzyn M, Walker B, Marison I, Stockar U von. 2003. Generally applicable fed-batch culture concept based on the detection of metabolic state by on-line balancing. *Biotechnology and Bioengineering* 82:627–639.
- Johnston M. 1999. Feasting, fasting and fermenting: Glucose sensing in yeast and other cells. *Trends in Genetics* 15:29–33.



- Junker BH, Wang HY. 2006. Bioprocess monitoring and computer control: key roots of the current PAT initiative. *Biotechnology and Bioengineering* 95:226–261.
- Käppeli O, Sonnleitner B, Blanch HW. 2008. Regulation of Sugar Metabolism in *Saccharomyces* -Type Yeast: Experimental and Conceptual Considerations. *Critical Reviews in Biotechnology* 4:299–325.
- Knepper A, Schleicher M, Klauke M, Weuster-Botz D. 2008. Enhancement of the NAD(P)(H) Pool in *Saccharomyces cerevisiae*. *Eng. Life Sci.* 8:381–389.
- Kristensen RN. 2002. *Fed-Batch Process Modelling for State Estimation and Optimal Control*. Copenhagen, Denmark: Nørhaven Digital.
- Lakowicz JR. 2006. *Principles of fluorescence spectroscopy*. 3rd ed. New York: Springer.
- Lei F, Rotbøll M, Jørgensen SB. 2001. A biochemically structured model for *Saccharomyces cerevisiae*. *Journal of Biotechnology* 88:205–221.
- Li JK, Asali EC, Humphrey AE, Horvath JJ. 1991. Monitoring cell concentration and activity by multiple excitation fluorometry. *Biotechnology progress* 7:21–27.
- Li JK, Humphrey AE. 1991. Use of fluorometry for monitoring and control of a bioreactor. *Biotechnology and Bioengineering* 37:1043–1049.
- Lindemann C, Marose S, Nielsen H, Scheper T. 1998. 2-Dimensional fluorescence spectroscopy for on-line bioprocess monitoring. *Sensors and Actuators B: Chemical* 51:273–277.
- Marose S, Lindemann C, Scheper T. 1998. Two-dimensional fluorescence spectroscopy: a new tool for on-line bioprocess monitoring. *Biotechnology progress* 14:63–74.
- Marquard D, Enders A, Roth G, Rinas U, Scheper T, Lindner P. 2016. In situ microscopy for online monitoring of cell concentration in *Pichia pastoris* cultivations. *Journal of Biotechnology* 234:90–98.
- Martens H, Naes T. 1989. *Multivariate Calibration*.
- Mehmood T, Liland KH, Snipen L, Sæbø S. 2012. A review of variable selection methods in Partial Least Squares Regression. *Chemometrics and Intelligent Laboratory Systems* 118:62–69.
- Mullen RJ, Monekosso D, Barman S, Remagnino P. 2009. A review of ant algorithms. *Expert Systems with Applications* 36:9608–9617.
- O'Toole M, Diamond D. 2008. Absorbance based light emitting diode optical sensors and sensing devices. *Sensors*:2453–2479.
- Otto M. 1999. *Chemometrics: Statistics and computer application in analytical chemistry*.

- Ozcan S, Dover J, Rosenwald AG, Wolfl S, Johnston M. 1996. Two glucose transporters in *Saccharomyces cerevisiae* are glucose sensors that generate a signal for induction of gene expression. *Proc. Natl. Acad. Sci. USA* 93:12428–12432.
- Pallotta ML, Brizio C, Fratianni A, Virgilio C de, Barile M, Passarella S. 1998. *Saccharomyces cerevisiae* mitochondria can synthesise FMN and FAD from externally added riboflavin and export them to the extramitochondrial phase. *FEBS Letters* 428:245–249.
- Pham HTB, Larsson G, Enfors S. 1998. Growth and energy metabolism in aerobic fed-batch cultures of *Saccharomyces cerevisiae*: Simulation and model verification. *Biotechnology and Bioengineering*:474–482.
- Ranzan C, Strohm A, Ranzan L, Trierweiler LF, Hitzmann B, Trierweiler JO. 2014. Wheat flour characterization using NIR and spectral filter based on Ant Colony Optimization. *Chemometrics and Intelligent Laboratory Systems* 132:133–140.
- Rhee JI, Kang T. 2007. On-line process monitoring and chemometric modeling with 2D fluorescence spectra obtained in recombinant *E. coli* fermentations. *Process Biochemistry* 42:1124–1134.
- Schalk R, Georg D, Staubach J, Raedle M, Methner F, Beuermann T. 2017. Evaluation of a newly developed mid-infrared sensor for real-time monitoring of yeast fermentations. *Journal of bioscience and bioengineering* 123:651–657.
- Shamsipur M, Zare-Shahabadi V, Hemmateenejad B, Akhond M. 2006. Ant colony optimisation: A powerful tool for wavelength selection. *J. Chemometrics* 20:146–157.
- Shane B, Snell Esmond E. 1976. Transport and metabolism of vitamin B6 in the yeast *Saccharomyces carlsbergensis* 4228. *The Journal of Biological Chemistry*:1042–1051.
- Shimizu K, Marikawa M, Mizutani I S, Iijima S, Matsubara M, Konayashi T. 1988. Comparison of control techniques for baker's yeast culture using an automatic glucose analyzer. *Journal of Chemical Engineering Japan*:113–117.
- Singh GP, Goh S, Canzoneri M, Ram RJ. 2015. Raman spectroscopy of complex defined media: Biopharmaceutical applications. *J. Raman Spectrosc.* 46:545–550.
- Solle D, Geissler D, Stärk E, Scheper T, Hitzmann B. 2003. Chemometric modelling based on 2D-fluorescence spectra without a calibration measurement. *Bioinformatics* 19:173–177.
- Sonnleitner B, Käppeli O. 1986. Growth of *Saccharomyces cerevisiae* is controlled by its limited respiratory capacity: Formulation and verification of a hypothesis. *Biotechnology and Bioengineering*:927–937.

- Sporty J, Lin S, Kato M, Ognibene T, Stewart B, Turteltaub K, Bench G. 2009. Quantitation of NAD<sup>+</sup> biosynthesis from the salvage pathway in *Saccharomyces cerevisiae*. *Yeast* (Chichester, England) 26:363–369.
- Srinivas SP, Mutharasan R. 1987. Inner filter effects and their interferences in the interpretation of culture fluorescence. *Biotechnology and Bioengineering*:769–774.
- Stärk E. 2000. Bioprozessanalytik durch Online-Vorhersage von Bioprozessgrößen mittels 2D-Fluoreszenzspektroskopie und multivariater Auswerteverfahren.
- Tukey JW. 1974. *Exploratory Data Analysis*: Addison-Wesley, Reading, Mass.
- Vemuri GN, Eiteman MA, McEwen JE, Olsson L, Nielsen J. 2007. Increasing NADH oxidation reduces overflow metabolism in *Saccharomyces cerevisiae*. *Proceedings of the National Academy of Sciences of the United States of America* 104:2402–2407.
- Walker GM. 1998. *Yeast Physiology and Biotechnology*.
- Wold S, Sjöström M, Eriksson L. 2001a. PLS-regression: a basic tool of chemometrics. *Chemom Intell Lab Syst* 58:109–130.
- Wold S, Sjöström M, Eriksson L. 2001b. PLS-regression: a basic tool of chemometrics. *Chemometrics and Intelligent Laboratory Systems* 58:109–130.
- Yang F, Pan J, Zhang T, Fang Q. 2009. A low-cost light-emitting diode induced fluorescence detector for capillary electrophoresis based on an orthogonal optical arrangement. *Talanta* 78:1155–1158.

# **Appendixes**

## **A Affidavit**



UNIVERSITY OF  
HOHENHEIM

Annex 2 to the University of Hohenheim doctoral degree regulations for Dr. rer. Nat.

**Affidavit according to Sec. 7(7) of the University of Hohenheim doctoral degree regulations for Dr. rer. Nat.**

1. For the dissertation submitted on the topic

.....  
Development of an on-line process monitoring for  
.....  
yeast cultivations via 2D-fluorescence spectroscopy  
.....

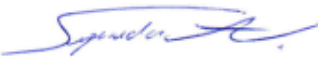
I hereby declare that I independently completed the work.

2. I only used the sources and aids documented and only made use of permissible assistance by third parties. In particular, I properly documented any contents which I used - either by directly quoting or paraphrasing – from other works.
3. I did not accept any assistance from a commercial doctoral agency or consulting firm.
4. I am aware of the meaning of this affidavit and the criminal penalties of an incorrect or incomplete affidavit.

I hereby confirm the correctness of the above declaration: I hereby affirm in lieu of oath that I have, to the best of my knowledge, declared nothing but the truth and have not omitted any information.

Stuttgart, 20.09.2018

Place and Date



Signature

## **B Curriculum Vitae**

# Supasuda Assawajaruwan

Körschstraße 11, 70599 Stuttgart, Germany

Tel: (+49)176 84586331 E-Mail: [assawa.supasuda@gmail.com](mailto:assawa.supasuda@gmail.com)

---

## Education

- 10/2014 – Present                    **Ph.D. in Process Analytics**  
University of Hohenheim, Stuttgart, Germany  
Expected graduation: Dec 2018
- 10/2011 – 02/2013                    **Masters of Process Engineering**  
Offenburg University of Applied Sciences, Offenburg, Germany  
Average grade: 1.7  
Thesis at *Deutsches Zentrum für Luft- und Raumfahrt (DLR), Stuttgart*:  
“Calculation of thermodynamic properties for alternative energy resources and processes of production of organic carbonates based on CO<sub>2</sub> as a feedstock”
- 06/2007 – 04/2011                    **Bachelor of Biotechnology**  
Mahidol University, Bangkok, Thailand  
Average grade: 1.3  
Thesis at *University at Albany, Albany, NY, USA*:  
“Fabrication and characterization of polyhydroxyalkanoates 3D-scaffolds and their in vitro biocompatibility study with murine submandibular gland cells”

## Work experience

- 10/2014 – present                    **Research assistant** at University of Hohenheim
- developing the process of an on-line monitoring for yeast cultivations via 2D fluorescence spectroscopy
  - doing statistical data analysis and mathematical models, i.e., Chemometrics

- supervising Bachelor and Master students for projects and theses
  - being responsible for the laboratory teaching
- 07/2013 – 09/2014      **Research scientist** at Offenburg University of Applied Sciences
- designed and optimized the fermentation process for cellulase enzyme producing bacteria
  - optimized the fermentation process for high productivity of biogas
  - established the chemical and biological analysis methods
  - supervised students for theses and projects
- 10/2010 -02/2011      **Intern** at Department of Life Science, University at Albany, NY, USA
- implemented mouse cell line culture
  - created the scaffolds from the biodegradable plastics, i.e., PHAs, PLA, PCL and chitosan
  - performed the chemical and biological analysis methods for animal cell lines and scanning electron microscope

**Additional skills**

Languages

Thai (native)  
 English (excellent command)  
 German (very good command)  
 Chinese (basic knowledge)

Computer skills

Microsoft Office (Word, Excel, PowerPoint)  
 MATLAB, R and SPSS  
 Unscrambler® software

Other skills

Six Sigma (Yellow belt), SAP  
 Lean Management & Kaizen Practitioner

**Interests and activities**

Traveling, Badminton, Board games, Painting, Volleyball

**Reference**

**Prof. Dr. Bernd Hitzmann**  
 Head of Process Analytics and Cereal Science Department at  
 University of Hohenheim, Garbenstraße 23, 70599 Stuttgart  
[bernd.hitzmann@uni-hohenheim.de](mailto:bernd.hitzmann@uni-hohenheim.de)